

**THE BREAD WHEAT HARDNESS SCENARIO OF THE  
SOUTHERN AND WESTERN CAPE: INTRODUCING THE PARTICLE  
SIZE INDEX (PSI) METHOD AND FOURIER TRANSFORM NEAR  
INFRARED (FT-NIR) SPECTROSCOPY CALIBRATIONS**

**LOUISE VAN ZYL**

Thesis presented in partial fulfilment for the degree of

**MASTER OF SCIENCE IN FOOD SCIENCE**

In the Department of Food Science  
Faculty of Agricultural Sciences  
University of Stellenbosch



**Study Leader:** Dr. M. Manley  
**Co-study Leader:** Dr. B.G. Osborne

December 1999

## DECLARATION

I, the undersigned, hereby declare that the work contained in this thesis is my own original work and that I have not previously in its entirety or in part submitted it at any other university for a degree.

08 - 02 - 2000

Louise van Zyl

Date

## ABSTRACT

Fourier transform near infrared spectroscopy (FT-NIR), the particle size index (PSI) method and scanning electron microscopy were used to investigate the bread wheat hardness scenario of the Southern and Western Cape in South Africa.

The effect of differences in sample holder composition on FT-NIR calibration and prediction results were investigated. Different calibrations were derived for protein and moisture content of 92 South African whole wheat flour samples using three different sample holders. Best results were achieved with borosilicate-glass vials, followed by soda-glass vials and the conventional sample cup with a sapphire-glass base provided with the spectrophotometer. Differences in results due to the use of different sample holders were investigated using correlation coefficients ( $r$ ) and maximum distances ( $d$ ) of a number of individual spectra and by performing analysis of variance (ANOVA) on the predicted values for independent validation of the different calibration models. The effect of compositional differences within both the borosilicate-glass and the soda-glass vials were investigated by means of ANOVA on the predicted values of a single sample presented to the spectrophotometer in a number of individual vials. All differences were found to be statistically insignificant ( $P \leq 0.05$ ). The sapphire-glass sample cup provided with the spectrophotometer could therefore be replaced by one of the vial-types investigated in which each sample could be stored and presented to the spectrophotometer individually.

The bread wheat hardness scenario of the Southern and Western Cape were investigated by deriving a FT-NIR hardness calibration for 198 ground bread wheat samples and using the particle size index (PSI) test as reference method. Particle size index results indicate that the investigated bread wheat cultivars have a very wide hardness range of 37.05 - 60.50%. The influence of genotype, location, protein content and moisture content on wheat hardness was investigated by means of ANOVA, Student's t-test, correlation analysis and regression analysis. Significant differences ( $P \leq 0.05$ ) in hardness was found over cultivars, while a positive linear relationship with protein content and a negative linear relationship with moisture content exist. The wheat samples were subsequently presented to the spectrophotometer in individual borosilicate-glass vials. A FT-NIR calibration was

derived by performing PLS regression on baseline-corrected spectra and the model validated using independent validation. Excellent results were achieved with a SEP, RMSEP and  $r$  of 2.13%, 4.53% and 0.89, respectively.

Wheat hardness of South African cultivars was further investigated by means of a comparative scanning electron microscopy (SEM) study performed on South African and Canadian wheat cultivars of different hardnesses. For each cultivar a cross section of the endosperm and a sample of the whole wheat flour were examined. The South African durum wheat, Kronos and the Canadian durum wheat had similar kernel endosperm and flour structures with tightly-packed protein-starch matrixes and a high degree of starch damage. Canadian and South African bread wheats reveal a large range of hardnesses and therefore a great difference in kernel endosperm and flour structure. The continuity of the protein-starch matrix, the degree of starch damage and the structure of starch granules differ within the bread wheat class, with T4 and SST 75 being, respectively, the hardest and the softest of the examined South African cultivars. The structure of the South African and Canadian soft wheat cultivars have a high resemblance, both revealing a discontinuous matrix, free starch granules and little or no starch damage. Results confirm the theory that wheat hardness is determined by the strength of the protein-starch bond and that hardness-related structural differences exist within especially the South African and Canadian bread wheats.

It can be concluded that the bread wheat class of the Southern and Western Cape is significantly ( $P \leq 0.05$ ) influenced by genotype, protein and moisture content and encompasses wheats of a very wide hardness range. A new system of categorising South African wheats for commercial purposes that acknowledges these differences by including kernel hardness measurements, could be beneficial to the milling and baking industries. The PSI method and FT-NIR spectroscopy have been established as successful methods for such determinations on South African wheat cultivars.

## UITTREKSEL

Fourier transformasie naby infrarooi (FT-NIR) spektroskopie, die partikelgrootte-indeks (PGI) metode en skandeer-elektronmikroskopie (SEM) is gebruik om die broodkoringhardheid .scenario van die Suid- en Wes-Kaap in Suid-Afrika te ondersoek.

Die effek van verskille in monsterhouerkomposisie op FT-NIR kalibrasie en voorspellingsresultate is ondersoek. Verskillende kalibrasies is ontwikkel vir proteïen- en voginhoud van 92 Suid-Afrikaanse heelkoringmeelmonsters deur gebruik te maak van drie verskillende monsterhouertipes. Die beste resultate is verkry met borosilikaat-glasflessies, gevolg deur soda-glasflessies en die konvensionele monsterhouer met 'n saffier-glasbasis wat saam met die spektrofotometer verskaf is. Verskille in resultate as gevolg van die gebruik van verskillende monsterhouers is ondersoek deur gebruik te maak van die korrelasiekoëffisiënte ( $r$ ) en maksimum afstande ( $d$ ) van 'n aantal individuele spektra en deur analyse van variansie (ANOVA) op voorspelde waardes vir onafhanklike validasie van die verskillende kalibrasie-modelle. Die effek van komposisionele verskille binne die borosilikaat-glas en soda-glasflessies is ondersoek deur middel van ANOVA op voorspelde waardes van 'n enkele monster wat blootgestel is aan die spektrofotometer in 'n aantal individuele flessies. Daar is gevind dat alle verskille statisties onbeduidend is ( $P \leq 0.05$ ). Die saffier-glasmonsterhouer wat saam met die spektrofotometer verskaf word, kan dus vervang word met een van die ondersoekte flessie tipes waarin elke monster individueel gestoor en aan die spektrofotometer blootgestel kan word.

Die broodkoringhardheid scenario van die Suid- en Wes-Kaap is ondersoek deur 'n FT-NIR hardheid kalibrasie vir 198 gemaalde broodkoringmonsters te ontwikkel waar die partikelgrootte-indeks (PGI) metode as verwysingsmetode gebruik is. Volgens die PGI resultate het die ondersoekte broodkoringkultivars 'n wye hardheidsreeks van 37.05 - 60.50%, wat daarop dui dat die broodkoringklas in die Suid- en Wes-Kaap korings van 'n besondere wye reeks van hardhede bevat. Die invloed van genotipe, lokaliteite, proteïen- en voginhoud op graanhardheid is met behulp van statistiese ontledings ondersoek. Betekenisvolle verskille in

hardheid is gevind in monsters van verskillende genotipe ( $P \leq 0.05$ ). Hardheid toon verder 'n positiewe lineêre verband met proteïen- en 'n negatiewe lineêre verband met voginhoud.

Monsters is aan die spektrofotometer blootgestel in individuele borosilikaat-glasflessies. 'n FT-NIR kalibrasie is gevolglik ontwikkel deurdat die som van kleinste kwadrate (PLS) regressie uitgevoer is op basislyn-gecorrigeerde spektra. Die model is gevalideer met behulp van onafhanklike validasieprosedures. Goeie resultate is verkry met 'n standaardfout van voorspelling (RMSEP), standaardfout van voorspelling gekorrigeer vir oorhelling (SEP) en 'n korrelasiekoëffisiënt ( $r$ ) van onderskeidelik 4.53%, 2.13% en 0.89 behaal. Die resultate van die studie dui daarop dat beide die PGI en die FT-NIR metodes suksesvol gebruik kan word om korrelhardheid van Suid-Afrikaanse broodkorings te bepaal.

Om die koringhardheid van Suid Afrikaanse korings verder te bestudeer, is 'n vergelykende skandeer-elektronmikroskopie studie op 'n aantal Suid-Afrikaanse en Kanadese koringkultivars van verskillende hardhede uitgevoer. 'n Kruisseksie van die endosperm en 'n monster van die heelkoringmeel van elke kultivar is ondersoek. Die Suid-Afrikaanse durumkoring, Kronos, en die Kanadese durumkoring het eenderse endosperm- en meelstrukture met styfgepakte proteïen-stysel matrikse en 'n hoë graad van styselbeskadiging getoon. Suid-Afrikaanse en Kanadese broodkorings het 'n groot variasie in hardheid en dus ook in endosperm- en meelstruktuur openbaar. Die kontinuïteit van die proteïen-stysel matriks, die graad van styselbeskadiging en die struktuur van die styselgranules het onderlinge verskille getoon met T4 en SST 75 wat, onderskeidelik, die hardste en die sagste van die ondersoekte Suid-Afrikaanse broodkorings was. Die struktuur van die Suid-Afrikaanse en Kanadese sagtekoringmonsters toon 'n groot ooreenkoms. Beide het 'n los matriks, vry styselgranules en min of geen styselbeskadiging. Resultate van die SEM studie staaf die teorie dat koringhardheid bepaal word deur die sterkte van die proteïen-styselbinding en dui ook op hardheidsverwante strukturele verskille binne en tussen veral die Suid-Afrikaanse en Kanadese broodkorings.

Daar kan verder ook afgelei word dat die broodkorings van die Suid- en Wes-Kaap betekenisvol beïnvloed word deur genotipe, proteïen- en voginhoud en dat die

broodkoringklas korings van 'n baie wyer reeks hardhede insluit. Daarom is 'n nuwe sisteem vir die katagoriserings van Suid Afrikaanse broodkorings wat korrelhardheid-bepalings insluit, moontlik nodig. Die PGI metode en FT-NIR spektroskopie is daargestel as suksesvolle metodes vir sulke bepalings op Suid-Afrikaanse koringkultivars.

## ACKNOWLEDGEMENTS

I would like to express my sincere gratitude to the following persons and institutions that have formed an integral part of this research:

Dr. M. Manley, my study leader and senior lecturer at the Department of Food Science, University of Stellenbosch, for her consistent guidance and support during this study and preparation of this thesis;

Dr. Brian Osborne, my co-study leader and Head, Grain Science and Milling, BRI Australia Limited, NSW, Australia, for his guidance during this study, specifically regarding the Fourier transform near infrared spectroscopy results;

Prof. T.J. Britz, Chairman of the Department of Food Science, University of Stellenbosch, for his interest and support throughout my studies;

Ms. M. Reeves for her help with administrative work and computer assistance;

Mr. G.O. Sigge, Mr. E. Brooks and Ms. L. Maas for technical assistance during the execution of experimental procedures;

Southern Associated Maltsters (Pty) Ltd., Caledon, South Africa, for protein and moisture content determinations on certain wheat samples;

Mr. R. van Zyl, ARC Infruitec-Nietvoorbij, Stellenbosch, South Africa, for his assistance with the scanning electron microscopy study;

The Department of Agronomy and Pastures, University of Stellenbosch, for the use of their Buhler Mlu and Cyclone mills;

The Winter Cereal Research Trust for financing this study;



The National Research Foundation for a NRF Grant Holder's bursary; and

My family, friends and fellow post-graduate students for their encouragement and understanding throughout my studies.

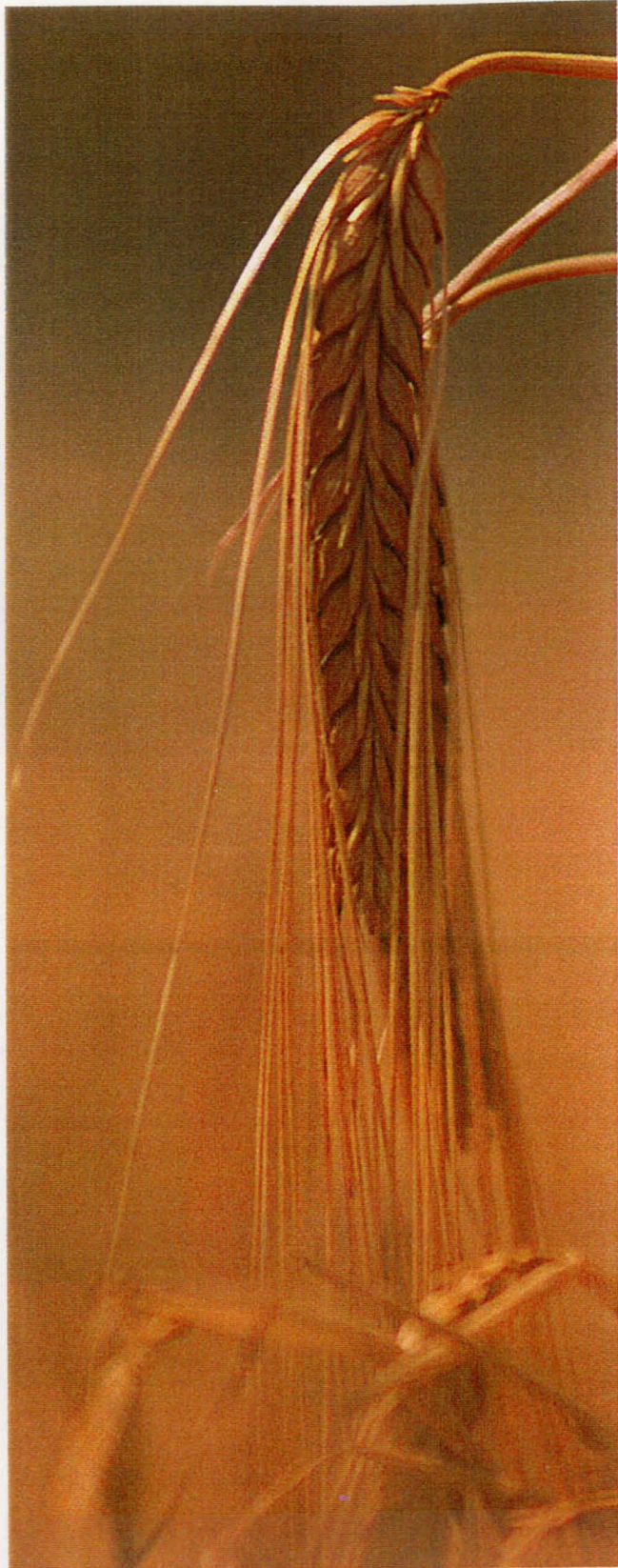
## CONTENTS

Chapter	Page
Declaration	ii
Abstract	iii
Uittreksel	v
Acknowledgements	viii
1. Introduction	1
2. Literature review	7
3. Using different sample holders in determining protein and moisture content in whole wheat flour by means of Fourier transform near infrared (FT-NIR) spectroscopy	61
4. Deriving grain hardness calibrations for Southern and Western Cape ground wheat samples by means of the particle size index (PSI) method and Fourier transform near infrared (FT-NIR) spectroscopy	91
5. A comparative scanning electron microscopy (SEM) study of South African and Canadian wheats of different hardnesses	118
6. General discussion and conclusions	149

Language and style used in this thesis are in accordance with the requirements of the *International Journal of Food Science and Technology*. This thesis represents a compilation of manuscripts where each chapter is an individual entity and some repetition between chapters has, therefore, been unavoidable.

## Chapter 1

### Introduction



## Chapter 1

### INTRODUCTION

There are thousands of known species and varieties of the genus *Triticum* (wheat), the principle wheats of commerce being the varieties of the species of *T. eastivum*, *T. durum* and *T. compactum* (Kent & Evers, 1994). These wheats need to be classified on a non-botanical basis for commercial purposes. The major distinguishing factors are grain texture (grain hardness or softness), winter or spring habit, red or white bran and protein content and quality. Of these, grain texture one of the most important factors affecting the quality and functionality of wheat. It affects the way in which wheat must be tempered for milling, the yield and particle size, shape and density of flour particles, the end-use properties in milling and the production of bread, soft wheat products and noodles (Pomeranz & Williams, 1990; Kent & Evers, 1994; Ohm *et al.*, 1998).

Despite its importance there is no clear definition for wheat hardness. It has been described as "the resistance to fracture upon grinding, slicing, abrasion or indentation of a single kernel or bulk samples" (Anjum & Walker, 1991) and as "difficult to penetrate or separate into fragments" (Pomeranz & Williams, 1990). There are many theories on the mechanism of wheat hardness. The most widely accepted one is that wheat hardness is determined by the differences in strength of the cohesion between starch and protein at the interface in the endosperm (Barlow *et al.*, 1973; Simmonds *et al.*, 1973; Kent & Evers, 1994).

In South Africa wheat is divided into 3 classes: hard wheat (for bread-making); soft wheat (for biscuit-making); and durum wheat (for pasta-making). Most wheat in South Africa forms part of the hard wheat class (Van Deventer, 1999). Hardness differences between cultivars within the same class are not uncommon. These intraclass as well as interclass hardness differences are influenced mainly by genotype (Pomeranz & Williams, 1990; Carver, 1994; Kent & Evers, 1994). In the past the distinction between hard and soft wheats was maintained by breeding programs which preserved the kernel morphology of

wheat generally recognised as hard or soft wheats (Norris *et al.*, 1989; Delwiche & Norris, 1993). In Canada and the USA crossbreeding has led to the mixing of hardness classes, making it increasingly difficult to distinguish between hard and soft wheats on the basis of kernel morphology. The same problem might occur in South Africa where wheat is not yet specified or categorised according to wheat hardness (Van Deventer, 1999). However, in the new free market system in South Africa, the price of wheat is playing an important role, and since the price is customary based on class in other wheat producing countries (Norris *et al.*, 1989), determining wheat hardness will become important in the South African wheat, milling and baking industries.

The measuring of wheat hardness dates back to the work of Cobb (1896) who measured the force needed to "bite" a kernel. At present there are more than a hundred different ways in which to measure wheat hardness (Cutler & Brinson, 1939; Norris *et al.*, 1989; Pomeranz & Williams, 1990). The majority of methods measure how the kernel breaks rather than absolute hardness and usually evaluate hardness-related phenomena by measuring some property of the wheat during or after grinding (Hoseney *et al.*, 1988; Norris *et al.*, 1989). In South Africa wheat hardness is currently determined by means of break flour yield and flour extraction (Wessels, 1999). In the United Kingdom the air jet sieve method is used successfully, while in Canada, Australia and the USA the particle size index (PSI) method is preferred (Norris *et al.*, 1989). These methods are based on the fact that wheat of different hardnesses produces flours of different particle sizes upon grinding (Cutler & Brinson, 1939). In the last two decades near infrared (NIR) reflectance and transmittance spectroscopy have been employed to successfully define wheat hardness or softness (AACC, 1983; Norris *et al.*, 1989; Williams, 1991; Delwiche & Norris, 1993; Delwiche *et al.*, 1995; Manley, 1995).

Near infrared spectroscopy is a quantitative and/or qualitative method by which the concentration of a specific component or a physical characteristic of a sample is related to the spectral data collected for that sample by means of a calibration model (Bradley, 1986; Osborne *et al.*, 1993). This method is

especially advantageous for the routine analysis of samples where the existing method is time-consuming or involves the use of expensive reactants. It is a simple, precise and non-destructive method by which multiple analysis can be done in one operation and the results are obtained within ten seconds to three minutes, depending on the spectrophotometer used (Wheling, 1994).

Near infrared (NIR) spectroscopy is capable of differentiating between wheats of different hardnesses because of its sensitivity to variance in particle size and particle size distribution of the ground wheat. Radiation scattering properties are used to define wheat hardness or softness (Pomeranz & Williams, 1990). Near infrared spectroscopy has also been used successfully for the hardness measurement of whole grain (Williams, 1991; Delwiche *et al.*, 1995; Manley, 1995). No Fourier transform near infrared (FT-NIR) spectroscopy work has, however, been done on wheat kernel hardness.

Scanning electron microscopy (SEM) has been successfully used in providing information on wheat hardness by examining hardness-related structural differences between wheats of different hardnesses (Barlow *et al.*, 1973; Moss *et al.*, 1980; Glenn & Saunders, 1990). This technique provides magnified images by the use of electrostatic or electromagnetic lenses with fast-moving electrons as illumination and is used to study the outside features of bulk material (Watt, 1997).

The aim of this study was to determine the wheat hardness scenario in the Southern and Western Cape in South Africa by means of the particle size index (PSI) test and FT-NIR reflectance spectroscopy of whole wheat flour samples, and assisted by scanning electron microscopy (SEM) studies of a number of whole grain and ground wheat samples.

## References

- AACC (1983). Wheat hardness as determined by near infrared reflectance, Method 39-70. In: *Approved methods of the AACC (8<sup>th</sup> edition)*. UK: Association of American Cereal Chemist Inc.
- Anjum, F.M. & Walker, E.R. (1991). Review on the significance of starch and protein to wheat kernel hardness. *Journal of Food Agriculture*, **56**, 1-13.
- Barlow, K.K. Buttrose, M.S., Simmonds, D.H. & Vesk, M. (1973). The nature of the starch-protein interface in wheat endosperm. *Cereal Chemistry*, **50**, 443-454.
- Bradley, E.B. (1986). Introduction to spectroscopic methods. In: *Instrumental Analysis (edited by G.D. Christian & J.E. O'Reilly)*. Pp. 144-157. Massachusetts, USA: Allyn and Bacon Inc.
- Carver, B.F. (1994). Genetic implications of kernel NIR hardness on milling and flour quality in bread wheat. *Journal of the Science of Food and Agriculture*, **65**, 125-132.
- Cobb, N.A. (1896). The hardness of grain in the principle varieties of wheat. *Agricultural Gazette N.S.W.*, **7**, 279-299 (as cited by Pomeranz & Williams, 1990).
- Cutler G. H. & Brinson, G.A. (1939). The granulation of whole meal and a method of expressing it numerically. *Cereal Chemistry*, **12**, 120.
- Delwiche, R. & Norris K.H. (1993). Classification of hard red wheat by near-infrared diffuse reflectance spectroscopy. *Cereal Chemistry*, **70**, 29-35.
- Delwiche, R., Chen, Y. & Hruschka, W.R. (1995). Differentiation of hard red wheat by near infrared analysis of bulk samples. *Cereal Chemistry*, **72**, 243-247.
- Glen, G.M. & Saunders, R.M. (1990). Physical and structural properties of wheat endosperm associated with grain texture. *Cereal Chemistry*, **67**, 176-182.
- Hoseney, R.C., Wade, P. & Finley, J.W. (1988). Soft wheat products. In: *Wheat Chemistry and Technology Volume II (3<sup>ed</sup> edition)* (edited by Y. Pomeranz). Pp. 407-456. Minnesota, USA: American Association of Cereal Chemists Inc.

- Kent, N.L. & Evers, A.D. (1994). *Kent's Technology of Cereals* (4<sup>th</sup> edition). Pp. 1-5, 78-82, UK: Elsevier Science Ltd.
- Manley, M. (1995). *Wheat hardness by near infrared (NIR) spectroscopy: New insights*, PhD. Thesis, University of Plymouth, United Kingdom.
- Moss, R., Stenvert, N.L., Kingswood, K. & Pointing, G. (1980). The relationship between wheat microstructure and flourmilling. *Scanning Electron Microscopy*, **3**, 613-620.
- Norris, K.H., Hruschka, W.R., Bean, M.M. & Slaughter, D.C. (1989). A definition of wheat hardness using near infrared reflectance spectroscopy. *Cereal Foods World*, **34**, 696-704.
- Ohm, J.B., Chung, O.K. & Deyoe, C.W. (1998). Single kernel characteristics of hard winter wheats in relation to milling and baking quality. *Cereal Chemistry*, **75**, 125-131.
- Osborne, B.G., Fearn, T. & Hindle, P.H. (1993). *Practical NIR Spectroscopy with Practical Implications in Food and Beverage Analysis* (2<sup>ed</sup> edition). Pp. 1-71. Essex, UK: Longman Group UK Ltd.
- Pomeranz, Y. & Williams, P.C. (1990). Wheat hardness: its genetic, structural, and biochemical background, measurement and significance. In: *Advances in Cereal Science and Technology* (edited by Y. Pomeranz). Pp. 471-458. Minnesota, USA: American Association of Cereal Chemists Inc.
- Simmonds, D.H., Barlow, R.R. & Wrigley, C.W. (1973). The biochemical basis of grain hardness in wheat. *Cereal Chemistry*, **50**, 553-562.
- Van Deventer, C.S. (1999). Koringbedryf moet kyk na nuwe klasifikasiesistelsel. *Landbouweekblad*, **1098**, 10-13.
- Watt, I.M. (1997). The electron microscope family. In: *The Principles and Practice of Electron Microscopy*, 2<sup>nd</sup> edition. Pp. 59-135. Cambridge, UK: Cambridge University Press.
- Wehling, R.L. (1994). Infrared spectrometry. In: *Introduction to the Chemical Analysis of Foods* (edited by S.S. Nielsen). Pp. 344,350. Boston, USA: Jones and Bartlett Publishers.

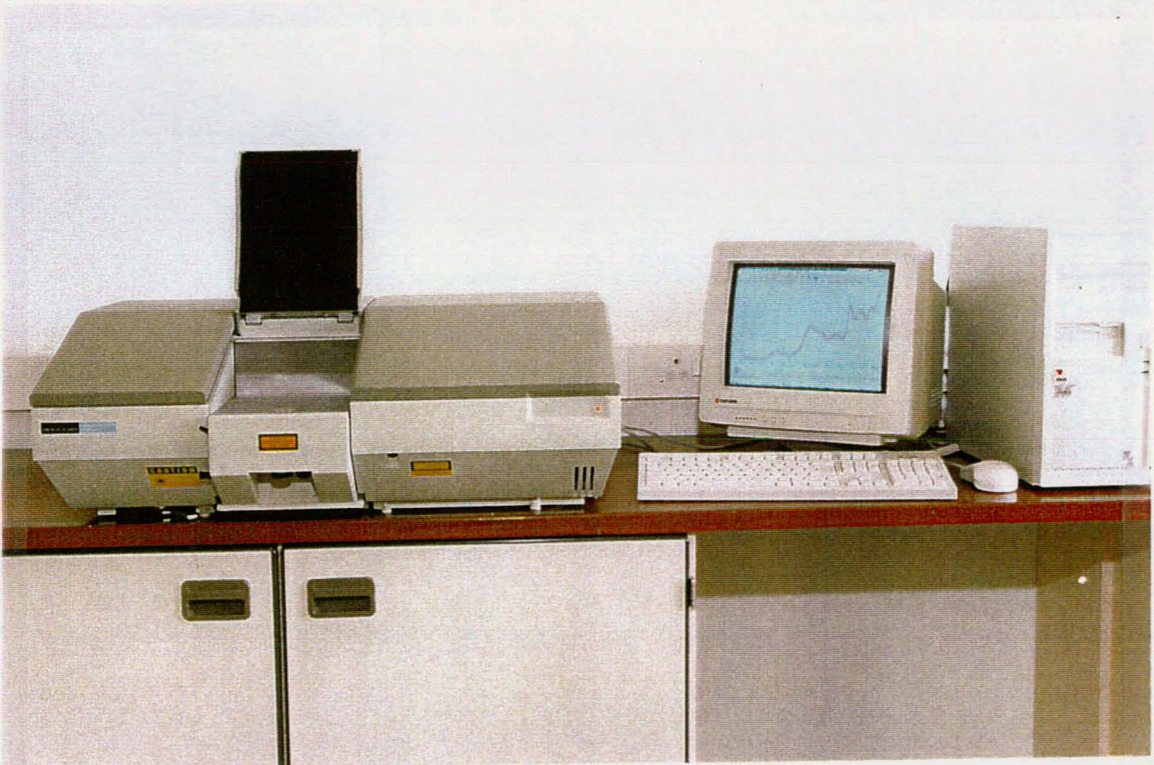


Wessels, A. (1999). Personal communication. Manager of product quality and development. Pioneer Food Group Ltd., Cape Town, South Africa.

Williams, P.C. (1991). Prediction of kernel texture in whole grains by near infrared transmittance. *Cereal Chemistry*, **68**, 112-114.

## Chapter 2

### Literature Review



## Chapter 2

### LITERATURE REVIEW

#### A. NEAR INFRARED SPECTROSCOPY

Spectroscopy can be described as a quantitative and/or qualitative analytical method by which the spectra of resonance peaks involving nuclei, atoms, ions or molecules are studied (Bradley, 1986). These peaks are indicative of energy changes arising from radiation-matter interactions such as absorption, emission or diffraction. The theoretical basis for this interaction is the quantized nature of energy transfer from the radiation field to matter (absorption), or vice versa (emission).

Spectroscopic methods differ in the species being analysed, the type of radiation-matter interaction to be monitored and the region of electromagnetic spectrum used in the analysis. Spectroscopic methods commonly used for traditional laboratory food analysis are based on the absorption or emission of radiation in the ultraviolet-, visible-, infrared- and radio frequency ranges (Penner, 1994).

The infrared (IR) region lies between the visible and the microwave regions on the electromagnetic spectrum (Figure 1). It comprises all the electromagnetic waves with wavenumbers between 12 500 and 10  $\text{cm}^{-1}$  (corresponding to wavelengths between 800 and 100 000 nm) (Anonymous, 1997a). The infrared region is divided into the near-infrared, mid-infrared and far-infrared regions. These regions differ with respect to the type of molecular energy levels that can be studied as well as the experimental techniques used.

Measurements in the near infrared (NIR) spectral region, stretching from 12 500 to 4000  $\text{cm}^{-1}$  (corresponding to 800 - 2500 nm), are more widely used for quantitative food analysis than are far- and mid-infrared measurements (Wehling, 1994). Near-infrared radiation can excite harmonics of molecular vibrations as well as low energy electronic transitions in molecules and crystals. Transmittance or diffuse reflectance techniques are used to record small differences in absorption, which is then transformed into an analytical result by means of complex regression mathematics (Wehling, 1994).

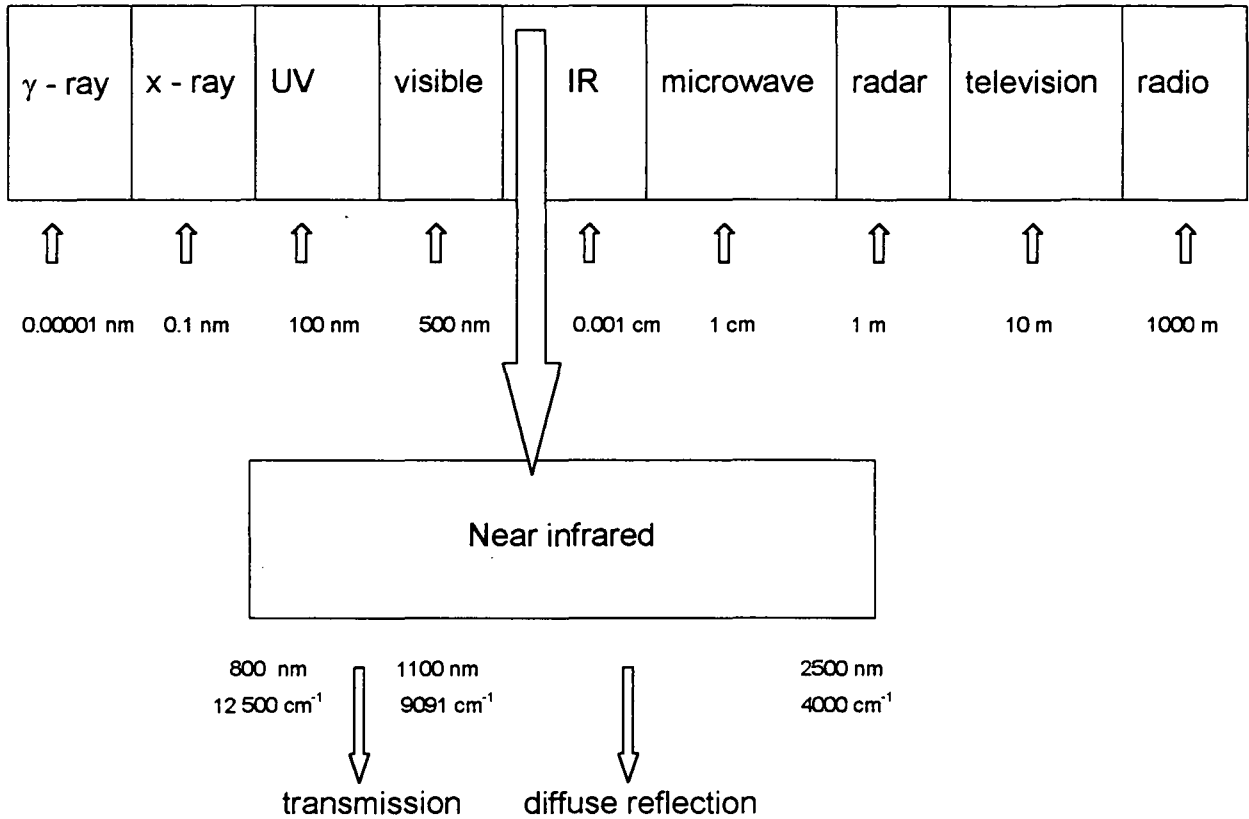


**Figure 1.** Electronic spectrum indicating the NIR region.

Fourier transform near infrared (FT-NIR) spectroscopy refers to a method where the sample sees all the wavelengths in the region of interest at all times instead of the traditional dispersive method where it sees only a small portion at a time (Bradley, 1986; Wetzel, 1998). It is accomplished by recording the intensity at the detector as a function of optical path difference traversed by two NIR beams in a Michelson interferometer. The method delivers a time-domain spectrum and must be converted to the traditional frequency-domain using the Fourier transform.

### **A 1. History and development of NIR spectroscopy**

Herschel recorded the first NIR spectrum in 1800 in Europe when he continued his measurements of heat energy of solar emission beyond the red portion of the visible spectrum. It was not until 1881, however, that Abney & Festing (1881) first photographically measured the NIR spectra of several organic liquids. Already they realized the importance of bonds involving hydrogen in the production of NIR absorptions.

In the early 1900's Coblentz (1905) measured the spectra of 19 compounds from 12 500 - 34 722  $\text{cm}^{-1}$  (corresponding to 288-800 nm). He observed that compounds with similar chemical groupings have characteristic absorption bands in the IR region. Coblentz's findings have since been extended to show that the nature of the chemical structures bonded to the specific group influences the exact wavelengths of absorption (Osborne *et al.*, 1993).

Up to the 1950's the NIR region was still being neglected because rapid measurement was not possible until photoelectric detectors had been invented (Osborne, 1981). However, research during the second World War led to the invention of such a detector, called the Cary 14, in 1954 (Osborne *et al.*, 1993).

Karl Norris (1964) was the first to use the NIR region for food analysis when he developed a new method for measuring the moisture content in grain. By using a computer correlation transform technique he was able to eliminate the interferences of protein, starch and oil he was experiencing during his moisture measurements. By pioneering the technique of multiple wavelength readings on a sample he also made

the simultaneous determination of several constituents possible. Norris's continuous research led to the development of practical NIR transmittance spectroscopy of intact cereal grains in 1979 (Osborne *et al.*, 1993). This meant that the need to grind the sample was eliminated. Karl Norris is referred to by many as the "father" of NIR spectroscopy for developing the first commercial instrument designed specifically for NIR measurements, called the Dickey- John Grain Analysis Computer, in 1971.

## **A 2. Advantages, disadvantages and applications of NIR analysis**

Foods and beverages are processed to detailed quality specifications which require many analytical determinations on the raw materials, the process intermediates and the final product (Osborne *et al.*, 1993). The chemical methods of the past are proving to be inadequate to meet the growing demand for rapid, cost-effective analysis in the food and beverage industry.

The NIR spectroscopic method of analysis is an instrumental method for the rapid and reproducible measuring of the chemical composition of a sample. The four main advantages of this method, apart from its precision, would be its speed, the simplicity of sample preparation, multiplicity of analysis with one operation, and the nonconsumption of the sample (Wehling, 1994; Wetzel, 1998). A measurement can be made in as little as ten seconds, although the average would be closer to 30 seconds to three minutes. Little or no sample preparation is needed and the technique can be used by employees without extensive training. It is also applicable for on-line measuring systems.

Fourier transform near infrared (FT-NIR) spectroscopy has the added advantages of improved speed and resolution, or signal-to-noise ratio, over the conventional NIR method (Bradley, 1986). However, its main advantage is its multiplex or Fellgett's advantage, namely that information from all spectral elements is measured simultaneously (Griffiths & de Haseth, 1986). Furthermore, Jacquinot discovered that the maximum allowed solid angle of the collimated beam passing through an interferometer of a Fourier transform instrument is greater than the solid angle of the collimated beam of the same cross-sectional area at the prism or grating

of a monochromator measuring at the same resolution. The Fellgett and Jacquinot advantages combine to form the fundamental basis for the improved performance of FT-NIR spectrophotometers over monochromators of dispersive NIR spectrophotometers.

The main disadvantages of the NIR spectroscopic method would be the instrumentation requirements, the high initial cost of the instrumentation, dependence on calibration procedures and the complexity in the choice of data treatment (Wheling, 1994). The method used to lack in sensitivity for minor constituents, but this is becoming increasingly less of a problem.

Applications of NIR spectroscopy in the food industry date back to 1938 and the work of Ellis & Bath (1938) who reported studies on gelatin. Today NIR is commonly used to determine especially the major constituents in food (Williams & Stevenson, 1990). NIR spectra of food constituents show broad bands which comprise envelopes of overlapping absorptions corresponding mainly to overtones and combinations involving C-H, O-H and N-H chemical bonds.

There are several areas where NIR analysis can be applied in the food industry (Williams & Stevenson, 1990). Analysing raw materials can ensure that specifications can be met in the finished product. By analysing the product at critical stages during processing its composition can be monitored. It is further necessary to analyse the finished product to verify that specifications have been met. By-products should also be analysed to determine their value for future sale. Another increasingly important application is the analysis of effluents and other wastes for pollution control (Williams & Stevenson, 1990; Osborne *et al.*, 1993).

Examples of current applications of NIR in foods include the analysis of kernel hardness, protein and moisture in wheat (Hunt *et al.*, 1977; Williams, 1991), fat, protein and total solids in fermented milks (Rodriguez-Otero & Hermida, 1995; Rodriguez-Otero *et al.*, 1997), ethanol, glycerol, glucose and fructose in wine (Garcia-Jares & Medina, 1997), firmness of kiwifruit (McClone *et al.*, 1997) and the soluble solids in peaches (Peiris *et al.*, 1998). Any substance, however, that absorbs in the NIR region and is present at levels of a few tenths of a percent or greater has the potential to be analysed by NIR spectroscopy (Wehling, 1994).

### A 3. Fundamentals of NIR spectroscopy

#### Electromagnetic radiation properties

Electromagnetic radiation, of which NIR radiation forms a part, is an alternating electromagnetic field in space. A graphical representation of a plane polarized electromagnetic wave is shown in Figure 2. The wave is referred to as plane polarized because the oscillating electric and magnetic fields making up the wave are each limited to a single plane (Penner, 1994). Both the electric and the magnetic vectors are perpendicular to each other and to the direction of the wave propagation.

Radiation has a dual nature: wavelike and particulate (Penner, 1994). Propagation-associated phenomena such as interference, diffraction and refraction, are best explained using the wave theory. Its interaction with matter, the basis of absorption and emission, though, is best explained in terms of its particulate nature.

The harmonic wavelike character of radiation can be described by a number of properties including its wavelength, wavenumber, frequency and velocity of propagation (Osborne *et al.*, 1993). The relationship between these properties is (equation 1):

$$\bar{\nu} = \frac{1}{\lambda} = \frac{\nu}{V} \quad \dots 1$$

where  $\bar{\nu}$  = wavenumber

$\lambda$  = wavelength

$\nu$  = wave frequency

$V$  = velocity of propagation



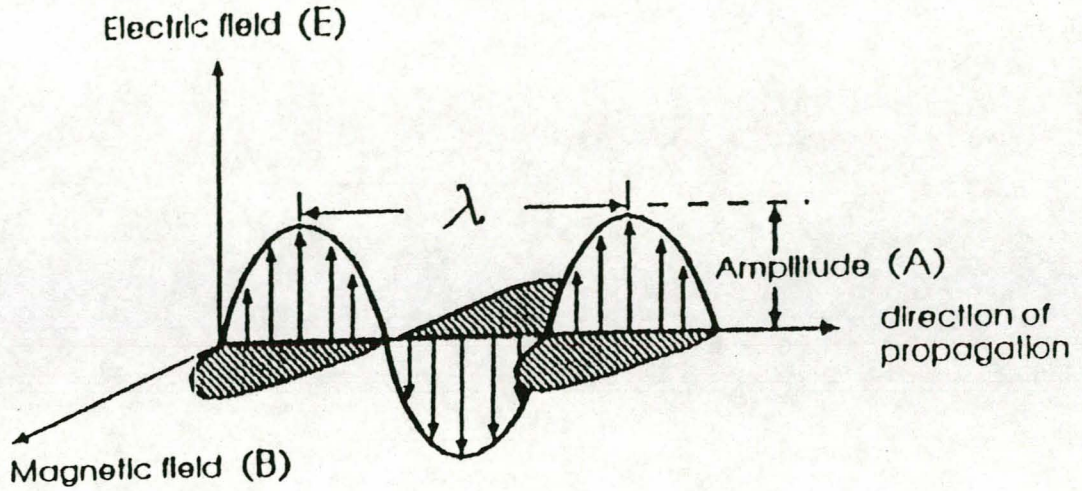


**Figure 2.** A plane-polarized electromagnetic radiation propagating along the x-axis. The electric and magnetic fields are in phase, perpendicular to each other and to the direction of propagation (Penner, 1994).

The frequency of an electromagnetic wave is determined only by the source of radiation and thus stays constant in different media (Penner, 1994). The velocity, however, will be influenced slightly by the medium through which the wave is propagating. Changes in wavelength will be proportionate to changes in wave velocity.

If we consider electromagnetic radiation as a simple harmonic wave, its simple harmonic motion has the properties of the sine wave defined by equation 2 (Osborne *et al.*, 1993).

$$y = A \sin \theta \quad \dots 2$$

Although the wave properties of radiation can never be ignored, absorption and emission of radiation are best understood by considering light to be comprised of many particles, or discrete quanta of energy, called photons (Bradley, 1986). The energy of a photon is defined in equation 3 in terms of the frequency of the associated wave.

$$E = h\nu = \frac{hc}{\lambda} \quad \dots 3$$

where  $E$  = energy [J]

$h$  = Planck's constant ( $6.62 \times 10^{-34}$  Jsec<sup>-1</sup>)

$\nu$  = radiation frequency [Hz]

The amount of energy transferred per photon during absorption or emission is also given by equation 3 commonly referred to as the Einstein-Planck relation (Bradley, 1986). This relation indicates that the energy of a photon of monochromatic radiation is dependent only on its wavelength or frequency. Furthermore it is important to remember that the intensity of a beam of radiation depends on the quantity of photons per unit time per unit area, and also that the quantum energy per photon is constant at any given radiation frequency.

## Properties of vibrating molecules

### *The harmonic oscillator*

Interatomic bonds behave like springs and have elastic properties. Many fundamental frequencies can be roughly calculated by assuming that the band energies arise from the vibration of such ideal diatomic oscillators (Ciurczak, 1992). It essentially obeys Hook's law in that the restoring force,  $F$ , exerted by the spring is proportional to the distance,  $y$ , it has traveled from the equilibrium position (equation 4). Furthermore the total energy of the bond is proportional to the frequency of the vibration. The frequency of an interatomic bond and the vibrational energy for any molecule are given by equations 5 & 6, respectively.

$$F = -k y \quad \dots 4$$

where  $k$  - force constant

$$\nu = \frac{1}{2\pi} \sqrt{\frac{k}{\mu}} \quad \dots 5$$

where  $\nu$  = vibrational frequency

$\mu$  = reduced mass of the two atoms

$$E = (\nu + \frac{1}{2}) h\nu \quad \dots 6$$

According to the classical spring model the energetics of the system undergoes cyclic conversions from potential energy to kinetic energy (Osborne *et al.*, 1993). The simple harmonic motion that the molecule's energy undergoes is shown in Figure 3. At equilibrium position the kinetic energy is at a maximum and the potential energy is zero. As the spring compresses or stretches, the potential energy increases and the kinetic energy decreases until the potential energy reaches a maximum and the kinetic energy is zero at the maximum amplitude.

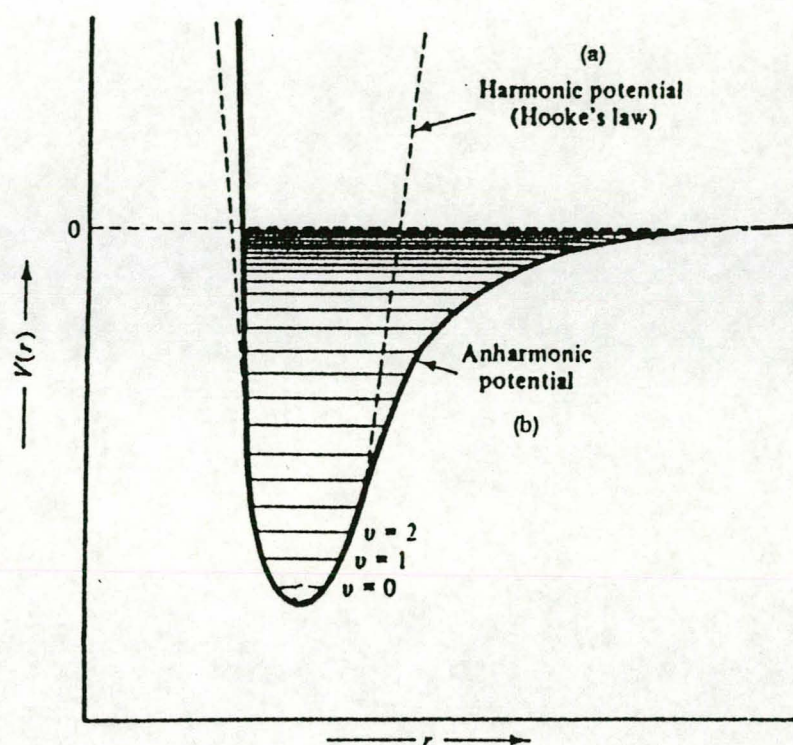


**Figure 3.** Energy diagram of vibrational mode as (a) an ideal diatomic oscillator or (b) an actual anharmonic diatomic oscillator (Ciurczak, 1992).

The equation (7) by which the system's energy can be calculated at any given point reads

$$E = \frac{ky^2}{2} \quad \dots 7$$

where  $y$  is the distance traveled from the equilibrium position (Osborne *et al.*, 1993). This works fairly well for true diatomic molecules and also for the average value of two atoms stretching within a polyatomic molecule. Unfortunately it approximates the average or centre frequency of the bond and is therefore of little value, since in real molecules the electron-withdrawing or -donating properties of neighbouring atoms determine the bondstrength, length and therefore also the frequency. It is these differences, however, that cause a real spectrum to develop.

#### *The quantum theory and energy levels*

In 1900 Max Planck proposed that an oscillator's energy is quantized. This means that the potential or internal energy of molecules or atoms does not vary continuously, but rather in a series of discrete steps (Osborne *et al.*, 1993; Wetzel, 1998). Any change in an oscillator's energy content can therefore only occur by means of a transition between certain allowed internal energy levels brought about by the absorption or emission of discrete packets of energy or quanta. The potential energy spacings between allowed internal energy levels will be unique for every species and may be used as a "fingerprint" in qualitative absorption spectroscopy. Planck further proposed that the frequency of the electromagnetic radiation needed for such a transition is related to the change in energy (equation 8).

$$\Delta E = h\nu \quad \dots 8$$

Potential energy levels for an organic molecule is depicted in Figure 4 as a partial molecular energy level diagram (Penner, 1994). Three electronic energy

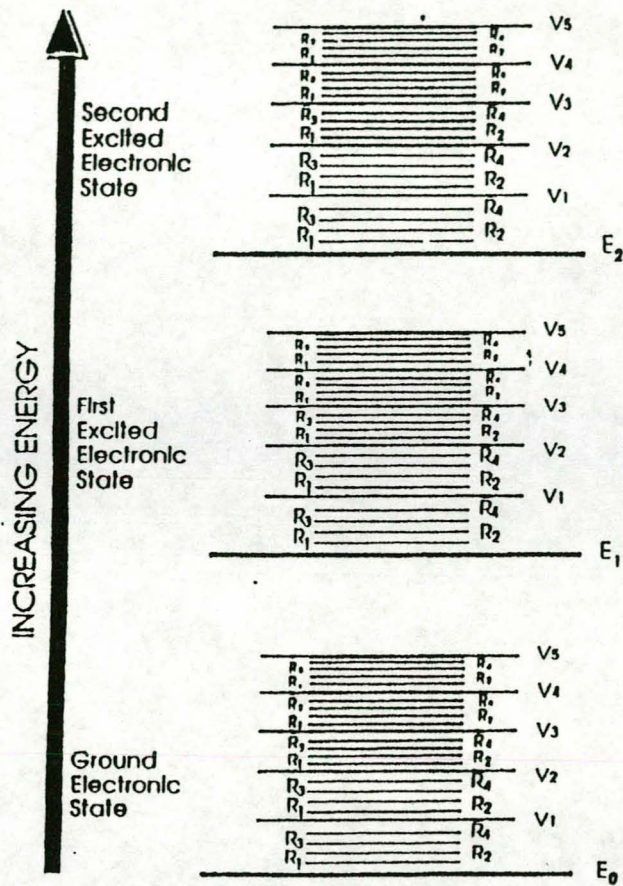


**Figure 4.** Partial molecular energy level diagram depicting three electronic states (where  $E_i$  = electronic energy levels,  $V_i$  = vibrational energy levels and  $R_i$  = rotational energy levels) (Penner, 1994).

states, the lowest of which is the ground state, are depicted. If an electronic transition takes place it results in the electron changing from orbital or energy level. This necessarily results in a change in the electron's as well as the molecule's potential energy. The magnitude of the energy difference between the ground state and the first excited states, for the atoms' valence electrons and the molecule's bonding electrons are generally of the same range as the energy content of photons associated with ultraviolet and visible light radiation (Penner, 1994).

Each electronic energy state has its own corresponding vibrational and rotational energy levels (Penner, 1994). Atoms, though, do not have these corresponding energy levels and therefore may appear less complicated. The difference in energy levels associated with the vibrating motions of the atoms that comprise a molecule are much less than those of the molecular electronic levels and are of the same magnitude as the energy of photons associated with radiation in the IR, including the NIR, region. Energy differences between rotational energy levels are even smaller and are of the same magnitude as the energy content of photons of microwave radiation.

A vibrating molecule can absorb IR radiant energy to move from the lowest vibrational level to the first excited level only if the frequency of the radiation is identical to the initial frequency of vibration within the molecule (Wehling, 1994; Wetzel, 1998). These frequencies are referred to as fundamental absorptions and give rise to IR spectra, provided that an electric moment exists across the vibrational bond. Should the molecule be raised to a higher excited state, it will be due to the absorption of radiation frequencies that are the relevant number of times that of the fundamental frequency. These absorptions are called overtones and have a relatively low intensity. For example, if a molecule in its ground state absorbs radiant energy with a frequency that is twice that of the fundamental frequency, it will be excited to the second excited vibrational state and the absorption will be referred to as the first overtone. It is the absorption of these overtone frequencies by vibrating molecules that give rise to spectra in the NIR region. Another theoretical possibility in this region is the occurrence of combination or difference bands (Osborne *et al.*, 1993; Penner, 1994). This is possible when two or more different vibrations interact

to give bands with frequencies that is the sum or the difference of multiples of their fundamental frequencies.

The selection rules for the quantum-mechanically treated harmonic oscillator only allow vibrational transitions in which  $\nu$  changes by one ( $\Delta\nu = \pm 1$ ) (Osborne *et al.*, 1993). It therefore only explains the observed absorption bands due to fundamental modes of molecular vibration. It does not explain the presence of overtone bands in the NIR region that arise from "forbidden" transitions ( $\Delta\nu = \pm 2, \pm 3, \dots$ ). These transitions can, however, be explained by approaching molecules as anharmonic oscillators.

#### *Anharmonic oscillator*

Real molecules do not obey the laws of simple harmonic motion exactly, just like real bonds, although elastic, do not obey Hook's law exactly. When two atoms approach each other, the coulombic repulsion between their nuclei causes the potential energy to rise more rapidly than predicted by the harmonic approximation (Osborne *et al.*, 1993; Penner, 1994). At interatomic distances at which dissociation occurs the potential energy levels will level off, as can be seen in Figure 3. Notice that the two curves in Figure 3 are almost identical at low potential energies. The success of the harmonic model stems from this fact.

An anharmonic oscillator behaves like a harmonic oscillator, but with an oscillating frequency which decreases with increasing radiation frequency (Osborne *et al.*, 1993). The selection rules for anharmonic oscillators are  $\Delta\nu = \pm 1, \pm 2, \pm 3 \dots$  (Osborne *et al.*, 1993; Penner, 1994). They are the same as for harmonic oscillators but with the additional possibility of larger jumps. In practice, though, this probability diminishes rapidly so that only jumps due to  $\Delta\nu = \pm 1, \pm 2$ , and sometimes  $\pm 3$  have intensities strong enough to be observed.



### *Modes of vibrations for molecules*

A vibration can be either of a stretching or a bending nature (Osborne *et al.*, 1993). Stretching involves the type of vibration in which there is a continuous change in interatomic distances along the axis of the bond between the two atoms. In the case of a triatomic group of atoms stretching may be symmetrical or asymmetrical (Figure 5). Bending vibrations involve a change in bond angle and can be further classified into four types: scissoring; rocking; wagging; and twisting as depicted in Figure 5.

Each of these vibrational modes could give rise to overtones or combinations observable in the NIR region (Osborne *et al.*, 1993). The intensity of these bands will depend on the degree of anharmonicity. Hydrogen, being the lightest of atoms, causes the bonds it is involved in to vibrate with large amplitude when stretching. This motion would therefore deviate significantly from the harmonic oscillator theory. This explains why most absorption bands observed in the NIR arise from overtones of hydrogenic stretching vibrations involving functional groups, or combinations involving stretching and bending vibrational modes of such groups.

### **Modes of radiation-sample interaction**

When monochromatic radiation interacts with a sample it can either be transmitted, absorbed or reflected (Murray, 1988), and according to the law of conservation of energy (equation 9),

$$E = P_a + P_t + P_r \quad \dots 9$$

where  $P_a$  = radiant power of absorption

$P_t$  = radiant power of transmission

$P_r$  = radiant power of reflection

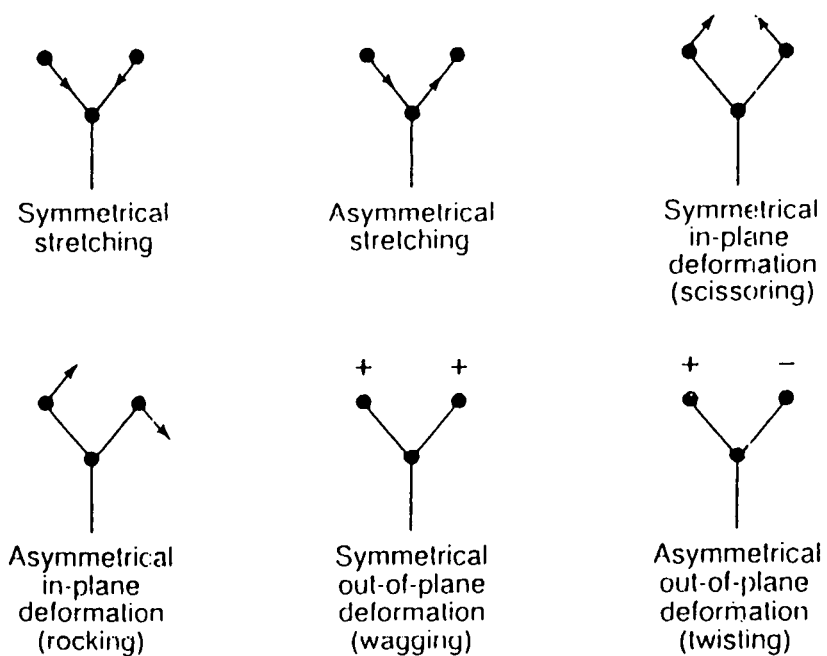


**Figure 5.** Modes of vibration of a group  $AX_2$  (Osborne *et al.*, 1993).

In transmittance spectroscopy the reflected component can be eliminated by using a control or solvent blank (Murray, 1988). This technique commonly makes use of higher frequency energy,  $12\,500 - 9091\text{ cm}^{-1}$  (corresponding to 800-1100 nm), due to its greater depth of penetration. In reflectance spectroscopy, again, the transmitted component is eliminated by using a large enough sample thickness that all the light is either absorbed or reflected and none passed right through the sample.

### *Transmission of radiation*

Radiation propagates through a medium, other than a vacuum, through the temporary polarization of the particles of the medium. This polarization is caused by the interaction of the electric vector of the radiation with electrons which causes them to oscillate with respect to their nuclei (Osborne *et al.*, 1993; Wetzel, 1998). When radiation crosses the boundary between two media with different refractive indexes, the direction of propagation changes abruptly. This phenomena is called refraction. The process of transmission is stepwise where the oscillating particles act as intermediates and where diffraction often occurs.

### *Absorption of radiation*

Absorption of radiation by an atom or molecule can be defined as the process in which energy from a photon of electromagnetic radiation is transferred to the absorbing species (Penner, 1994). The atom or molecule will have an increase in internal energy equivalent to the amount of energy in the particular photon that was absorbed and will consequently be raised to a more excited state. If one plots photon energy against the relative absorption of radiation composed of photons of that energy, one observes the characteristic absorption spectrum of that species.

The Beer-Lambert law describes the attenuation of the transmitted radiation by an absorbing sample (Osborne *et al.*, 1993; Wetzel, 1998). It states that the fraction of radiation energy,  $P$ , absorbed by an infinitesimal thickness of sample is proportional to the number of molecules, in other words

$$\frac{-dP}{P} = kdn \quad \dots 10$$

and after integrating

$$-\ln \frac{P_t}{P_o} = kn \quad \dots 11$$

where  $P_o$  = power of incident radiation

$P_t$  = power of transmitted radiation

$n$  = number of molecules in the beam's path

Since  $n$  is proportional to the concentration,  $c$ , of the sample molecules and the thickness,  $b$ , through which the radiation passes,

$$\log \frac{P_o}{P_t} = abc \quad \dots 12$$

where  $a$  = a constant called absorptivity

The fraction of radiation,  $P_o / P_t$ , transmitted by the sample is measured and is called the transmittance,  $T$ . This again is converted to the absorbance,  $A$ , which is defined by

$$A = \log \frac{I}{T} = \log \frac{P_o}{P_t} \quad \dots 13$$

so that equation 11 becomes

$$A = abc \quad \dots 14$$

If the Beer-Lambert relationship holds true, a plot of absorbance against concentration will result in a straight line through the origin with slope  $ab$ , and from which  $a$  may be determined easily (Osborne *et al.*, 1993).

### *Emission of radiation*

Emission is essentially the opposite of absorption in that it is that process by which energy is released by an atom or molecule in the form of a photon of radiation (Penner, 1994). Molecules that were raised to an excited state usually only remain in that state for a short while before relaxing back to the ground state. The most common relaxation process is for the molecule to convert its energy to kinetic energy in small steps by colliding with other molecules. Energy can also be lost by emission of a photon. This process is referred to as fluorescence or phosphorescence. In all cases the relaxation process is driven by the tendency of a species to exist in the lowest possible energy state.

### *Reflection of radiation*

For an opaque and non-absorbing sample the incident radiation will be reflected. Specular reflection and/or diffuse reflection can occur (Honings, 1985). Specular reflection takes place at the first surface the incident radiation encounters and can be described by the Fresnel equations. When the angle of incidence is zero degrees, the fraction of radiation power reflected is given by equation 15 (Osborne *et al.*, 1993).

$$\frac{P_r}{P_o} = (n_2 - n_1)^2 \quad \dots 15$$

where  $n_1$  and  $n_2$  = refractive indexes of the two mediums

Diffusely reflected radiation penetrates into part of the sample before being reflected back to the surface (Honings, 1985). Between the initial penetration and

the final exiting any radiation inside the sample undergoes constant absorption as described by equation 16 called Lambert's law.

$$A = \frac{4\pi K b}{\lambda_o} \quad \dots 16$$

where A = absorbance

K = absorption index of the sample

b = average pathlength

$\lambda_o$  = wavelength of monochromatic incident light measured in a vacuum

A large number of NIR analysis applications involve solid samples whose absorbance spectra are measured by the diffuse reflectance technique (Osborne *et al.*, 1993). Currently it is common practice to use equation 17 to relate a sample's diffuse reflectance to its composition.

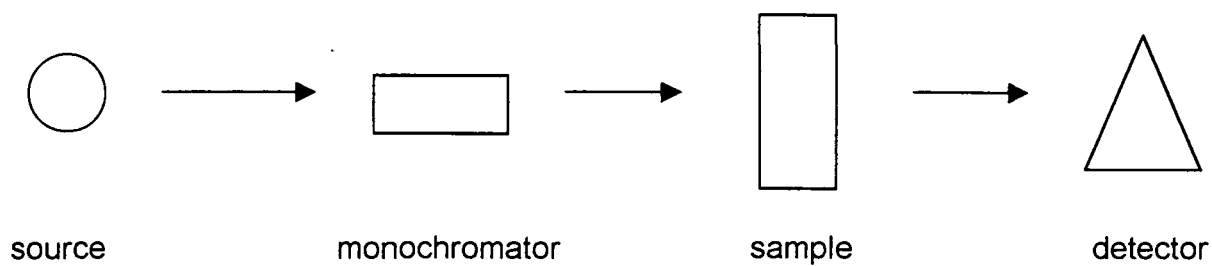
$$\log \frac{R}{R_o} = abc = A \quad \dots 17$$

where R = diffused reflected radiation from the sample

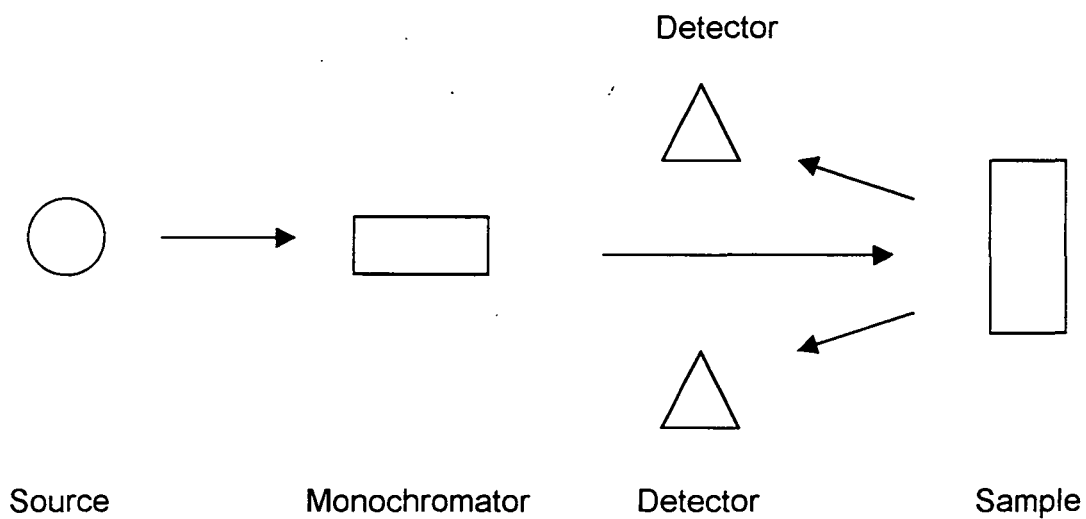
$R_o$  = diffused reflected radiation from a white standard

#### **A 4. NIR spectroscopic instrumentation**

The building blocks for all spectrophotometers are essentially the same (Bradley, 1986). A source of electromagnetic energy, the sample to be investigated, an analyser, a detector and a recorder are needed. The setup may sometimes include further instruments such as an electronic amplifier of the detected energy and an interferometer. A block diagram of a typical spectrophotometer, both in transmittance and diffuse reflectance mode, is depicted in Figure 6.



a) Near infrared transmittance



b) Near infrared reflectance

**Figure 6.** Basic instrument configurations for (a) reflectance and (b) transmittance (Workman & Burns, 1992).

## Source

Except for non-thermal radiation, NIR absorption spectroscopy requires a broad source of energy which spans the spectral region from the visible to  $3333\text{ cm}^{-1}$  (corresponding to 3000 nm). Ideally the spectral energy distribution and the power output should be constant (Osborne *et al.*, 1993).

Near infrared sources are inert solids that are electrically heated and produce intensity-vs-wavelength curves characteristic of black body radiation (Kincaid, 1986). The tungsten filament bulb is usually the preferred source for NIR instruments. It is normally operated at around 2400 K, and its life of several thousand hours can be greatly extended by underrunning. Unfortunately the conventional filament bulb often has an extended filament and a large envelope to minimize the effect of tungsten deposition so that it is not a compact source. Quartz halogen bulbs overcome the tungsten loss problem and are available running from temperatures of 2600 to 3200 K.

Although the NIR sources are almost always incandescent filaments and produce broad emission, there are other types of emitters that are non-thermal and emit radiation from much narrower range of wavelengths down to individual emission lines (Osborne *et al.*, 1993). The most important examples of this type of NIR source are light-emitting diodes, laser diodes and lasers. These sources are more efficient, power consumption is reduced and it can be electronically modulated.

## Analysers

The method by which light is spectrally modulated or selected defines the optical operating principle of an NIR instrument. In dispersive systems a monochromator or filter is used to isolate a specific portion of the radiation, while an interferometer is used in interferometric systems (Osborne *et al.*, 1993).



### *Dispersive systems*

In dispersive systems wavelengths of light are separated spatially, usually angularly. Prisms, filters or diffraction gratings can be used to select the correct wavelengths from a broad-band thermal radiation source (Osborne *et al.*, 1993).

The prism is the classical dispersing element, but it is an inefficient arrangement with low and non-linear dispersion and is therefore not often used (Osborne *et al.*, 1993).

Optical filters are used to pass or reject certain frequencies or bands of frequencies (Bradley, 1986). There are three main types of filters, namely cut-in or cut-out, bandpass and band rejection filters. A fourth type of filter is called a restrahlen filter and is only used in reflection (Bradley, 1986). It reflects only a narrow range of frequencies. This type of filter is useful in suppressing unwanted orders from a grating.

Certain wavelengths of light can also be selected by means of diffraction gratings. The word diffraction implies the effects that are produced when portions of waveforms are cut off. A grating is a parallel array of equidistant grooves that is spaced closely together. A diffraction grating can be used in either transmission or reflection, although the latter is much more commonly practiced (Bradley, 1986).

### *Interferometric systems*

When dispersive systems are used radiation is dispersed so that the detector only views a small portion of the available frequencies or wavelengths at one time (Bradley, 1986). The resulting record of intensity-vs-frequency or wavelength is said to be the frequency domain spectrum. A very different way to achieve the same goal would be to measure the intensity or radiant power of many wavelengths as a function of time (Bradley, 1986). This would be time-domain spectroscopy or Fourier transform spectroscopy, because the time-domain spectrum is converted into a conventional frequency-domain spectrum by a Fourier transform using a digital computer.

It is necessary to modulate the incoming beam so as to convert the frequency of the incoming radiation to a frequency that can be followed by the appropriate detector (Kincaid, 1986). This optical transformation is accomplished with a Michelson interferometer. The intensity at the detector is recorded as a function of the optical path difference transversed by two light beams in this interferometer, and is termed the interferogram.

The first two-beam interferometer was designed by Michelson in 1891. It creates the condition for optical interference by splitting light into two beams and then, after introducing a path difference, recombines them as illustrated in Figure 7 (Osborne *et al.*, 1993). A beam-splitter is fixed at a 45° angle between two mirrors that are perpendicular to each other. The beam splitter divides the light equally between the beams and also recombines them after they have been reflected back by the mirrors. Half of the light is reflected back in the direction of the source, while the other half can be collected by a detector. One mirror stays fixed while the other can be moved parallel with the beam of radiation. The radiation source is usually polychromatic so that the interferogram resulting from the sample-radiation interaction will be a sum of sine waves. Their individual amplitudes represent the intensities of corresponding spectral elements. A frequency decomposition, by taking a Fourier transform, is required to construct the spectrum (Osborne *et al.*, 1993).

While the Michelson interferometer is used most often in FT-NIR spectroscopy, other interferometers do exist. The Fabry-Perot interferometer is used in high resolution applications, for example atomic spectroscopy and measuring narrow-band laser line widths. The Mach-Zender interferometer, again, is mostly used to measure refraction index changes in gasses and in interference microscopes to image transparent samples (Tissue, 1996).

## Detectors

The most widely used detectors in the NIR range are the compound lead-salt semi conductors (Osborne *et al.*, 1993). Lead sulphide (PbS) is used over the range 400 - 10 000  $\text{cm}^{-1}$  (corresponding to 1000 - 2500 nm) and is more sensitive than lead selenide (PbSe) which is used over the range 2500 - 3500 nm.

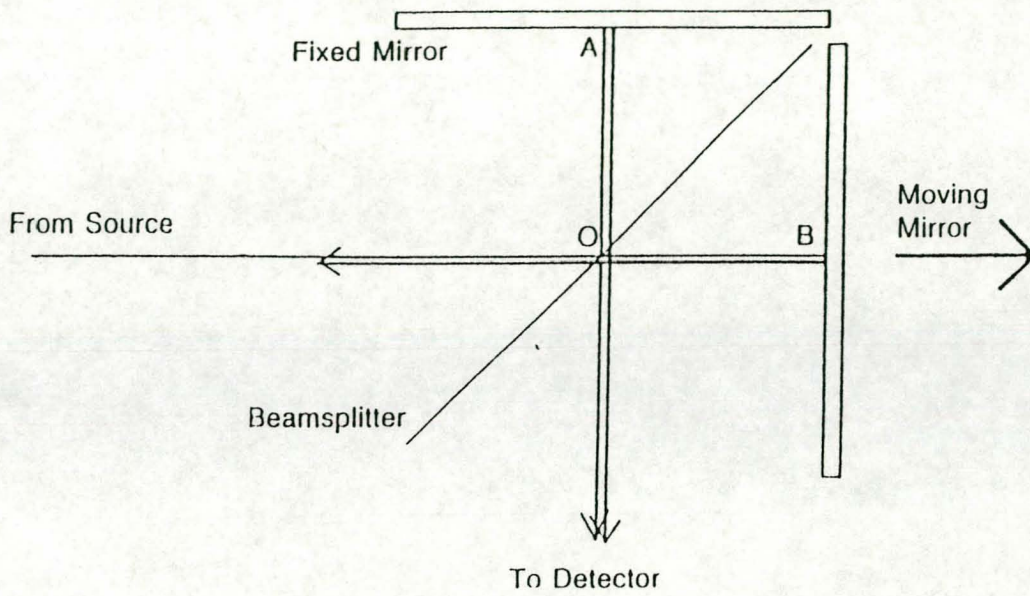


**Figure 7.** Michelson interferometer schematic diagram (Osborne *et al.*, 1993).

## A 5. Near infrared (NIR) calibrations

The goal of the calibration is to calculate a mathematical model relating the NIR spectra to the values obtained by the reference method (Workman, 1992). The model must be most sensitive to changes in concentration and least sensitive to non-concentration related factors. It is important to remember that the accuracy of a calibration is highly dependent on the accuracy of the results of the reference method.

Near infrared calibrations are made difficult by the complexity of the spectra (Osborne *et al.*, 1993). The peak of interest will most likely be overlapped by other interfering peaks. Furthermore reflectance is strongly dependent on the scattering properties of the sample.

The first step in the calibration process is to construct a data matrix,  $\mathbf{X}$  (often being  $\log 1/R$ ), from the instrument responses at selected wavelengths for a given calibration sample set (Beebe & Kowalski, 1987). A matrix of concentration values,  $\mathbf{Y}$ , is then obtained using a reference method. Next the mathematical method that will best reproduce  $\mathbf{Y}$  given the  $\mathbf{X}$  matrix must be chosen. The different calibration methods differ in their assumption of how to best estimate  $\mathbf{Y}$  from  $\mathbf{X}$ .

### *Multiple linear regression (MLR)*

Multiple linear regression assumes that the best approach to estimate concentration is to find the linear combination of the variables in  $\mathbf{X}$  that minimizes the errors in reproducing  $\mathbf{Y}$  (Beebe & Kowalski, 1987). Spectral intensities at selected wavelengths are used and concentration is a function of absorption in an inverse Beer's law model, so that

$$\mathbf{Y} = \mathbf{XS} + \mathbf{E} \quad \dots 25$$

where  $\mathbf{S}$  = matrix of regression coefficients

$\mathbf{E}$  = matrix of errors associated with the MLR model

The regression coefficients are chosen as to minimize the sum of squared errors. Because data compression is achieved by eliminating most of the spectral information, the wavelengths used must be well chosen to prevent a high error (Martin, 1992). A variety of the forward stepwise regression is most commonly used to select the correct wavelengths (Osborne *et al.*, 1993). An equation is built by adding wavelengths one at a time, each chosen so that the resulting equation has the smallest residual sum of squares possible. The starting point for the procedure can either be a wavelength known to be important for the specific measurement, or the pair of wavelengths which gives the best two-term equation. The addition of wavelengths is terminated when the added term ceases to be statistically significant.

The MLR method is the most popular method used in systems where there are no non-linearities, no interferences or interactions with other constituents and a low noise (Martin, 1992). Other estimation procedures for fitting equations that could be used in cases where the x's are highly correlated would be the ridge regression and the latent root regression.

#### *Fourier transforms*

Multiple linear regression can be generated by using Fourier coefficients rather than log 1/R spectral data (Martin, 1992). This method is advantageous because of the speed of computation and also because it eliminates the problem of wavelength selection and intercorrelation present with log 1/R data. Furthermore more terms can be used in the equation without running the risk of overfitting.

#### *Full spectrum models*

Due to the multicollinearity among spectral measurements and the resulting redundant information in the spectrum, a reduction in data is usually necessary when performing calibration procedures (Næs & Isaksson, 1991). Multiple linear regression uses wave selection methods to reduce spectral data. Full-spectrum methods, however, uses the information in all the spectral variables and then compresses it down to a few essential variables, components or factors before

regression. The quantity of spectral data is thus reduced, avoiding overfitting problems without discarding any useful information. The different approaches to data reduction between the wavelength selection methods and the full-spectrum methods are illustrated in Figure 8.

The two most important full-spectrum methods currently in use would be the principle component regression (PCR) and partial least square (PLS) regression techniques. To understand the essence of these methods one must visualise a multi-dimensional system for which new variables will be created (Osborne *et al.*, 1993).

Plotting the  $\log 1/R$  data of a set of samples at a given large amount of wavelengths against each other, one will create a multitude of axis in a multi-dimensional space. Each point on the plot will represent a sample and the distance in each dimension represents the spectral data of the different wavelengths. Reducing the amount of spectral data therefore translates to reducing the dimensions in space needed to represent the data. An easy way of achieving this is to project the points onto a smaller dimensional subspace. By performing these projections, new variables or factors that are linear combinations of the original data is created. The difference between PCR and PLS comes in the choosing of the particular planes onto which to project the points. Principle component analysis (PCA) assumes that by capturing most of the variability in the points, most of the information will be retained (Beebe & Kowalski, 1987). Principle component analysis therefore selects projections that maximize the variability in the projected points. The first principle component will therefore be found in the direction of maximum variability of the data as to maximize the amount of spectral information in the first variable. Whether the factors correlate with the reference data is not taken into account (Osborne *et al.*, 1993). The number of components to be used in the regression equation is decided by such methods as independent or cross-validation. Multiple regression follows PCA and is used to relate the few principle components to the reference data.

Partial least squares differs from PCA in that its factors are constructed by using a criterion that balances the need to capture as much variation in the spectral data as possible, as well as the correlation between the factors and the reference data (Osborne *et al.*, 1993).

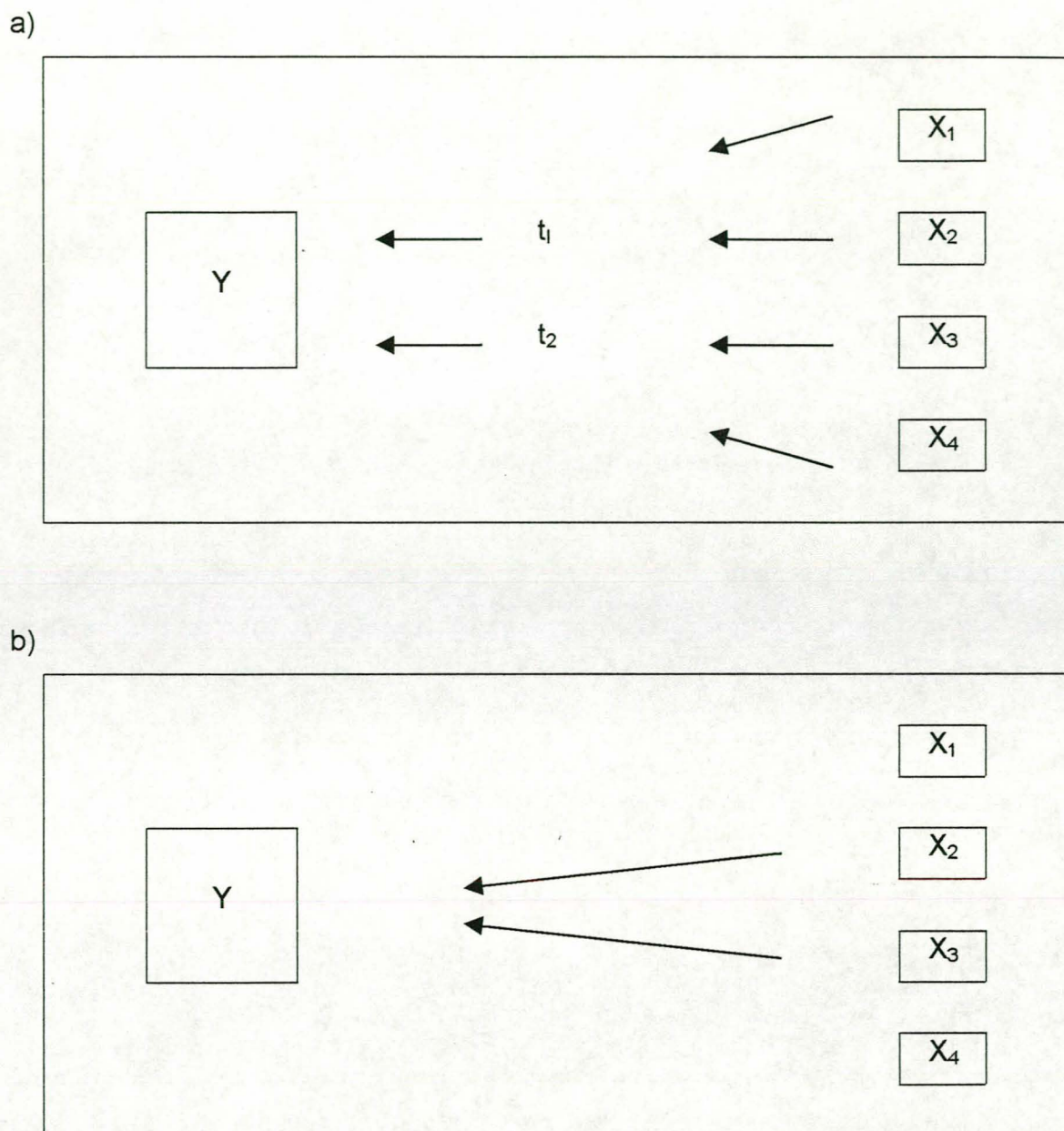


**Figure 8.** Illustration of data compression/reduction: (a) illustrates how full-spectrum methods combine all variables into a few components,  $t_1$  and  $t_2$ , before regression; and (b) illustrates that wavelength selection methods use only some of the variables (in this case  $x_2$  and  $x_3$ ) in the regression (Næs & Isaksson, 1991).

### *Non-linear models*

Artificial neural networks were recently developed to calibrate non-linear systems. In Figure 9 a small forward-feed network is shown. Each of the six nodes on the left of the figure receives one piece of spectral data and distributes it to the nodes in the middle or "hidden" layer (Osborne *et al.*, 1993). Each of these nodes receives six pieces of spectral data and which are combined in a weighed linear sum and transformed by a non-linear transfer function before being sent to the final node. Here the three impulses are again combined and put out as a predicted reference measurement.

### **Model selection**

When choosing a calibration model the nature of the samples, the reliability of the reference data and time constraints must be taken into account (Martin, 1992). The MLR model works well in systems where there is no co-linearity, but due to the long process of wavelength selection that is required it can be time consuming. This is not a problem with PCR and PLS, and they have the further advantage of reduced noise as the useful spectral information is concentrated into the first few factors.

It is general practice to develop a number of models and then selecting and testing the best against an independent set of validation samples, or by cross validation. The goodness of a calibration model can also be assessed statistically (Martin, 1992). The correlation coefficient ( $r$ ), the standard error of estimate or calibration (SEE or SEC), the standard error of prediction (SEP), the root mean standard error of prediction (RMSEP) and the F-statistic are most often used. The SEP and RMSEP give an estimate of the magnitude of the errors expected when independent samples are predicted when using the model (Osborne *et al.*, 1993, Anonymous, 1997b). The standard error of calibration (SEC) is the differences between the predicted and actual values at the calibration stage. The standard error of estimate (SEE) for the regression gives an indication of the quality of the fit of the regression. The coefficient of determination ( $R^2$ ) of the full model gives the



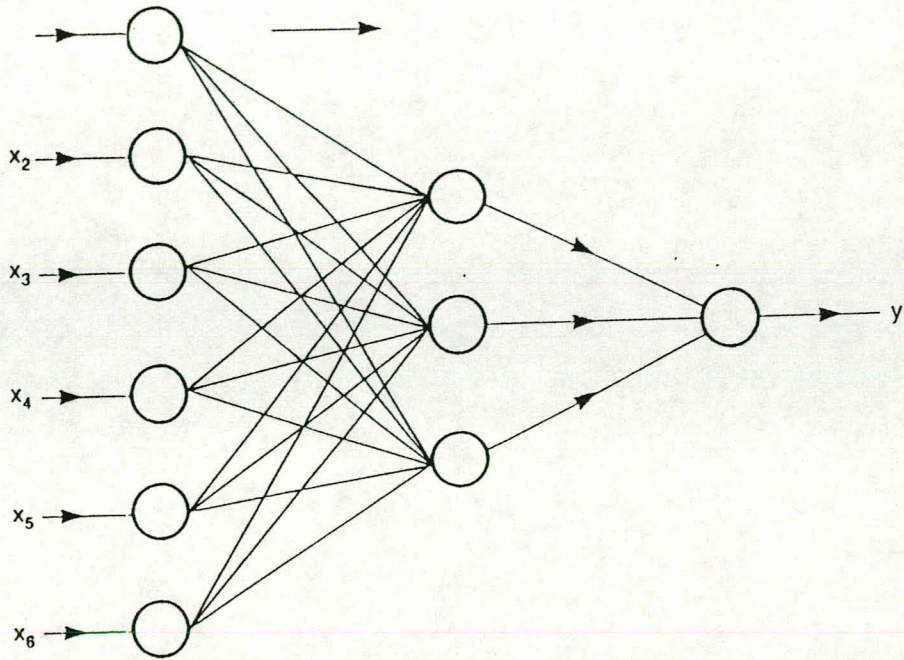


**Figure 9.** A simple feed-forward artificial neural network (Osborne *et al.*, 1993).

proportion of variability of the property that is described by the model. The correlation coefficient ( $r$ ) is the square root of the coefficient of determination. The F-value is used to determine whether the property variance accounted for by the model is significantly better than the residual property variance. A poor regression will give a low ( $<3$ ) F-value (Anonymous, 1997b). A good calibration model would therefore have low SEP, RMSEP, SEC and SEE values and high  $r$ ,  $R^2$  and F-values. The number of factors or principle components chosen should be such that it is enough to capture as much of the variability in the spectral data as possible, but not so much that there is a risk of over fitting, which would result in poor results when predicting independent samples.

## **B. WHEAT HARDNESS**

### **B 1. Introduction**

Cereals are the fruits of cultivated grasses of the monotyledenous family *Gramineae* (Kent & Evers, 1994). The principle crops are wheat, barley, oats, rye, rice, maize, sorghum and the millets. Of these, wheat is arguably the most important, comprising more than 30% of the world's cereal cultivated surface and being the world population's major source of carbohydrates and protein. Furthermore wheat flour has the unique ability of forming a visco-elastic, gas-retaining dough giving rise to a broad spectrum of products of economic significance (Kent & Evers, 1994).

The place and time of the origin of the wheat plant is not known with certainty, but it is agreed upon that even centuries before recorded history various species were cultivated for human consumption in the Mediterranean area (Shellenberger, 1964). There are also numerous archeological finding sustaining the believe that wheat was cultivated in particularly Persia, Egypt, Greece and Europe (Kent & Evers, 1994). Percival (1921) believed that bread wheat originated by hybridization from an emmer type and wild species of grass.

The structure of a wheat kernel can be seen diagrammatically in Figure 10. Wheat kernels are rounded on the dorsal side and have a longitudinal crease the

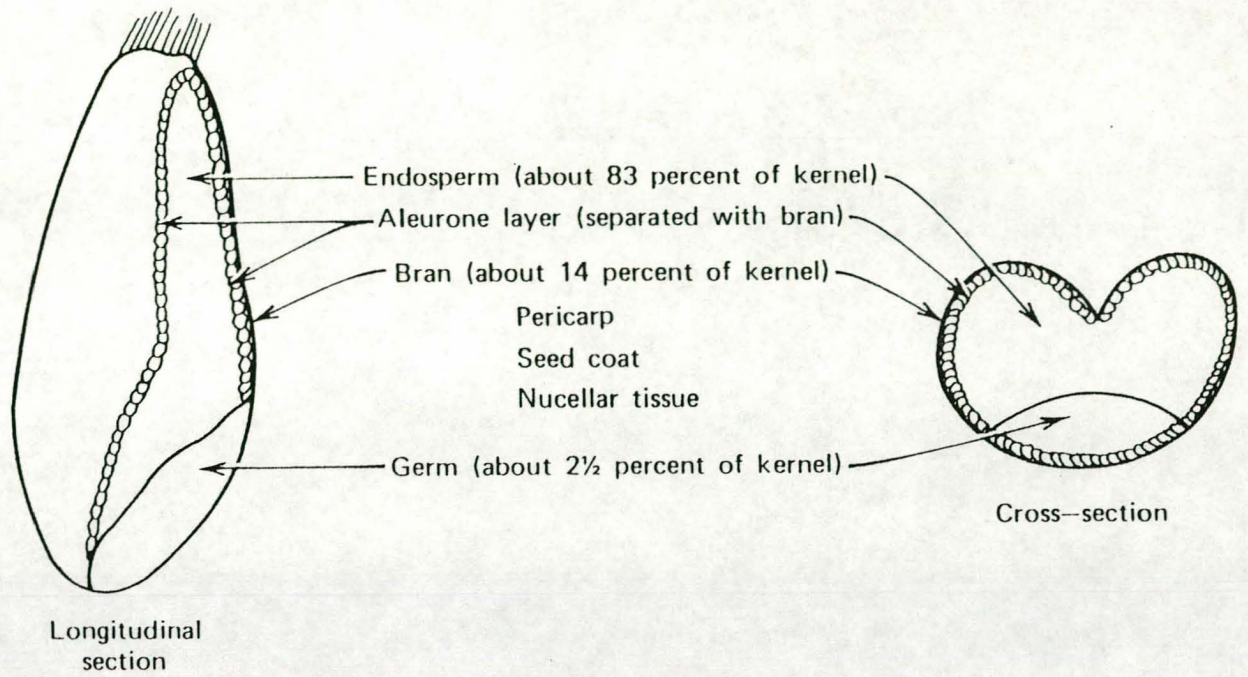


**Figure 10.** A diagram of the structure of a wheat kernel (Hoseney, 1994).

length of the ventral side (Matz, 1991; Hosenev, 1994; Kent & Evers, 1994). A multilayered pericarp surrounds the entire seed. The outer pericarp consists of remnants of thin-walled cells and is what wheat millers call the beeswing. The inner pericarp is composed of intermediate cells, cross-cells and tube cells. The total pericarp comprises about 5% of the kernel. The seed coat is firmly joined to the tube cells on the outside and the nucellar epidermis on the inside. It consists of three layers: a thick outer cuticle; a layer that contains pigments; and a thin inner cuticle.

The aleuronlayer is generally one cell thick and completely surrounds the kernel, covering both the starchy endosperm and the germ (Matz, 1991; Hosenev, 1994). The aleuron cells are thick walled, cube-shaped and starch-free. The germ comprises about 2.5 - 3.5% of the kernel and is composed of two major parts – the embryonic axis, and the scutellum which functions as a storage organ (Hosenev, 1994).

The endosperm is composed of three types of cells: peripheral; prismatic; and central (Matz, 1991; Hosenev, 1994). The peripheral cells are the first row of small cells inside the aleuronlayer. Several rows of elongated prismatic cells follow with the central cells being inside the prismatic cells and having irregular shapes and sizes. The content and cell walls of the endosperm make up flour. The endosperm is packed with starch cells imbedded in a protein matrix. The protein is mainly gluten, the storage proteins of wheat (Hosenev, 1994). In maturing wheat the gluten is synthesized in protein bodies, but as the wheat grows mature the protein bodies are compressed together in a matrix that appears mud or clay-like. The starch granules occur mainly as large lenticular granules and as small spherical granules.

There are thousands of known species and varieties of the genus *Triticum* (wheat), the principle wheats of commerce being varieties of the species of *T.aestivum*, *T. durum* and *T. compactum* (Kent & Evers, 1994). These species can be classified in various ways (Shellenberger, 1964). Hackel (1890) grouped them together, based upon their plant botany, into *vulgare* (common wheat or bread wheat), *durum* (Durum wheat), *compactum* (Club wheat), *turgidum* (Pollard wheat), *dicoccum* (Emmer), *spelta* (Spelt), *plonicum* (Polish wheat) and *dicoccum* (Einkorn). For commercial purposes, however, wheat must be classified by properties other

than botanical features. The major distinguishing factors are grain hardness or softness, winter or spring habit, red or white bran and protein content (Kent & Evers, 1994). Grain texture (hardness or softness) is the most important of these distinguishing factors because of its importance in the milling procedure and the end-use properties of the wheat.

## **B 2. Definition and significance**

Despite its importance there is no clear definition of kernel hardness. Anjum & Walker (1991) describe it as "the resistance to fracture upon grinding, slicing, abrasion, or indentation of a single kernel or bulk samples". Other definition includes "not easily penetrated or separated into parts" and "difficult to penetrate or separate into fragments". Softness of wheats, again, is defined as "easily disintegrating under stress" (Pomeranz & Williams, 1990). True wheat hardness is under strong genetic control by one or two major genes (Symes, 1965; Carver, 1994) and should not be confused with vitreous wheat. Vitreous wheat has a glass-like nature and is not genetically controlled, but is strongly influenced by environmental factors such as high temperatures and nitrogen availability during the maturing phase of development (Pomeranz & Williams, 1990).

It would appear through studies done by Barlow *et al.* (1973) and Simmonds *et al.* (1973) that differences in hardness between different wheat varieties are a result of differences in the strength of the adhesion between starch granules and storage proteins in the endosperm. They concluded that there is a high adhesion between starch and protein in hard wheats, causing a higher degree of fractures to occur through starch granules than at the interface between the starch and protein than is the case with soft wheats (Kent & Evers, 1994). The nature of the protein-starch bond is not known (Hoseney, 1994). However, the fact that protein and starch can be easily separated from each other after treatment of flour with water seems to indicate that the bond is broken or weakened by water. Research work has also shown that hard wheat contains a specific water soluble protein at the protein-starch interface that soft wheat do not contain (Hoseney, 1994).

Wheat hardness is of great significance in determining the quality of wheat. It affects the way in which wheat must be tempered for milling, the yield and particle size, shape and density of flour particles, the end-use properties in milling and the production of bread, soft wheat products and noodles (Kent & Evers, 1994; Ohm *et al.*, 1998).

Before milling wheat it is customary to temper it, in other words water is added to the dry grain after which it is allowed to rest for a period of time (Pomeranz & Williams, 1990; Larsen, 1970; Pomeranz *et al.*, 1984). Reducing hard wheat to flour requires more work than is the case with soft wheats, resulting in the starch being more damaged. Wheat texture influences the tempering process in that soft wheats absorb water faster due to cavities in their endosperm, thus needing a shorter tempering time than hard wheat.

Hard wheat and soft wheat mill differently and therefore yield flour particles with different characteristics. Fragmentations of the endosperm of hard wheats occur at cell boundaries, a weak point in the kernel, while the endosperm of soft wheats fractures in a random way (Hoseney *et al.*, 1988). Varieties of hard wheat yield coarse, gritty flour that is easily sifted. The flour consists of regular-shaped particles, many of which are single, or groups of, endosperm cells (Kent & Evers, 1994). Soft wheat varieties yield very fine flour that sieves poorly and consists of irregular-shaped fragments of endosperm cells.

The flour yield of wheat can be related to the way in which wheat fractures. Hard wheat cultivars fracture in such a way that the endosperm is more readily separated from the bran, resulting in a higher flour yield (Kent & Evers, 1994).

Wheat texture influences the end-use of flour through the effect it has on particle size and water absorption. The granular, starch-damaged flour formed by hard wheat varieties is of a higher milling and bread making quality than the flour of soft wheat (Carver, 1994). A high level of starch damage is desirable, because it increases the water absorption of the dough (Pomeranz & Williams, 1990). High water absorption is economic for the baker and important for crumb softness and bread keeping characteristics (Ohm *et al.*, 1998). The flour of soft wheat cultivars is

usually not suited for bread-making, but rather for biscuit-making (Carver, 1994; Pomeranz & Williams, 1990).

### **B 3. Intrinsic factors influencing wheat hardness**

The most important factor that governs the hardness of wheat is its genotype. Other factors that are also of great importance are the environment (growing location and season), protein content, moisture content, temperature and kernel size (Pomeranz & Williams, 1990).

#### *Genotype*

The differences in hardness between different classes of wheats is generally controlled by one major gene, *Ha*, situated on the 5 D chromosome (Carver, 1994; Kent & Evers, 1994). This gene controls the strength of the association between protein and starch in the endosperm which causes hardness of wheat.

#### *Environment*

The most important environmental factor affecting wheat hardness is the soil, and more specifically its moisture-holding capacity and available nitrogen and phosphorus. Studies show that if a specific wheat cultivar is grown in different locations with different soil types, there is indeed a variance in hardness (Aamodt & Torrie, 1935; Williams & Sobering, 1984). The heritability of texture is very strong relative to the environmental effect (Briggle *et al.*, 1968; Pomeranz & Williams, 1990).

Growing season influences protein content, kernel size and density as well as kernel texture (Moss, 1978; Pomeranz & Williams, 1990; Williams & Sobering, 1984). The magnitude of the differences in texture of wheat due to different seasons is of the same order as that due to different locations, the variance due to genotype still being far greater (Moss, 1978).

### *Protein content*

There is some disagreement on whether there is any relation between wheat hardness and protein content (Pomeranz & Williams, 1990). Some of the conflicting results can be explained when taking into consideration that in earlier studies hardness was visually estimated according to the degree of vitreousness of the kernels. While hardness does not seem to have any relation to protein, studies show that more vitreous kernels have a higher protein content (Miller *et al.*, 1982; Pomeranz & Williams, 1990).

### *Moisture content and temperature*

Moisture content has an indirect effect on texture in that methods of measuring wheat texture are influenced by the variation of moisture content within the sample set (Pomeranz & Williams, 1990).

### *Kernel size*

Large kernels requires more pressure to break and might give a false high hardness reading when such methods as crushing are implemented. It does, however, not affect measurement which involve grinding of bulk samples (Pomeranz & Williams, 1990).

## **B 4. Methods for measuring wheat hardness**

The measuring of wheat hardness dates back to the work of Cobb in the late 19<sup>th</sup> century (1896). He measured the force needed to "bite" a kernel in two and he was the first to apply a numerical figure to wheat kernel texture. At present there are more than a hundred different ways in which to measure wheat hardness (Cutler & Brinson, 1939; Hosney, 1987; Pomeranz & Williams, 1990; Williams, 1991; Gaines *et al.*, 1996). The absolute hardness of wheat is, however, difficult to measure due to the non-uniform shape of the grains. Therefore the majority of methods measure how the grain breaks rather than the absolute hardness. Most of these methods



evaluate hardness-related phenomena by measuring some property of the wheat during or after grinding (Hoseney *et al.*, 1988; Norris *et al.*, 1989).

Methods evaluating wheat whilst grinding include those measuring abrasion, work to grind and time to grind. Hard wheats grind much faster, but require more energy than do soft wheats (Hoseney *et al.*, 1988). The pearling index indicates how much of the surface of the kernel is abraded in a pearler, hard wheats being more resistant than soft wheats (Hoseney, 1987).

The single kernel characteristic system (SKCS) has recently been developed for classifying wheat and has showed potential for determining wheat quality parameters such as moisture, test weight and kernel hardness (Martin, 1993; Bechtel *et al.*, 1996; Gaines *et al.*, 1996; Ohm *et al.*, 1998). The SKCS is designed to isolate and weigh individual kernels and crushing them between a toothed rotor while progressively narrowing the crescent-shaped gap (Gaines *et al.*, 1996, Ohm *et al.*, 1998). This information is algorithmically processed to provide a hardness-index for each sample based on its kernel-crush profile, moisture, size and weight.

Those methods of determining kernel hardness by measuring a property after grinding usually measure some aspect of the resulting particle size distribution, hard wheats having larger mean particle sizes than soft wheats (Norris *et al.*, 1989). The most common method of this type is the particle size index (PSI). In the last decade radiation scattering properties have been used to define hardness or softness by means of near infrared reflectance as well as transmittance spectroscopy (Norris *et al.*, 1989; Williams, 1991).

#### *The particle size index (PSI) hardness test*

The majority of methods that test wheat hardness are grinding/sieving tests, most of which are modifications of the particle size index (PSI) method developed by Cutler & Brinson (1939) (Williams & Sobering, 1986a). This method is very precise, but time consuming, and involves the grinding of a bulk sample of wheat into flour after which it is sieved and the throughs weighed. This information is related to relative hardness in that the harder the wheat, the higher its mean particle size, and the lower the weight of the sifted flour.

### *NIR spectroscopy*

Near infrared (NIR) reflectance spectroscopy is capable of differentiating between wheats of different hardness because of its sensitivity to variation in particle size and particle size distribution (Pomeranz & Williams, 1990). The logarithm of the reciprocal of reflectance ( $\log 1/R$ ) at any point in the NIR spectrum increases with increasing particle size (Norris *et al.*, 1989). This technique was first applied by Sauer (1978). Today it is recognised as a reliable, rapid and easily standardisable technique for the measurement of wheat hardness (Osborne & Fearn, 1983; Williams & Sobering, 1986b; Hong *et al.*, 1989; Norris *et al.*, 1989; Williams, 1991; Delwiche & Norris, 1993, Delwiche *et al.*, 1995; Manley, 1995).

Delwiche & Norris (1993) classified hard red wheat by means of NIR diffuse reflectance spectroscopy. They measured the scattering of radiation of 100 ground wheat samples comprising of winter and spring wheats collected over 4 seasons. A 5 factor principle component regression (PCR) model gave accurate results with an average misclassification of 5%. In 1995 these same samples were used to perform NIR analysis on bulk whole grain wheat samples (Delwiche *et al.*, 1995). The reflectance spectra of the samples were collected by a NIR spectrophotometer equipped with a bulk transport cell attachment. An artificial neural network (ANN) model performed better than MLR, PCA or PLS regressions in classifying wheat hardness, with accuracies in the range of 95-98%.

Williams (1991) predicted wheat hardness of whole grains using NIR transmittance. He used an Infratec NIR transmittance instrument to record the spectra and PLS regression to compute the calibrations. The accuracy of the results of this method was equal to that of the reference method (PSI test) and slightly superior to the NIR reflectance method, having a  $r$  of 0.96 and a SEP of 3.37%.

The NIR spectroscopy method for determining wheat texture can easily be standardised as demonstrated by Williams & Sobering (1986b). They used the PSI test as reference method to calibrate a DICKEY-john GACIII and a Technicon InfraAlyzer 300. Their calibrations were transferable to 21 instruments, with an average  $r$  between collaborators of 0.98 and an average SEP of 2.67%. Norris *et al.*

(1989) also obtained excellent results in their collaborative study were no reference data was used.

## **B 5. Wheat hardness in South Africa**

In South Africa wheat is divided into three classes: hard wheat (for bread-making); soft wheat (for biscuit-making); and durum wheat (for pasta-making) (Anonymous, 1999; Van Deventer, 1999). The majority of wheats form part of the hard or bread wheat class. Hardness differences within and between classes are not uncommon and are influenced mainly by genotype. Currently, in South Africa, wheat is categorised into one of the three hardness classes by means of kernel morphology and genotype (Wessels, 1999). If there is some uncertainty as to the hardness class into which the cultivar should be categorised, kernel hardness relative to that of a standard cultivar will be measured by means of flour yield before subsequent classification. As a rule, however, wheat hardness is not used in classifying South African wheat for commercial purposes and no standard method for its measurement have been established. The bread wheat class, including the majority of South African wheats, are subclassified only on the basis of protein content and hectoliter mass (Table 1). However, since the price of wheat in other wheat producing countries, such as Canada (Table 2), is based on a sub-classification system that includes kernel hardness as a parameter, determining kernel hardness will become important in the new free market system in South Africa (Norris *et al.*, 1989; Delwiche & Norris, 1993; Van Deventer, 1999).

## **C. ELECTRON MICROSCOPY**

Electron microscopes refer to a family of instruments that produce magnified images by the use of electrostatic or electromagnetic lenses with fast-moving electrons as illumination. They give images of very high resolution over a very useful depth of field (Goldstein *et al.*, 1992; Watt, 1997). Transmission electron microscopy (TEM)

**Table 1.** The bread wheat sub-classification system currently used in South Africa (Wessels, 1999).

<b>Class B (bread wheat)</b>									
	<b>BP</b>			<b>BS</b>			<b>BL</b>		
<b>Protein (%)</b>	≥ 12			10-12			≤ 10		
	<b>BPS</b>	<b>BP1</b>	<b>BP2</b>	<b>BSS</b>	<b>BS1</b>	<b>BS2</b>	<b>BLS</b>	<b>BL1</b>	<b>BL2</b>
<b>Minimum hectoliter mass (kg)</b>	≥ 79	≥ 76	≥ 74	≥ 79	≥ 76	≥ 74	≥ 79	≥ 76	≥ 74

**Table 2.** The bread wheat sub-classification system currently used in Canada (Williams, 1999).

	<b>Sub-classes</b>	<b>PSI hardness value (%)</b>
<b>Bread wheat class</b>	Western extra strong	47 - 52
	Hard red spring	56 - 60
	Hard red winter	55 - 60
	Prairie red spring	57 - 61
	Prairie white spring	56 - 62

looks directly at the internal structure of the translucent specimen and use shorter wavelength electron illumination than scanning electron microscopy (SEM), which is used to study the outside features of bulk material.

### **C 1. Transmission electron microscopy (TEM)**

The simplest transmission electron microscope has two image forming lenses and is an exact analogy of the compound light microscope (Figure 11). An electron gun provides illumination that is concentrated on the specimen by a condenser lens (Watt, 1997). After the electrons passed through the specimen they are focussed by the objective lens into a magnified intermediate image. This image is then further enlarged by a projector lens and the final image is formed on a florescent screen or a photographic film.

Such a two-stage transmission electron microscope would have a magnification of about 10 000 times and a resolution of down to 5 nm (Watt, 1997). Additional magnification and higher resolution can be obtained by adding further imaging lenses. Presently there are several microscopes employing six imaging lenses that achieve magnification of up to 1 000 000 times and resolutions of fractions of nanometers (Watt, 1997).

### **C 2. Scanning electron microscopy (SEM)**

A fine probe of electrons is focussed at the surface of the specimen and scanned across it in a pattern of parallel lines (Goldstein *et al.*, 1992; Watt, 1997). A number of interactions can take place between the electron beam and the specimen leading to a wealth of information, schematically summarized in Figure 12. Signals due to electrons of radiation can be collected for every position of the incident electron probe. The signal is then amplified and used to vary the brightness of the trace on the cathode-ray tube that is being scanned in synchronism with the probe. The

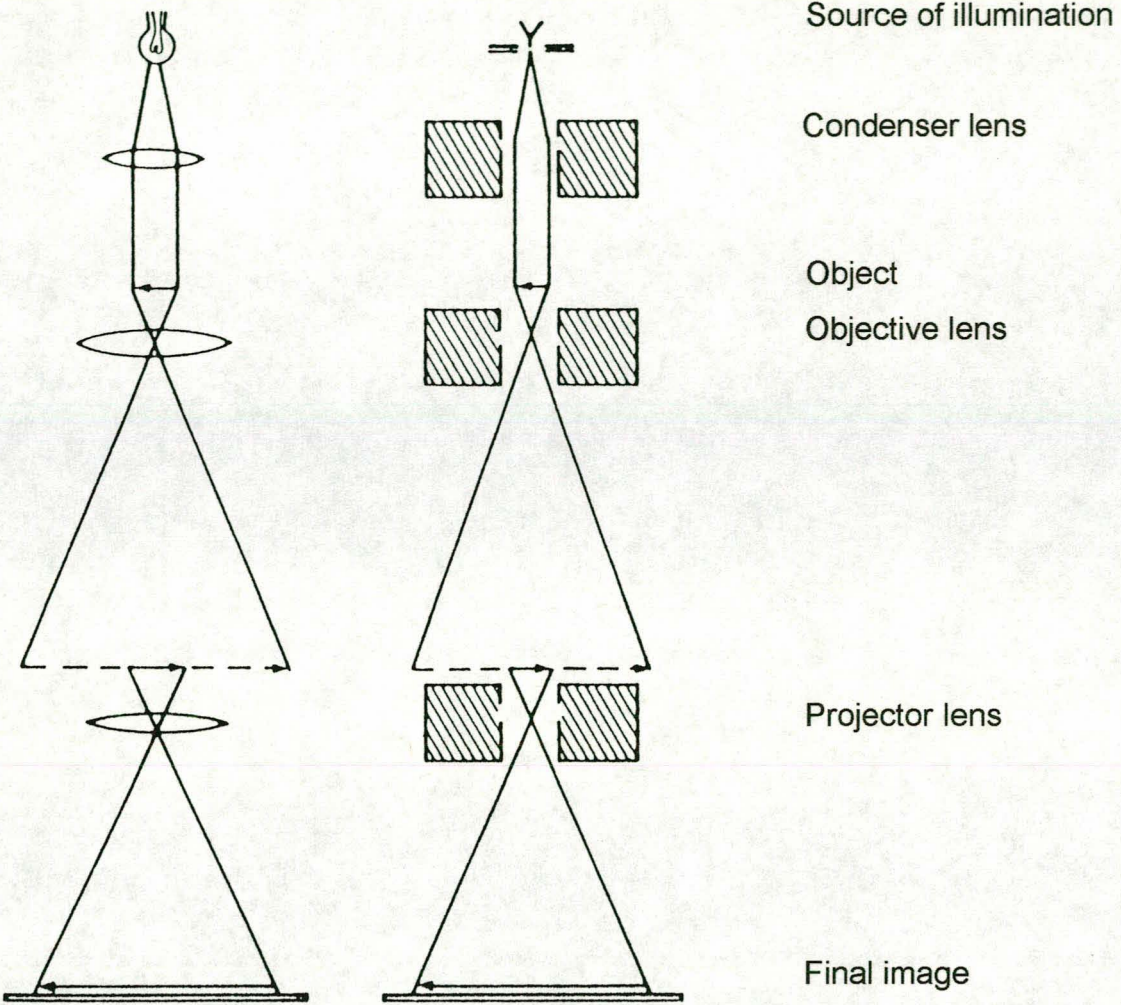


**Figure 11.** Light microscope and equivalent two-stage electron microscope (Watt, 1997).

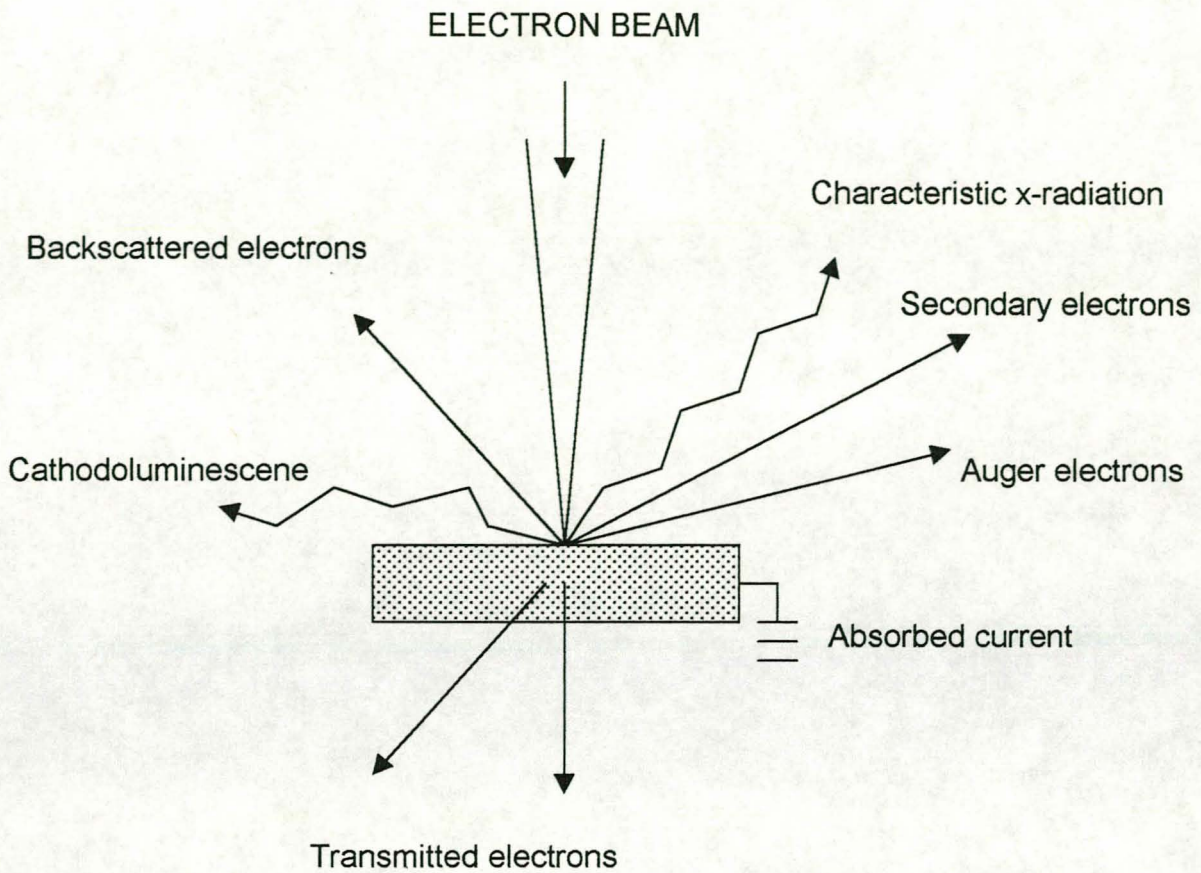


**Figure 12.** Schematic representation of the possible interactions between the electron and the specimen in an electron microscope.

magnification achieved is the ratio between the dimensions of the final image display and the field scanned on the specimen and can be up to 200 000 times (Watt, 1997).

### **C 3. Electron microscopy and wheat hardness**

Wheat hardness is determined by the strength of the adhesion between starch and protein molecules in the endosperm and in return determines the way in which the grain will fracture upon grinding (Barlow *et al.*, 1973; Kent & Evers, 1994). Electron microscopy can be an affective technique in determining hardness-related differences in the structure of the endosperm of whole and ground wheat (Barlow *et al.*, 1973, Hosenev & Seib, 1973; Moss *et al.*, 1980; Davis & Eustage, 1984; Glenn & Saunders, 1990; Freeman & Shelton, 1991). Hard wheats will reveal breakage at the cell walls and soft wheats will reveal breakage through the cells of the endosperm. Furthermore, the cells of the endosperm of hard wheats are packed more tightly and their cell walls are thicker than in soft wheats (Hosenev, 1994).

Scanning electron microscopy is preferred over light microscopy used in the past because of the great depth of focus available. The depth of focus afforded to the scanning electron microscope is 300 times that of the light microscope at equivalent magnifications (Evers, 1969). Furthermore light microscopy requires the use of an aqueous media, causes swelling of especially the protein molecules, giving the false impression of a very compact endosperm structure. The SEM does not need an aqueous medium and is therefore extremely useful in studying wheat structure (Moss *et al.*, 1980).

## **D. DISCUSSION**

Fourier transform near infrared analysis is a quantitative and/or qualitative method by which the concentration or a physical characteristic of a specific sample is related to the spectral data collected for that sample by means of a calibration model. This method is especially advantageous for the routine analysis of samples where the



existing method is time-consuming or involves the use of expensive reactants. It is a simple, precise, non-destructive method by which multiple analysis can be done in one operation and the results are achieved within 10 seconds to three minutes.

Many studies have been done on the determination of wheat hardness. Wheat hardness is defined as "not easily penetrated or separated into fragments" and it is of great significance in determining the quality and end-use properties of wheat. Currently South African wheats are classified only according to protein content and hectoliter mass. Wheat is not yet categorised or classified according to hardness and no standard method of determining hardness has been established in South Africa. Since the price of wheat in other wheat-producing countries are based on class where hardness is a parameter, establishing a method to determine hardness accurately may become essential in the new free market system in South Africa.

Methods of determining wheat texture other than NIR spectroscopy include the methods where the force needed to 'bite' the kernel is measured, the pearling test and the particle size index (PSI) test. These methods are, however, not ideal because most of them rather measure how the grain breaks than the absolute hardness, or they are time consuming. Near infrared or Fourier transform near infrared spectroscopy therefore seems to be the modern method of choice because of its speed and accuracy in using radiation scattering properties to define wheat texture. Electron microscopy can provide further useful information on hardness-related differences in the structure of the wheat endosperm.

## E. REFERENCES

- Aamodt, O.S. & Torrie, J.H. (1935). Studies on the inheritance of and the relationship between kernel texture and protein content in several spring wheat crosses. *Canadian Journal of Research. Section C, Botanical Sciences*, **13**, 79-88 (as cited by Pomeranz & Williams, 1990).
- Abney, W. & Festing, E.R. (1881). On the influence of the atomic grouping in the molecules of organic bodies on their absorption in the infrared region of the spectrum. *Philosophical Transactions of the Royal Society*, **172**, 887-918.
- Anjum, F.M. & Walker, C.E. (1991). Review on the significance of starch and protein to wheat kernel hardness. *Journal of the Science of Food and Agriculture*, **56**, 1-13.
- Anonymous. (1997a). *McGraw-Hill Encyclopedia of Science and Technology* (5<sup>th</sup> edition). Vol. 5. Pp. 184-185. USA: McGraw-Hill Inc.
- Anonymous. (1997b). *Spectrum QUANT+ User's Reference*. The Perkin-Elmer Corporation. Beaconsfield, UK: Technical Publishers.
- Anonymous (1999). Prysdiiferensieringsfaktore. *Graan/Grain Gazette*, April 1999, 6-10.
- Barlow, K.K., Buttrose, M.S., Simmonds, D.H. & Vesk, M. (1973). The nature of the starch-protein interface in wheat endosperm. *Cereal Chemistry*, **50**, 443-454.
- Beebe, K.R. & Kowalski, B.R. (1987). An introduction to multivariate calibration analysis. *Analytical Chemistry*, **59**, 1007-1017.
- Bechtel, D.B., Wilson, J.D. & Martin, C.R. (1996). Determining endosperm texture of developing hard and soft red winter wheats dried by different methods using the single-kernel wheat characterization system. *Cereal Chemistry*, **73**, 567-570.
- Bradley, E.B. (1986). Introduction to spectroscopic methods. In: *Instrumental Analysis* (edited by G.D. Christian & J.E. O'Reilly). Pp. 144-157. Massachusetts, USA: Allyn and Bacon Inc.
- Briggle, L.W., Yamazaki, W.T. & Hansen, J.D. (1968). Heritability of three quality characteristics in the F2 and F3 generations. *Crop Science*, **8**, 283-285.

- Carver, B.F. (1994). Genetic implications of kernel NIR hardness on milling and flour quality in bread wheat. *Journal of the Science of Food and Agriculture*, **65**, 125-132.
- Ciurczak, E.W. (1992). Principles of near-infrared spectroscopy. In: *Handbook of Near Infrared Analysis* (edited by D.A. Burns & E.W. Ciurczak). Pp. 7-8. New York, USA: Marcel Dekker Inc.
- Cobb, N.A. (1896). The hardness of grain in the principle varieties of wheat. *Agricultural Gazette N.S.W.*, **7**, 279-299 (as cited by Pomeranz & Williams, 1990).
- Coblentz, W.W. (1905). Investigations of infrared absorption spectra, part I. Publication No. 35, Washington: Carnegie Institute of Washington.
- Cutler, G.H. & Brinson, G.A. (1939). The granulation of wholemeal and a method of expressing it numerically. *Cereal Chemistry*, **12**, 120.
- Davis, A.B. & Eustage, W.D. (1984). Scanning electron microscope views of material from various stages in the milling of hard red winter, soft red winter and durum wheat. *Cereal Chemistry*, **61**, 182-186.
- Delwiche, R. & Norris, K.H. (1993). Classification of hard red wheat by near-infrared diffuse reflectance spectroscopy. *Cereal Chemistry*, **70**, 29-35.
- Delwiche, R., Chen, Y. & Hruschka, W.R. (1995). Differentiation of hard red wheat by near infrared analysis of bulk samples. *Cereal Chemistry*, **72**, 243-247.
- Ellis, J.W. & Bath, J. (1938). Modifications in near-infrared spectra of natural and synthetic fibres. *Journal of Chemistry and Physics*, **6**, 723-729.
- Evers, A.D. (1969). Scanning electron microscopy of wheat starch. *Die Stärke*, **4**, 96-99.
- Freeman, T.P. & Shelton, D.R. (1991). Microstructure of wheat starch: from kernel to bread, *Food Technology*, **45**, 164-168.
- Gaines, C.S., Finney, P.F., Fleege, L.M. & Andrews, L.C. (1996). Predicting a wheat hardness measurement using the single-kernel characterization system. *Cereal Chemistry*, **73**, 278-283.
- Garcia-Jares, C.M. & Medina, B. (1997). Application of multivariate calibration to the simultaneous routine determination of ethanol, glycerol, fructose, glucose and

- total residual sugars in botrytized-grape sweet wines by means of near infrared spectroscopy. *Fresenius Journal of Analytical Chemistry*, **357**, 86-91.
- Glenn, G.M. & Saunders, R.M. (1990). Physical and structural properties of wheat endosperm associated with grain texture. *Cereal Chemistry*, **67**, 176-182.
- Goldstein, J.I., Newbury, D.E., Echlin, P., Joy, D.C., Romig, A.D., Lyman, C.E., Fiori, C. & Lifshin, E. (1992). Electron optics. In: *Scanning Electron Microscopy and X-ray Microanalysis, 2<sup>nd</sup> edition*. Pp. 21-67. New York, USA: Plenum Press.
- Griffiths, P.R. & de Haseth, J.A. (1986). Foreword. In: *Fourier Transform Infrared Spectrometry*. Pp. v-vii. Canada: John Wiley and Sons Inc.
- Hackel, E. (1890). *The true Grassia*. New York, USA: Henry Holt and Co. (as cited by Shellenberger, 1964).
- Herschel, F.W. (1800). Investigation of the power of the prismic colours to heat and illuminate objects; with remarks that prove the different refrangibility of radiant heat. To which is added, an inquiry into the method of viewing the sun advantageously with telescopes of large apertures and high magnifying powers. *Philosophical Transactions of the Royal Society*, **90**, 255-283.
- Hong, B.H., Rubenthaler, G.L. & Allan, R.E. (1989). Wheat pentosans. II. Estimating kernel hardness and pentosans in water extracts by near infrared reflectance. *Cereal Chemistry*, **66**, 374-377.
- Honings, D.E. (1985). Near infrared analysis. *Analytical Instrumentation*, **1**, 22-24.
- Hoseney, R.C. (1987). Wheat hardness. *Cereal Foods World*, **32**, 320-322.
- Hoseney, R.C. (1994). *Principles of Cereal Science and Technology* (2<sup>nd</sup> edition). Pp. 6-12. Minnesota, USA: American Association of Cereal Chemists Inc.
- Hoseney, R.C. & Seib, P.A. (1973). Structural differences in hard and soft wheat. *The Bakers Digest*, **47**, 26-28,56.
- Hoseney, R.C., Wade, P. & Finley, J.W. (1988). Soft wheat products. In: *Wheat Chemistry and Technology Volume II* (3<sup>rd</sup> edition) (edited by Y. Pomeranz). Pp. 407-456. Minnesota, USA: American Association of Cereal Chemists Inc.
- Howard, A., Leake, H.M. & Howard, G.L.C. (1913). The influence of the environment on the milling and baking qualities of wheat in India. No.2. The experiments of

- 1909-10 and 1910-11. *Memoirs of the Department of Agriculture of India*, **5**, 49-103 (as cited by Pomeranz & Williams, 1990).
- Hunt, W.H., Fulk, D.W., Elder, B. & Norris, K. (1977). Collaborative study on infrared reflectance devices for the determination of protein in hard red winter wheat and for protein and oil in soybeans. *Cereal Foods World*, **22**, 143-144.
- Kent, N. L. & Evers, A.D. (1994). *Kent's Technology of Cereals* (4<sup>th</sup> edition). Pp. 1-5, 78-82. Oxford, UK: Elsevier Science Ltd.
- Kincaid, J.R. (1986). Infrared and raman spectrometry. In: *Instrumental Analysis* (2<sup>nd</sup> edition) (edited by G.D. Christian & J.E. O'Reilly). Pp. 228-233. Newton, USA: Allyn and Bacon Inc.
- Larsen, R.A. (1970). Milling. In: *Cereal Technology* (edited by S.A. Matz). Pp. 1-43. Connecticut, USA: The AVI Publishing Company Inc.
- Manley, M. (1995). *Wheat hardness by near infrared (NIR) spectroscopy: New insights*, PhD. Thesis, University of Plymouth, United Kingdom.
- Martin, K.A. (1992). Quantitative analysis. In: *Recent Advances in Near Infrared Reflectance Spectroscopy*. Pp. 337-343. New York, USA: Marcel Dekker Inc.
- Martin, C.R., Rousser, R. & Brabec, D.L. (1993). Development of a single-kernel wheat characterization system. *Transactions of the ASAE*, **36**, 1399-1404 (as cited by Betchel et al., 1996).
- Matz, S.A. (1991). Botany of the wheat plant. In: *The chemistry and Technology of Cereals as Food and Feed* (2<sup>nd</sup> edition). Pp. 6-16. New York, USA: Van Nostrend Reinhold/AVI.
- Miclone, V.A., Abe, H. & Kawano, S. (1997). Kiwifruit firmness by near infrared scattering. *Journal of Near Infrared Spectroscopy*, **5**, 83-89.
- Miller, B.S., Afework, S., Pomeranz, Y. & Bolte, I. (1982). Die relative Kornharte von "Dark Hard" und "Yellow Hard" winterweizen. *Getreide Mehl Brot*, **36**, 114-117.
- Moss, R., Stenvert, N.L., Kingswood, K. & Pointing, G. (1980). The relationship between wheat microstructure and flourmilling. *Scanning Electron Microscopy*, **3**, 613-620.
- Murray, I. (1988). Aspects of the interpretation of near infrared spectra. *Food Science and Technology Today*, **2**, 135-139.

- Næs, T. & Isaksson (1991). Multicollinearity and the need for data reduction. *NIR News*, **2**, 10-11.
- Norris, K.H. (1964). Reports on the design and development of a new moisture meter. *Agricultural Engineers*, **45**, 370-372.
- Norris, K.H., Hruschka, W.R., Bean, M.M. & Slaughter, D.C. (1989). A definition of wheat hardness using near infrared reflectance spectroscopy. *Cereal Foods World*, **34**, 696-704.
- Ohm, J.B., Chung, O.K. & Deyoe, C.W. (1998). Single-kernel characteristics of hard winter wheats in relation to milling and baking quality. *Cereal Chemistry*, **75**, 156-161.
- Osborne, B.G. (1981). Principles and practice of near infra-red (NIR) reflectance analysis. *Journal of Food Technology*, **16**, 13-19.
- Osborne, B.G. & Fearn, T. (1983). Collaborative evaluation of near infrared reflectance analysis for the determination of protein, moisture, and hardness in wheat. *Journal of the Science of Food and Agriculture*, **34**, 1011-1017.
- Osborne, B.G. & Fearn, T. & Hindle, P.H. (1993). *Practical NIR Spectroscopy with Practical Applications in Food and Beverage Analysis (2<sup>nd</sup> edition)*. Pp. 1-17, 13-14, 16-22, 36-47, 49-51, 67-71. Essex, UK: Longman Group UK Limited.
- Peiris, K.H., Dull, G.D., Leffler, R.G. & Kays, S.J. (1997). Nondestructive determination of soluble solids content of peach by near infrared spectroscopy. *Proceedings from the sensors for nondestructive testing international conference and tour, Orlando Florida*. (NRAES-97: Northeast Regional Agricultural Engineer Service Cooperative Extension).
- Penner, M.H. (1994). Basic principles of spectrometry. In: *Introduction to Chemical Analysis of Foods* (edited by S.S. Nielsen). Pp. 317-324. Boston, USA: Jones and Bartlett Publishers.
- Percival, J. (1921). *The wheat plant*. UK: John Duckworth and Co. (as cited by Pomeranz & Williams, 1990).
- Pomeranz, Y., Bolling, H. & Zwingelberg, H. (1984). Wheat hardness and baking properties of wheat flours. *Journal of Cereal Science*, **2**, 137-143.

- Pomeranz, Y. & Williams, P.C. (1990). Wheat hardness: its genetic, structural, and biochemical background, measurement, and significance. In: *Advances in Cereal Science and Technology* (edited by Y. Pomeranz). Pp. 471-548. Minnesota, USA: American Association of Cereal Chemist Inc.
- Rodriguez-Otero, J.L. & Hermida, M. (1995). Analysis of fermented milk products by near infrared reflectance spectroscopy. *Journal of the AOAC*, **79**, 817-821.
- Rodriguez-Otero, J.L., Centro, J.A. & Hermida, M. (1997). Application of near infrared transfectance spectroscopy to the analysis of fermented milks. *Milchwissenschaft*, **52**, 196-200.
- Sauer, W. (1975). Frühzeitige erfassung von qualitätsmerkmalen als grundlage für eine wirkungsvolle selektion in der weizenzüchtung. I. Bestimmung der mechanisch besschädigten stärke als Mass für kornhärte und wasseraufnahme. *Muehle Mischfuetter techn.*, **11**, 521-522 (as cited by Pomeranz & Williams, 1990).
- Shellenberger, J.A. (1964). Production and utilization of wheat. In: *Wheat Chemistry and Technology* (edited by I. Hlynka). Pp. 1-12. Minnesota, USA: American Association of Cereal Chemist Inc.
- Simmonds, D.H., Barlow, R.R. & Wrigley, C.W. (1973). The biochemical basis of grain hardness in wheat. *Cereal Chemistry*, **50**, 553-562.
- Symes, K.J. (1965). The inheritance of grain hardness in wheat as measured by the particle size index. *Australian Journal of Agricultural Resources*, **16**, 113-123 (as cited by Pomeranz & Williams, 1990).
- Tissue, B.M. (1996). *Near-infrared absorption spectroscopy (NIR)*. <http://www.scimedia.com/chem-ed/spec/vib/nir.htm> (August, 1997).
- Van Deventer, C.S. (1999). Koringbedryf moet kyk na nuwe klassifikasiestelsel. *Lanbouweekblad*, **1098**, 10-13.
- Watt, I.M. (1997). The electron microscope family. In: *The Principles and Practice of Electron Microscopy*, 2<sup>nd</sup> edition. Pp. 59-135. Cambridge, UK: Cambridge University Press.

- Wehling, R.L. (1994). Infrared spectrometry. In: *Introduction to the Chemical Analysis of Foods* (edited by S.S. Nielsen). Pp. 344, 350. Boston, USA: Jones and Bartlett Publishers.
- Wessels, A. (1999). Personal communication. Manager of product quality and development. Pioneer Food Group Ltd., Cape Town, South Africa.
- Wetzel, D.L.B. (1998). Analytical near infrared spectroscopy. In: *Instrumental Methods in Food and Beverage Analysis* (edited by D.L.B. Wetzel & G. Charalambous). Pp. 141-195. New York, USA: Elsevier.
- Williams, P.C. (1991). Prediction of wheat kernel texture in whole grains by near infrared transmittance. *Cereal Chemistry*, **68**, 112-114.
- Williams, P.C. & Sobering, D.C. (1984). Influence of variables on wheat hardness. *Cereal Foods World*, **29**, 498.
- Williams, P.C. (1999). Personal communication. Grain Research Laboratory. Canadian Grain Commission, Canada.
- Williams, P.C. & Sobering, D.C. (1986a). Attempts at standardization of hardness testing of wheat. I. The grinding / sieving (Particle Size Index) method. *Cereal Foods World*, **31**, 359-364.
- Williams, P.C. & Sobering, D.C. (1986b). Attempts at standardization of hardness testing of wheat. II. The near infrared reflectance method. *Cereal Foods World*, **31**, 417-420.
- Williams, P.C. & Stevenson, S.G. (1990). Near-infrared reflectance analysis: Food industry applications. *Trends in Food Science and Technology*, **1**, 44-48.
- Workman, J.J. (1992). NIR spectroscopy calibration. basics. In: *Handbook of Near Infrared Analysis* (edited by D.A. Burns & E.W. Ciurczak). Pp. 247-280. New York, USA: Marcel Dekker Inc.
- Workman, J.J. & Burns, D.A. (1992). Commercial NIR instrumentation. In: *Handbook of Near Infrared Analysis* (edited by D.A. Burns & E.W. Ciurczak). Pp. 37-52. New York, USA: Marcel Dekker Inc.



## Chapter 3

Using different sample holders in determining protein and moisture content in whole wheat flour by means of Fourier transform near infrared (FT-NIR) spectroscopy



## Chapter 3

# USING DIFFERENT SAMPLE HOLDERS IN DETERMINING PROTEIN AND MOISTURE CONTENT IN WHOLE WHEAT FLOUR BY MEANS OF FOURIER TRANSFORM NEAR INFRARED (FT-NIR) SPECTROSCOPY

### Summary

A Fourier transform near infrared (FT-NIR) spectrophotometer was used to record the spectra of 92 whole wheat flour samples presented in three different sample holders. The conventional sample cup with a sapphire-glass base (provided with the spectrophotometer), borosilicate-glass vials and soda-glass vials were used. Calibrations were derived for protein and moisture content, respectively, of whole wheat flour by performing partial least square (PLS) regression on multiplicative scatter corrected (MSC) spectra and tested using independent validation procedures. Best results were obtained with the sample set analysed in the borosilicate-glass vials. The standard error of prediction (SEP), root mean standard error of prediction (RMSEP) and the correlation coefficient ( $r$ ) were, respectively, 0.51%, 1.16% and 0.92 for the protein calibration model, and 0.15%, 0.38% and 0.94 for the moisture calibration model. The differences in spectral data due to the use of the different sample holders were investigated using correlation coefficients ( $r$ ) and maximum distances ( $d$ ). The significance of differences in prediction results was determined by performing an analysis of variance (ANOVA) on predicted protein and moisture values. Differences within each type of sample holder were also determined. All differences were found to be statistically insignificant ( $P \leq 0.05$ ).

### Keywords

Fourier transform near infrared spectroscopy, moisture, protein, sample holder

## Introduction

Near infrared (NIR) reflectance analysis is a quantitative method by which the concentration of a specific component of a sample is related to the spectral data collected for that sample by means of a calibration model (Bradley, 1986; Osborne *et al.*, 1993). This method was first applied to foodstuffs in the early 1900's by Ellis & Bath (1938). Over the years it has become an increasingly popular quantitative analytical method, finding application in a wide range of agricultural and pharmaceutical commodities (Williams & Stevenson, 1990; Osborne *et al.*, 1993; Li Yoon *et al.*, 1998). Studies on cereal and grain composition, in particular protein and moisture content of wheat and flour, have been especially widespread (Hunt *et al.*, 1977; Law & Tkachuk, 1977; Miller *et al.*, 1977; Osborne *et al.*, 1982; Osborne & Fearn, 1983a; Osborne & Fearn, 1983b; Osborne *et al.*, 1993; Delwiche, 1998).

Millers need to monitor the protein content of flour to confirm the expected composition of the grist (Osborne *et al.*, 1993). Any deviation would require a correction by adjusting the grist or the milling conditions. Decisions on blending streams for the production of a flour of a given specification can be based upon NIR determinations of, for example, protein, moisture and hardness performed on individual mill streams.

Williams *et al.* (1981) used NIR reflectance spectroscopy to derive protein calibrations for hard red wheat flours collected from three different millstreams. An individual calibration of the samples collected at each millstream was derived, as well as a combined calibration where all the samples were included using a Neotec GQA 31EL spectrophotometer. The results of the three individual flour stream calibrations were excellent with standard error of prediction (SEP) values of, respectively, 0.12%, 0.07% and 0.20%, while the results of the combined calibration were also good.

In another interesting study moisture in white flour, ground wheat and whole wheat was determined by means of near infrared reflectance spectroscopy using a single calibration (Osborne, 1987). Near infrared data of the 68 combined samples were obtained at  $5155\text{ cm}^{-1}$  (1940 nm) and  $4329\text{ cm}^{-1}$  (2310 nm) using a Technicon InfraAlyzer.300B instrument, and the

spectra were recorded using a Pacific Scientific Mk I 6350 Research Composition Analyser. The residual standard error of prediction and of calibration were 0.22% and 0.24%, respectively.

Most of these earlier studies on wheat and flour were carried out with reflectance instruments equipped with either filter wheels or tilted filters (McShane, 1989). The filter instruments have the disadvantage of a limited ability to employ different spectral regions that correspond to known absorption bands of common constituents in foodstuffs. Scanning instruments, grating monochromators or interferometers, however, is more flexible, less sensitive to matrix changes and has greater opportunities for the use of sophisticated calibration algorithms (McShane, 1989).

Sorvaniemi *et al.* (1993) used Fourier transform near infrared (FT-NIR) reflectance spectroscopy (equipped with an interferometer) to obtain protein and moisture calibrations of roller milled and commercially milled wheat flours using the Perkin Elmer FT-IR/NIR 1700X spectrophotometer. Multiplicative scatter correction (MSC) and partial least square (PLS) regression were carried out on the data. The standard error of prediction (SEP) and correlation coefficient ( $r$ ) values for the commercially milled samples were, respectively, 0.63% (dry basis) and 0.91 for the protein, and 0.19% and 0.85 for the moisture calibration model. Standard error of prediction (SEP) and  $r$  values for the roller milled samples, again, were 0.40% (dry basis) and 0.92, respectively for protein, and 0.16% and 0.97, respectively, for moisture.

The manufacturers of the Perkin Elmer Spectrum IdentiCheck FT-NIR spectrophotometer developed protein and moisture calibrations for 70 ground wheat samples by using PLS regression on second derivative spectra (Anonymous, 1997a). They achieved SEP and  $r$  values of, respectively, 0.28% and 0.98 for the protein model, and 0.49% and 0.96, respectively, for the moisture model.

When performing any NIR or FT-NIR spectroscopic analysis it is important not to overlook the importance of sample presentation. Studies showed that this can be an even more important variable than sample grinding, and that it may be necessary to do multiple measurements on the same sample to average out the variation caused by sample presentation

(Mark & Tunnel, 1995; Williams, 1992). One important sample presentation parameter is the sample holder material. Li Yoon *et al.* (1998) presented a number of pharmaceutical excipients in sample holders made from either quartz, soda-glass or clear neutral glass, to a NIR spectrophotometer. The differences in absorbance spectra arising from the use of different sample holders were quantified in terms of correlation coefficients ( $r$ ) and maximum distances ( $d$ ). They concluded that all three sample holders could be used for applications except those that are most exact in nature.

The aim of the study was to examine the influence of variation in sample holder composition on spectral absorbance and FT-NIR predicted values. The conventional sample cup provided with the spectrophotometer has a flat base of sapphire-glass and is used to present powders to the instrument. The process of emptying, cleaning and refilling it for each sample is, however, very inconvenient and time consuming. The ideal sample cup should be easy to fill, disposable, cheap and should not absorb NIR radiation. Samples were therefore also scanned in soda-glass vials and borosilicate-glass vials. The samples can be stored in these containers, placed directly on the IdentiCheck Reflectance Accessory (ICRA) unit and analysed. Should the differences inflicted by the different sample holders be statistically insignificant, the sapphire sample cup could be replaced by one of the more convenient vials.

Furthermore this study will also give insight into the accuracy with which protein and moisture content of South African wheat flour can be determined by means of the Perkin Elmer Spectrum IdentiCheck FT-NIR spectrophotometer.

## **Materials and methods**

### *Samples*

A total of 92 South African wheat samples from the 1995 and 1996 seasons were collected from different localities (Sersantsriver, Napier, Moorreesburg, Jonaskraal, Dunghye Park, Heidelberg, Boontjieskraal, Riebeeck-Wes and

Welgevallen). Thirteen different cultivars (Nantes, Dias, Palmiet, SST 16, SST 38, SST 55, SST 57, SST 65, SST 66, SST 68, Chokka, Adam Tas and Kariega) were used. The wheat samples were milled according to the Buhler Mlu method (AACC, 1983a) using the Falling Number KT-120 laboratory mill, obtaining whole wheat flour samples.

#### *Reference methods*

Protein determinations were performed in duplicate on the flour samples using a modified AACC Kjeldahl method (AACC, 1983b) and the Tecator Kjeltac System 1. A wheat flour sample (1 g) was accurately weighed into a Kjeldahl digestion tube. One selenium Kjeldahl catalyst tablet (Saarchem) and 18 ml 98% nitrogen-free sulphuric acid (Merck) were added. The sample was digested in the Tecator 1007 digestion System at 420°C for one hour, removed and allowed to cool down before 45 ml distilled water were added. A solution of 100 mg bromochresol green (BDH Chemicals Ltd) and 70 mg methyl red (Saarchem) were made up to 100 ml with methanol (B & M Scientific cc). Of this solution 12.5 ml were added to 1 l 4% boric acid (Saarchem). An erlenmeyer flask, containing 40 ml of the boric acid indicator solution, and the digestion tube containing the sample were placed in their respective positions in the Tecator 1002 Distillation Unit. Using the alkali dispenser, 85 ml of approximately 32% sodium hydroxide (Saarchem) were added to the sample, followed by distillation of the sample for 4 minutes. The content of the Erlenmeyer flask was titrated against standardised 0.2 N sulphuric acid (Merck). The same procedure was carried out for a digestion tube containing no sample to determine the blank value. The nitrogen content and the respective protein content were then calculated using equations 1 & 2.

$$\% \text{ N} = \frac{0.14 \times C \times B}{m} \quad \dots 1$$

where  $C$  = normality of sulphuric acid

$B$  = difference between titration volume of sample and titration volume of blank (ml)

$m$  = mass of sample (g)

$\% \text{ N}$  = nitrogen content

$$\% \text{ Protein} = \% \text{ N} \times 5.7 \quad \dots 2$$

Duplicate moisture determinations were performed on the flour samples according to a modified method of James (1995). The sample (5 g) was placed into a dry metal dish and dried in a Heraeus vacuum oven for 2 hours at 68 - 72°C. It was subsequently cooled down in a desiccator and the percentage moisture calculated according to equation 3.

$$\% \text{ moisture} = \frac{(w_2 - w_3)}{(w_2 - w_1)} \times 100 \quad \dots 3$$

where  $w_1$  = weight of sample before drying (g)

$w_2$  = weight of sample + metal dish before drying (g)

$w_3$  = weight of sample + metal dish after drying (g)

The standard error of laboratory (SEL) of both reference methods were determined by means of equation 4.

$$SEL = \sqrt{\frac{\sum (y_1 - y_2)^2}{2n}} \quad \dots 4$$

where  $y_1$  and  $y_2$  = values of duplicate determinations

$n$  = amount of samples analysed

### *Fourier transform near infrared measurements*

Samples were stored in air-tight vials until their spectra were recorded. Reflectance spectra of the 92 whole flour samples were recorded using the Perkin Elmer Spectrum IdentiCheck FT-NIR spectrophotometer. The IdentiCheck Reflectance Accessory (ICRA) and the Spectrum IdentiCheck Version 2.00 software programme were used. Spectra were recorded from 10 000  $\text{cm}^{-1}$  to 4000  $\text{cm}^{-1}$  at intervals of 4  $\text{cm}^{-1}$  and at a resolution of 16  $\text{cm}^{-1}$ . It is important that spectra are collected at the correct resolution. A FT-NIR spectrophotometer collects a spectrum by scanning a moving mirror to produce an optical path difference between two arms of an interferometer, creating an interferogram (Anonymous, 1997b). The farther the moving mirror scans the higher the resolution, the longer the interferogram and the finer the structure is resolved in the spectrum. By using the lowest adequate resolution you reduce the data collection time and improve the signal-to-noise ratio.

Each final spectrum was the average of 16 scans. The interleaved mode was used, where the instrument performs a series of interleaved sample and background scans, compensating for any instrument variation. The total number of data points for each spectrum was 1501 points.

The spectra of each of the 92 samples were collected with the samples being presented to the instrument in the conventional sample cup with a sapphire-glass base provided by Perkin Elmer, borosilicate-glass vials (Cromacol) and a soda-glass vials (Lasec) respectively, creating three sets of data. When the conventional sample cup was used, the cup had to be emptied, cleaned and refilled for each new sample. Care was taken to always fill it in the same way - by simply pouring the sample, followed by gentle tapping of the sample holder twice.

### *Calibration development*

Both the Spectrum Quant+ Version 4.10 software programme (provided by Perkin Elmer) and the Unscrambler Version 6.11 software programme (kindly provided by Foss Development (UK) Ltd) were used to derive the various



calibrations. Both programmes were used to ascertain the appropriate number of PLS factors to be applied and to obtain both standard error of prediction (SEP) and root mean standard error of prediction (RMSEP) values. Partial least square (PLS) regression was performed on multiplicative scatter corrected data and the resulting calibration models tested by means of independent validation. For this the sample set of 92 was divided into a calibration set, consisting of 61 samples, and a validation set, consisting of 31 samples. This procedure was followed in the case of all three data sets for both protein and moisture content. For each of the different calibrations the standard error of prediction (SEP) (equation 5), the root mean standard error of prediction (RMSEP) (equation 6), correlation coefficient ( $r$ ), bias and F-value were determined to express the accuracy of the calibration model.

$$SEP = \sqrt{\frac{\sum_{i=1}^n (\hat{y}_i - y_i - bias)^2}{n-1}} \quad \dots 5$$

where  $\hat{y}_i$  = predicted property of the  $i^{\text{th}}$  standard of the independent validation sample set

$y_i$  = actual property of the  $i^{\text{th}}$  standard

$n$  = number of spectra

$bias$  = the average differences between reference and predicted values

$$RMSEP = \sqrt{\frac{\sum_{i=1}^n (\hat{y}_i - y_i)^2}{n-1}} \quad \dots 6$$

To quantify the effect of the various sample holder compositions on the spectra, the correlation coefficient,  $r$ , and the maximum distances,  $d$ , (Li Yoon *et al.*, 1998) between the spectral data of three samples, each collected in the sapphire-glass conventional sample cup, the borosilicate-glass vial and the

soda-glass vial were calculated using, respectively, equations 7 & 8. The three samples used were known to differ significantly in their protein content and the calculations were done for both the normal absorbance spectra as well as the second derivative spectra. The second derivative spectra were obtained using the Spectrum IdentiCheck Version 2.00 software programme. Student's t-test was performed on the results to determine whether the differences were significant or not. Analysis of variance (ANOVA) was performed on the independent validation predicted protein and moisture values to determine whether there was significant differences between the validation results of the different protein and moisture models, respectively. The significance of compositional differences within the two types of vials was also examined. For both vials the same whole flour sample was presented to the spectrophotometer in 10 individual vials, its protein content predicted and Student's t-test performed on the data.

$$r_{jk} = \frac{\sum x_{ij} x_{ik}}{\sqrt{(\sum x_{ij}^2 \sum x_{ik}^2)}} \quad \dots 7$$

where  $x_{ij}$  = absorbance value (nm) of the  $i^{\text{th}}$  wavelength for spectra j

$x_{ik}$  = absorbance value (nm) of the  $i^{\text{th}}$  wavelength for spectra k

$$d = \max [\text{abs}(x_{ij} - x_{ik})] \quad \dots 8$$

## Results and discussion

### *Reference methods*

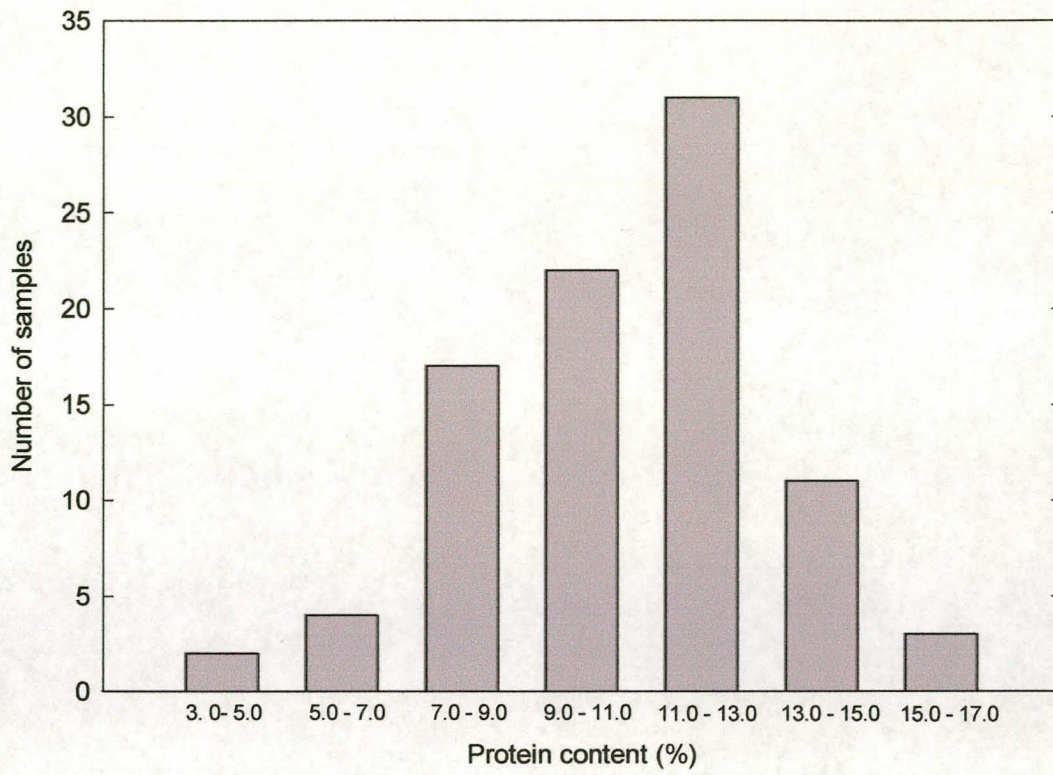
The average results of the reference protein and moisture determinations are tabulated in Table 1. The standard error of laboratory (SEL) of these methods were 0.34% and 0.70%, respectively. The distribution of the protein and moisture content values of the combined calibration and validation sets can be seen in Figures 1 & 2, respectively.

**Table 1.** Reference method results for protein and moisture content.

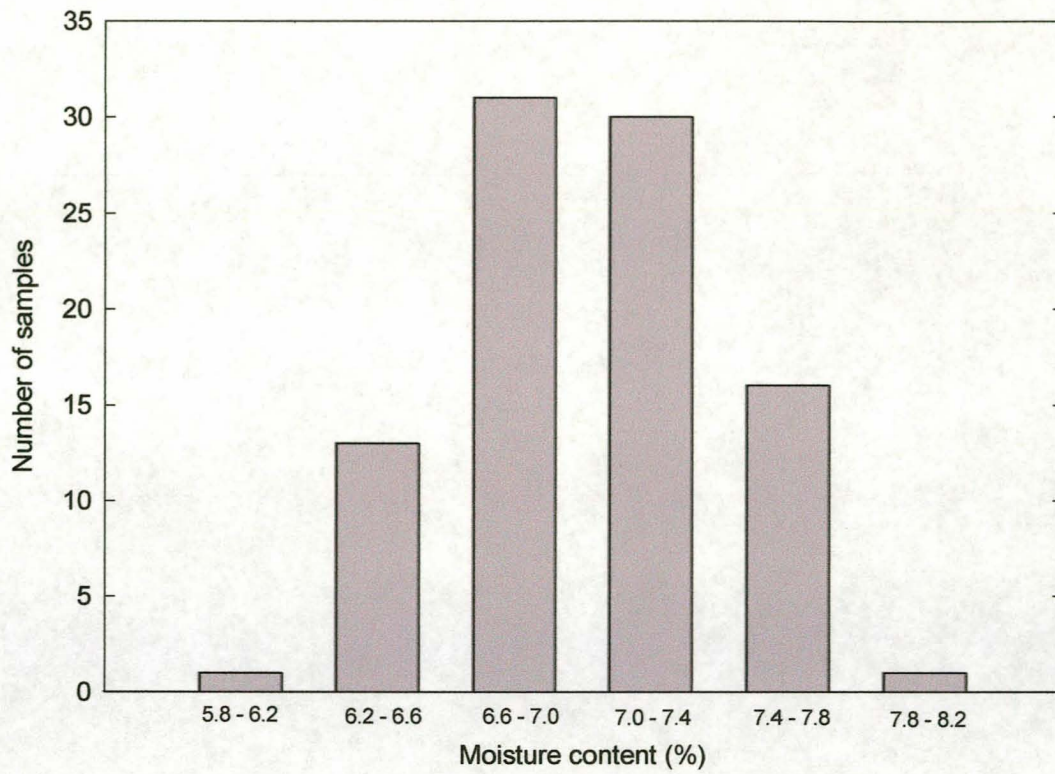
<b>Sample cultivar</b>	<b>Protein content (%)</b>	<b>Moisture content (%)</b>	<b>Sample cultivar</b>	<b>Protein content (%)</b>	<b>Moisture content (%)</b>
Nantes	12.09	6.46	Nantes	14.35	7.25
Dias	12.08	6.86	SST 57	13.06	7.18
Dias	13.94	6.91	Dias	10.36	6.94
Palmiet	13.62	7.10	Nantes	12.42	7.48
Palmiet	11.05	6.61	Dias	11.83	7.58
Dias	11.48	6.42	Dias	13.79	7.61
Nantes	11.54	6.70	SSt 57	6.15	7.65
Dias	15.54	6.20	Palmiet	13.17	7.44
Dias	14.25	6.69	Dias	8.11	7.85
SST 57	9.41	6.97	Nantes	11.52	6.31
Nantes	10.60	6.38	Nantes	11.27	7.20
Palmiet	10.98	6.32	Dias	11.00	7.45
Nantes	11.19	6.27	Nantes	8.86	6.76
Palmiet	11.75	6.61	Nantes	12.07	6.93
Nantes	15.44	6.61	Dias	9.67	7.15
Palmiet	8.07	6.68	Palmiet	10.89	7.07
SST 57	12.93	6.78	Palmiet	9.57	7.39
Nantes	7.48	6.40	Dias	14.90	7.45
Palmiet	13.76	6.30	Dias	12.17	7.27
SST 57	12.80	6.50	Palmiet	14.52	7.53
SST 57	6.26	7.20	Palmiet	9.32	6.93
SST 57	10.30	7.31	Palmiet	15.52	7.72
Palmiet	13.47	7.24	Palmiet	8.58	7.35
SST 57	8.57	7.33	Dias	10.96	7.44
SST 57	9.78	7.42	Nantes	11.73	7.30
SST 57	6.77	7.21	Dias	11.38	7.11
SST 57	11.91	7.28	Palmiet	11.72	7.31
SST 57	10.13	7.25	Nantes	16.12	7.29

Table 1 continued / ...

Sample cultivar	Protein content (%)	Moisture content (%)	Sample cultivar	Protein content (%)	Moisture content (%)
Nantes	10.27	7.34	Nantes	8.19	6.79
Palmiet	10.77	7.22	Chokka	8.20	7.15
SST 55	6.38	7.12	SST 65	6.71	7.20
SST 38	12.06	7.31	Adam Tas	7.86	7.11
SST 55	10.01	7.50	SST 66	5.85	7.12
Chokka	7.99	7.51	SST 16	4.79	6.97
Adam Tas	7.70	7.51	SST 65	8.19	6.73
Dias	10.53	7.66	SST 55	10.41	6.65
Palmiet	10.76	7.66	SST 38	11.08	6.71
Chokka	11.15	7.08	Nantes	11.93	6.50
Nantes	7.02	6.67	SST 66	11.64	6.65
Kariega	5.50	6.79	Palmiet	6.26	6.64
Kariega	9.32	6.64	SST 16	11.68	6.48
SST 66	10.60	6.91	Palmiet	11.04	6.80
SST 65	4.60	6.90	SST 57	11.38	6.84
SSt 38	5.30	6.79	Dias	7.52	6.41
Adam Tas	8.58	6.84	Kariega	10.65	6.63
SST 16	7.78	6.61	Dias	7.56	6.53



**Figure 1.** Protein content distribution of the flour samples.



**Figure 2.** Moisture content distribution of the flour samples.

### *Fourier transform near infrared measurements*

The absorbance spectra of a single flour sample, recorded in the sapphire-glass cup, the borosilicate-glass vial and the soda-glass vial, respectively, are presented in Figure 3, illustrating the differences in absorbance obtained when using different sample holders.

### *Calibration development*

The results of the three protein calibrations where the different sample holders were used are compared in Table 2. Table 3 contains the statistical results of the corresponding moisture calibrations. Scatter plots of the estimated versus actual values for the calibration sets of the various calibration models are illustrated in Figures 4 - 9. The corresponding scatter plots of the validation sample sets of the various calibration models are illustrated in Figures 10 - 15.

The best calibration results for protein content was obtained with the model where the spectra were recorded in the borosilicate-glass vials, followed by the soda-glass vials and the sapphire-glass cup. The borosilicate-glass model had the lowest SEP and RMSEP values of 0.15% and 1.16%, respectively, indicating a small expected error when independent samples are predicted using the respective calibration models. Furthermore the  $r$  value and the  $F$ -value, which corresponds to the signal to noise ratio in the model, were both the highest (0.92 and 302.8, respectively) for the model where borosilicate-glass vials were used. An analysis of variance (ANOVA) performed on the predicted values of the three calibrations, however, determined that no calibration model was significantly better than the other ( $P \leq 0.05$ ). Calibration results, however, compared well to flour protein NIR and calibration results of previous studies (Hunt *et al.*, 1977; Osborne *et al.*, 1982; Osborne & Fearn, 1983a), including a FT-NIR study by the manufacturers of the Perkin Elmer Spectrum IdentiCheck FT-NIR spectrophotometer, where SEP and  $r$  values of 0.28% and 0.98, respectively, were obtained (Anonymous, 1997a).

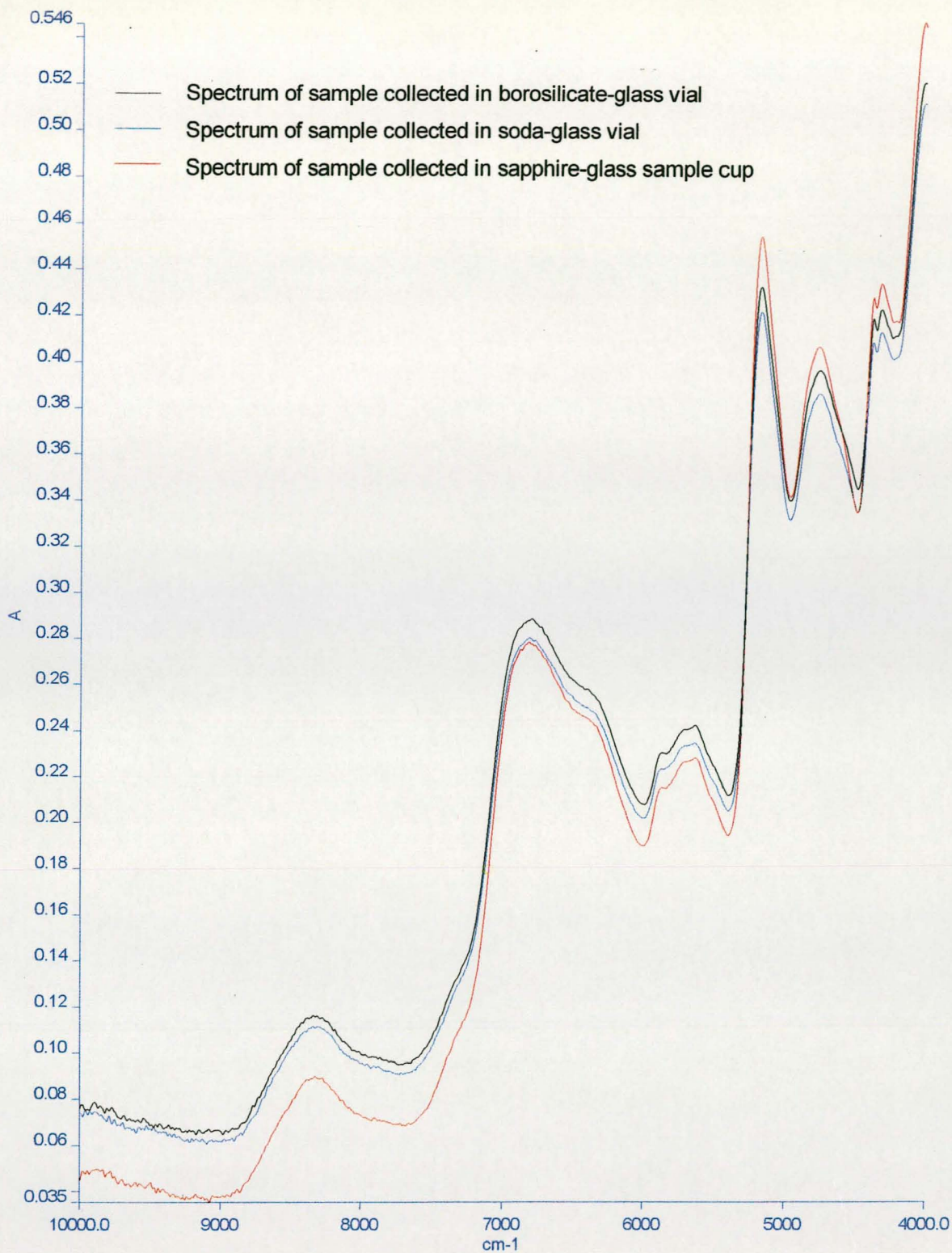


**Figure 3.** The absorbance spectra of the same sample presented to the spectrophotometer in the three different sample holders, respectively.



**Table 2.** Statistical results for protein calibrations using different sample holders (with a protein range of 5.30% - 16.12%).

	Borosilicate-glass vial	Soda-glass vial	Sapphire-glass cup
SEP (%)	0.51	0.80	0.83
RMSEP (%)	1.16	1.12	1.13
r	0.98	0.96	0.95
Bias	-0.20	-0.20	-0.22
F-value	320.8	155	138.7
# of factors	5	4	4

SEP = standard error of prediction

RMSEP = root mean standard error of prediction

r = correlation coefficient

**Table 3.** Statistical results for moisture calibrations using different sample holders (with a moisture range of 6.20% - 7.66%).

	Borosilicate-glass vial	Soda-glass vial	Sapphire-glass cup
SEP (%)	0.15	*	0.15
RMSEP (%)	0.38	0.41	0.43
r	0.94	0.92	0.94
Bias	0.02	0.01	-0.07
F-value	70.21	*	70.84
# of factors	6	6	6

\* = no values available

SEP = standard error of prediction

RMSEP = root mean standard error of prediction

r = correlation coefficient

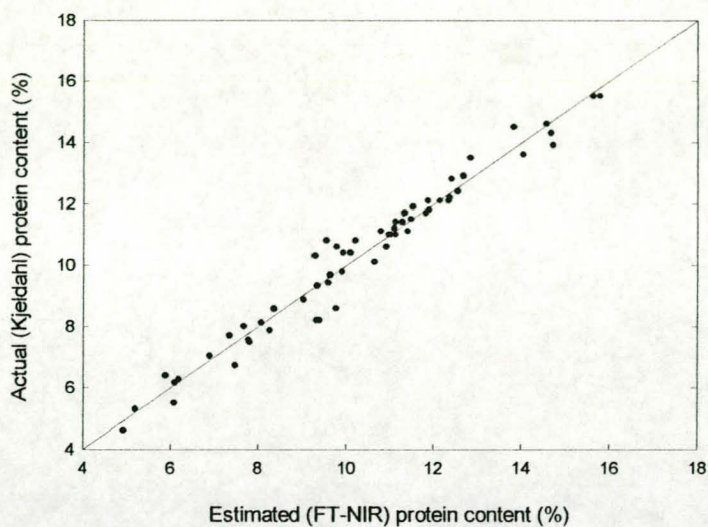


**Figure 4.** Scatter plot of the estimated versus actual protein content (%) for the calibration model where borosilicate-glass vials were used.

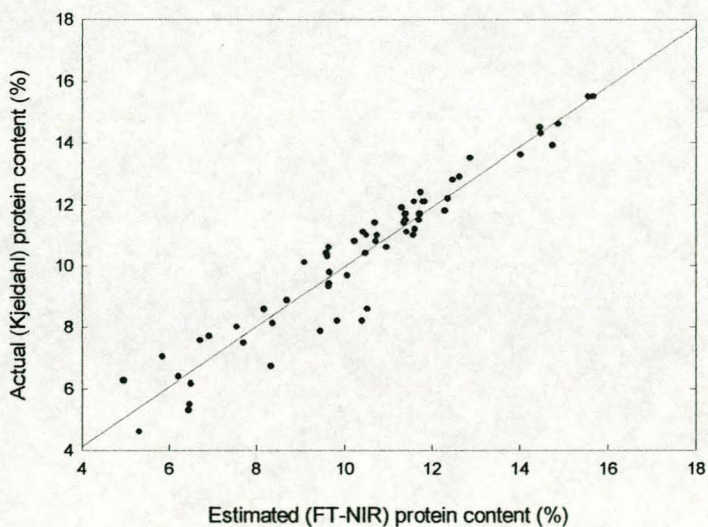


**Figure 5.** Scatter plot of the estimated versus actual protein content (%) for the calibration model where soda-glass vials were used.

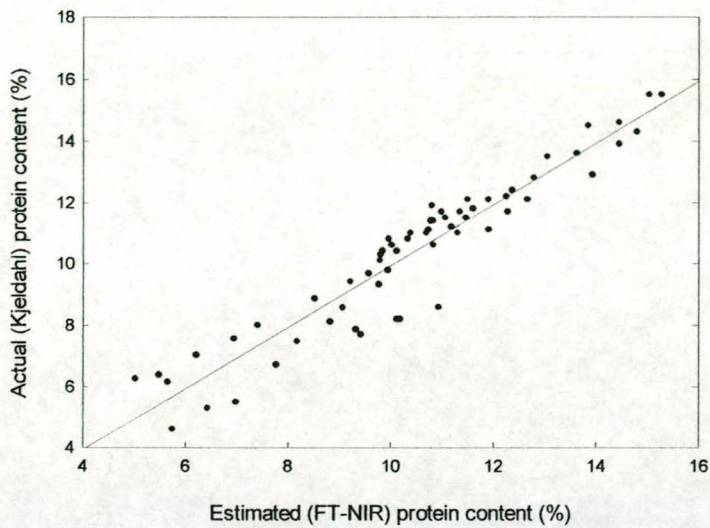


**Figure 6.** Scatter plot of the estimated versus actual protein content (%) for the calibration model where the sapphire-glass sample cup were used.

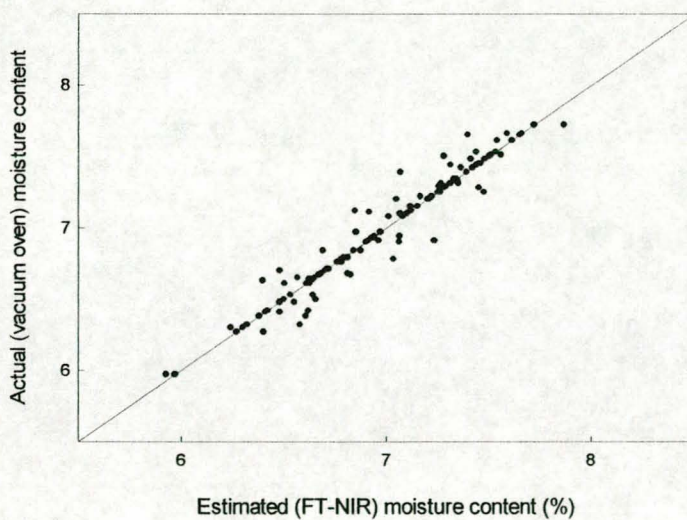


**Figure 7.** Scatter plot of the estimated versus actual moisture content (%) for the calibration model where borosilicate-glass vials were used.

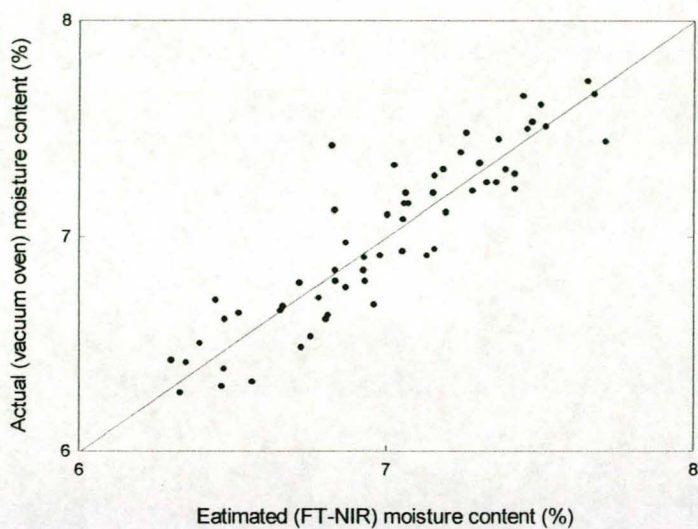


**Figure 8.** Scatter plot of the estimated versus actual moisture content (%) for the calibration model where soda-glass vials were used.

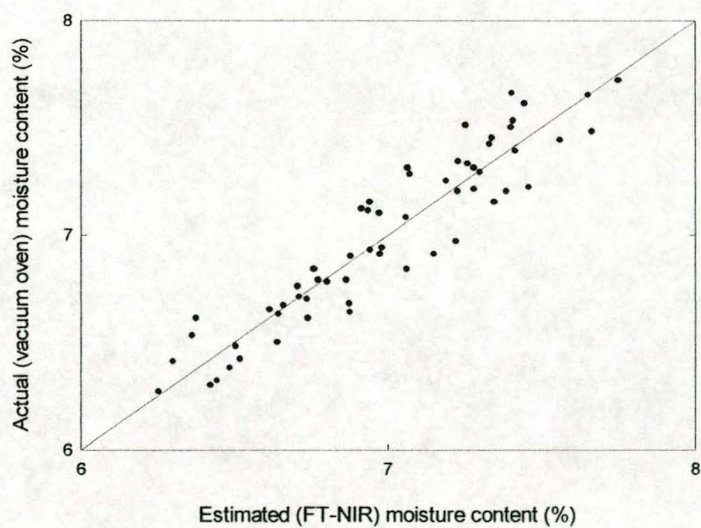


**Figure 9.** Scatter plot of the estimated versus actual moisture content (%) for the calibration model where the sapphire-glass sample cup was used.

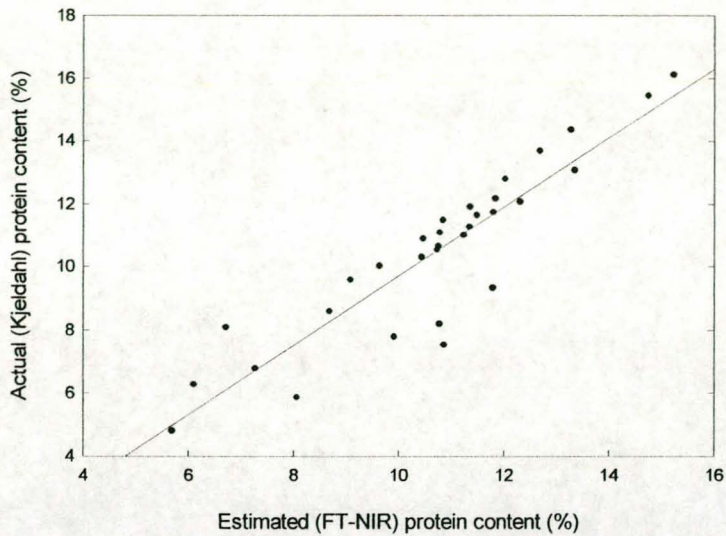


**Figure 10.** Scatter plot of estimated versus actual protein content (%) for the independent validation model where borosilicate-glass vials were used.

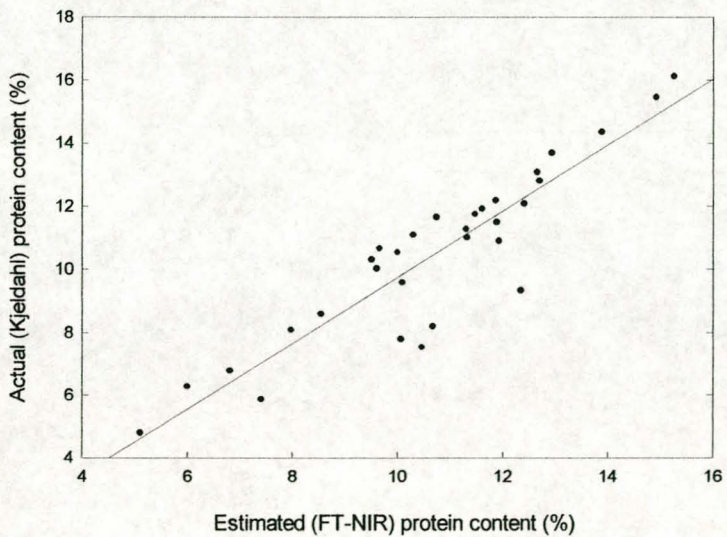


**Figure 11.** Scatter plot of estimated versus actual protein content (%) for the independent validation model where soda-glass vials were used.

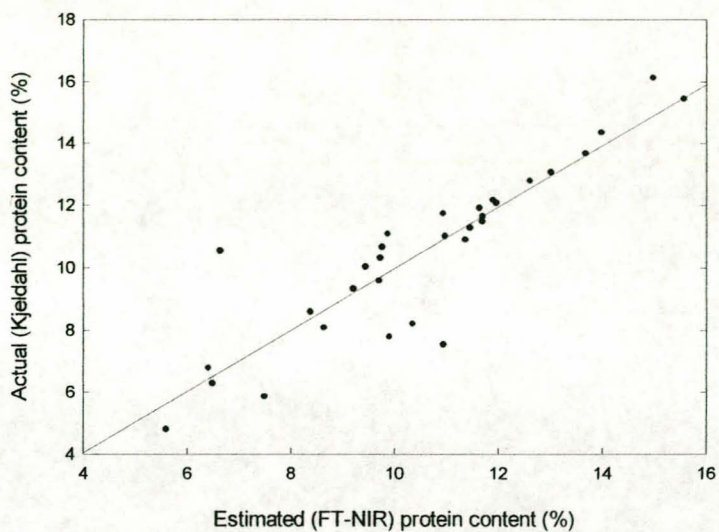


**Figure 12.** Scatter plot for the estimated versus actual protein content (%) for the independent validation model where the conventional sapphire-glass sample cup was used.

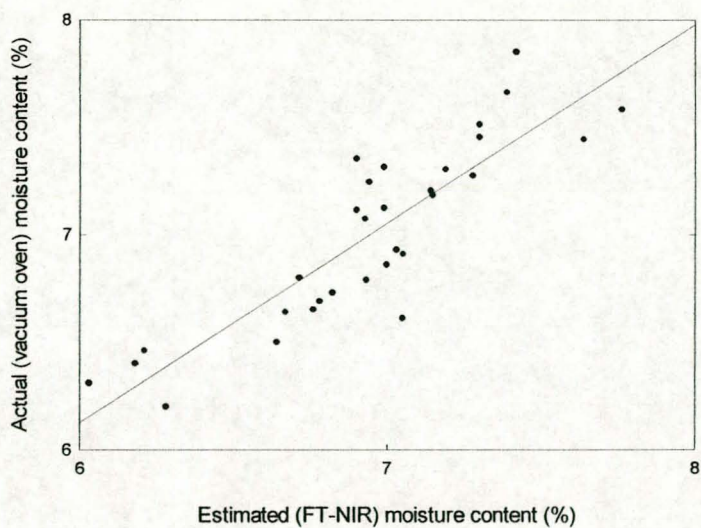


**Figure 13.** Scatter plot of the estimated versus actual moisture content (%) for the independent validation model where borosilicate-glass vials were used.

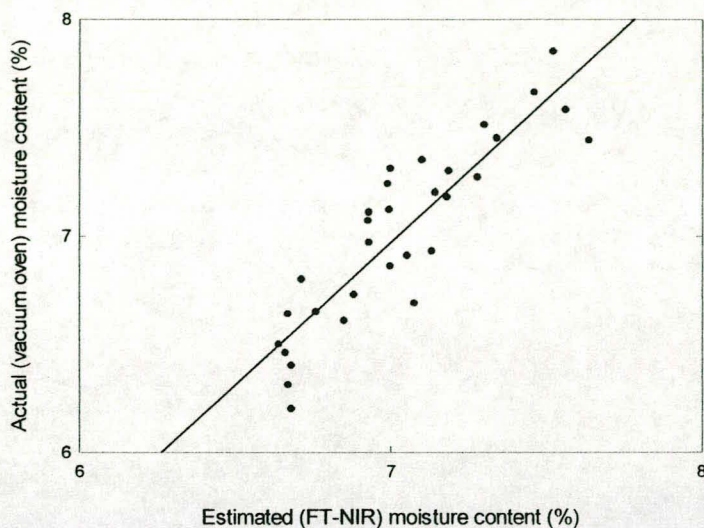


**Figure 14.** Scatter plot of the estimated versus actual moisture content (%) for the independent validation model where soda-glass vials were used.

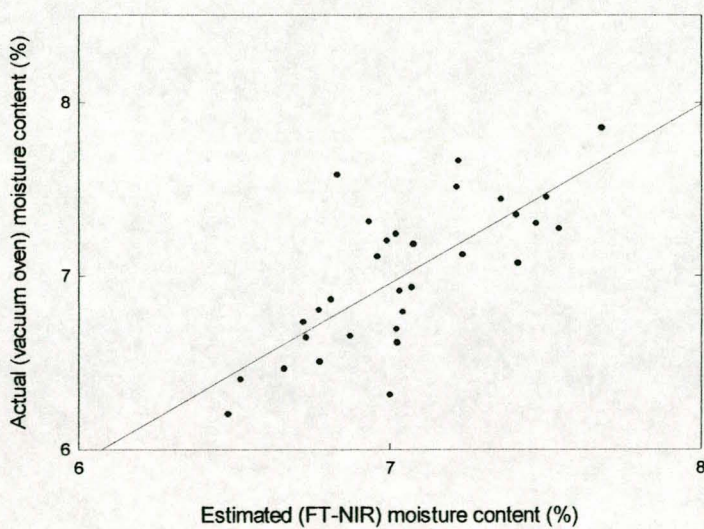


**Figure 15.** Scatter plot of the estimated versus actual moisture content (%) for the independent validation model where the conventional sapphire-glass sample cup was used.

The best moisture calibration was again obtained from the model where the borosilicate-glass vials were used. This model had the lowest SEP (0.15%) and RMSEP values (0.38%) together with high  $r$  (0.94) and  $F$ -values (70.21), but an ANOVA performed on the predicted moisture values again indicated no significant difference between the three different moisture calibrations ( $P \leq 0.05$ ). The moisture calibration results compared excellently with results obtained from flour moisture NIR (Hunt *et al.*, 1977; Osborne *et al.*, 1982; Osborne & Fearn, 1983a) and FT-NIR (Sorvaniemi *et al.*, 1993; Anonymous, 1997a) calibrations in previous studies. Sorvaniemi *et al.* (1993), for example, obtained a SEP and  $r$  value of 0.16% and 0.97, respectively, when flour was calibrated for moisture content, while the manufacturers of the Perkin Elmer Spectrum IdentiCheck FT-NIR spectrophotometer obtained results of 0.23% and 0.96, respectively (Anonymous, 1997a).

From the calibration results it would thus appear that there were indeed differences in spectral data when different sample holders were used, but that these differences did not significantly effect the accuracy of the different models. Correlation coefficients ( $r$ ) and the maximum distances ( $d$ ) of three of the samples (differing in protein content as seen in Table 4), were calculated to confirm the insignificance of the use of different sample holders on absorbance spectra (Tables 5 - 8). This was done for both their normal absorbance spectra and their second derivative spectra.

The correlation coefficient and maximum distance indicate that the spectra of samples presented in the soda-glass vials correlated better with spectra of samples presented in the sapphire-glass cup than with the spectra of samples presented in the borosilicate-glass vials. Furthermore the highest correlation among the sample holders were found between the soda-glass and borosilicate-glass vials. However, when Students'  $t$ -test was performed on the  $r$  and  $d$  results, it was found that the differences in absorbance values caused by these three sample holders were not significant ( $P \leq 0.05$ ).



**Table 4.** The protein content of the three samples used in the quantifying of differences caused by different sample holders.

Cultivar	Protein (%)
SST 57	11.91
Dias	14.90
Palmiet	6.26

**Table 5.** Correlation coefficient (r) results for normal absorbance spectra.

	$r_{(saph/boro)^*}$	$r_{(saph/soda)^*}$	$r_{(boro/soda)^*}$
<b>SST 57</b>	0.9966	0.9973	0.9999
<b>Dias</b>	0.9967	0.9959	1.0000
<b>Palmiet</b>	0.9959	0.9966	1.0000

$r_{(saph/boro)^*}$  = correlation coefficient between sample measured in the conventional cup and in the borosilicate-glass vials

$r_{(saph/soda)^*}$  = correlation coefficient between sample measured in the conventional cup and in the soda-glass vials

$r_{(boro/soda)^*}$  = correlation coefficient between sample measured in the soda-glass vials and in the borosilicate-glass vials

**Table 6.** Correlation coefficient (r) results for second derivative spectra.

	$r_{(saph/boro)^{\circ}}$	$r_{(saph/soda)^{\circ}}$	$r_{(boro/soda)^{\circ}}$
<b>SST 57</b>	0.998309	0.995285	0.995526
<b>Dias</b>	0.997119	0.992445	0.998207
<b>Palmiet</b>	0.997648	0.998087	0.998877

$r_{(saph/boro)^{\circ}}$  = correlation coefficient between sample measured in the conventional cup and in the borosilicate-glass vials

$r_{(saph/soda)^{\circ}}$  = correlation coefficient between sample measured in the conventional cup and in the soda-glass vials

$r_{(boro/soda)^{\circ}}$  = correlation coefficient between sample measured in the soda-glass vials and in the borosilicate-glass vials

**Table 7.** Maximum distance (d) results for normal absorbance spectra.

	$d_{(saph/boro)^{\circ}}$	$d_{(saph/soda)^{\circ}}$	$d_{(boro/soda)^{\circ}}$
<b>SST 57</b>	0.029352	0.025348	0.007607
<b>Dias</b>	0.025108	0.015188	0.013427
<b>Palmiet</b>	0.025842	0.023480	0.013622

$d_{(saph/boro)^{\circ}}$  = Maximum distance between sample measured in the conventional cup and in the borosilicate-glass vials

$d_{(saph/soda)^{\circ}}$  = Maximum distance between sample measured in the conventional cup and in the soda-glass vials

$d_{(boro/soda)^{\circ}}$  = Maximum distance between sample measured in the soda-glass vials and in the borosilicate-glass vials

**Table 8.** Maximum distance (d) results for second derivative spectra.

	$d_{(\text{saph}/\text{boro})}^{\circ}$	$d_{(\text{saph}/\text{soda})}^{\circ}$	$d_{(\text{boro}/\text{soda})}^{\circ}$
<b>SST 57</b>	0.000005	0.000005	0.000002
<b>Dias</b>	0.000004	0.000004	0.000002
<b>Palmiet</b>	0.000006	0.000005	0.000003

$d_{(\text{saph}/\text{boro})}^{\circ}$  = Maximum distance between sample measured in the conventional cup and in the borosilicate-glass vials

$d_{(\text{saph}/\text{soda})}^{\circ}$  = Maximum distance between sample measured in the conventional cup and in the soda-glass vials

$d_{(\text{boro}/\text{soda})}^{\circ}$  = Maximum distance between sample measured in the soda-glass vials and in the borosilicate-glass vials

Differences between individual vials of the same type were determined to be insignificant ( $P \leq 0.05$ ) by performing Student's t-test on the FT-NIR predicted values of the same sample presented in 10 individual soda-glass and borosilicate-glass vials, respectively.

## **Conclusions**

The Perkin Elmer Spectrum IdentiCheck FT-NIR spectrophotometer can be used successfully to derive protein and moisture calibrations for South African whole wheat flour. Using different sample holders (borosilicate-glass vials, soda-glass vials and the conventional sapphire-glass sample cup) does not effect FT-NIR calibration and prediction significantly ( $P \leq 0.05$ ). Therefore the sapphire-glass sample cup provided with the spectrophotometer can be replaced by the more convenient soda-glass or borosilicate-glass vials in presenting samples to the spectrophotometer. Accurate results can be obtained when this spectrophotometer is used to determine protein or moisture content of whole wheat flour.

## References

- Anonymous (1997a). *Perkin Elmer FT-NIR spectroscopy application note: The determination of protein and moisture in samples of wheat*. The Perkin Elmer Corporation. Beaconsfield, UK: Technical Publications.
- Anonymous (1997b). *Spectrum QUANT+ User's Reference*. The Perkin Elmer Corporation. Beaconsfield, UK: Technical Publications.
- AACC (1983a). Experimental milling: Buhler method, Method 22-20. In: *Approved Methods of the AACC (8th edition)*. UK: Association of American Cereal Chemists Inc.
- AACC (1983b). Crude Protein: improved Kjeldahl method for nitrate-free samples, Method 46-11. In: *Approved Methods of the AACC (8th edition)*. UK: Association of American Cereal Chemists Inc.
- Bradley, E.B. (1986). Introduction to spectroscopic methods. In: *Instrumental Analysis* (edited by G.D. Christian & J.E. O'Reilly). Pp. 144-157. Massachusetts, USA: Allyn and Bacon Inc.
- Delwiche, S.R. (1998). Protein content of single kernels of wheat by near-infrared reflectance spectroscopy. *Journal of Cereal Science*, **27**, 241-254.
- Ellis, J.W. & Bath, J. (1938). Modifications in near infrared absorption spectra of natural and synthetic fibres. *Journal of Chemistry and Physics*, **6**, 723-729.
- Hunt, W.H., Fulk, D.W., Elder, B. & Norris, K. (1977). Collaborative study on infrared reflectance devices for determination of protein in hard red winter wheat and for protein and oil in soybeans. *Cereal Foods World*, **22**, 143-144.
- James, C.S. (1995). Experimental Procedures. In: *Analytical Chemistry of Foods*. Pp. 73-74. UK: Blackie Academic & Professional.
- Law, D.P. & Tkachuk, R. (1977). Determination of moisture content in wheat by near infrared diffuse reflectance spectrophotometry. *Cereal Chemistry*, **54**, 874-881.

- Li Yoon, W., Jee, R.D., & Moffat, C. (1998). Optimisation of sample presentation for the near infrared spectra of pharmaceutical excipients. *Analyst*, **123**, 1029-1034.
- Mark, H. L. & Tunnel, D. (1995). Qualitative near-infrared reflectance analysis using Mahalanobis distances. *Analytical Chemistry*, **57**, 1449.
- McShane. (1989). Applying NIR to process control. *Journal of the American Oil Chemists' Society*, **66**, 641-643.
- Miller, B.S., Pomeranz, Y., Thompson, W.O., Nolan, T.W., Hughes, J.W., Davis, G. Jackson, N.G. & Fulk, D.W. (1978). Interlaboratory and intralaboratory reproducibility of protein determination in hard red winter wheat by Kjeldahl and near infrared procedures. *Cereal Foods World*, **23**, 198-201.
- Osborne, B.G. (1987). Determination of moisture in white flour, ground wheat and whole wheat by near infrared reflectance using a single calibration. *Journal of the Science of Food and Agriculture*, **38**, 341-346.
- Osborne, B.G., Douglas, S. & Fearn, T. (1982). The application of near infrared reflectance analysis to rapid flour testing. *Journal of Food Technology*, **17**, 355-363.
- Osborne, B.G. & Fearn, T. (1983a). Collaborative evaluation of universal calibrations for the measurement of protein and moisture in flour by near infrared reflectance. *Journal of Food Technology*, **18**, 453-460.
- Osborne, B.G. & Fearn, T. (1983b). Collaborative evaluation of near infrared reflectance analysis for the determination of protein, moisture and hardness in wheat. *Journal of the Science of Food and Agriculture*, **34**, 1011-1017.
- Osborne, B.G., Fearn, T. & Hindle, P.H. (1993). *Practical NIR Spectroscopy with Practical Application in Food and Beverage Analysis (2<sup>nd</sup> edition)*. Pp. 67-71, 145-156. Essex, UK: Longman Group UK Limited.
- Sorvaniemi, J., Kinnunen, A., Mälkki, Y. & Tsados, A. (1993). Using partial least squares regression and multiplicative scatter correction for FT-

NIR data evaluation of wheat flours. *Journal of Food Science and Technology*, **26**, 251-258.

Williams, P. C. (1992). Samples, sample presentation and sample selection. In: *Handbook of near infrared analysis* (edited by D. A. Burns & E. W. Ciurczak). Pp. 307-311. New York, USA: Marcel Dekker Inc.

Williams, P.C., Thompson, B.N., Wetzel, D., McLay, W. & Loewen, D. (1981). Near infrared instruments in flour mill quality control. *Cereal Foods World*, **26**, 234-237.

Williams, P.C. & Stevenson, S.G. (1990). Near infrared reflectance analysis: food industry applications. *Trends in Food Science and Technology*, **1**, 44-48.

## **Chapter 4**

**Deriving grain hardness calibrations for Southern and Western Cape ground bread wheat samples by means of the particle size index (PSI) method and Fourier transform near infrared (FT-NIR) spectroscopy**





## Chapter 4

### DERIVING GRAIN HARDNESS CALIBRATIONS FOR SOUTHERN AND WESTERN CAPE GROUND WHEAT SAMPLES BY MEANS OF THE PARTICLE SIZE INDEX (PSI) METHOD AND FOURIER TRANSFORM NEAR INFRARED (FT-NIR) SPECTROSCOPY

#### Summary

Two methods, the particle size index (PSI) method and Fourier transform near infrared (FT-NIR) spectroscopy, were successfully used in determining kernel hardness of 198 Southern and Western Cape ground bread wheat samples. Samples were presented to the Perkin Elmer Spectrum IdentiCheck FT-NIR spectrophotometer in individual borosilicate-glass vials. A hardness calibration was derived by applying partial least square (PLS) regression to baseline corrected spectra. Reference hardness results were determined by means of the PSI method. Independent validation was carried out on the calibration model. Excellent results were obtained with the model, having had a standard error of prediction (SEP) of 2.13%, a root mean standard error of prediction (RMSEP) of 4.53% and a multiple correlation ( $r$ ) of 0.89. Particle size index results indicate that the bread wheat class in the Southern and Western Cape includes wheats of a wide variety of hardnesses. Analysis of variance (ANOVA) and Student's  $t$ -test were used to determine whether significant differences in hardness values existed in wheats over different cultivars and different localities. Results showed statistically significant differences in hardness over cultivars ( $P \leq 0.05$ ). Protein and moisture content of all 198 samples were also determined and the relationship between hardness and protein and moisture content, respectively, determined by means of correlation analysis. It was found that hardness had a positive linear relationship with protein content and a negative linear relationship with moisture content within certain cultivars and localities.

## Keywords

Fourier transform near infrared spectroscopy, particle size index method, wheat hardness

## Introduction

Grain hardness is one of the most important distinguishing factors in classifying wheat for commercial purposes, affecting both its quality and functionality (Pomeranz & Williams, 1990; Kent & Evers, 1994; Ohm *et al.*, 1998). It plays a major role in the way in which wheat must be tempered for milling, the yield and particle size, shape and density of flour particles as well as the end-use properties in milling and the production of bread, soft wheat products and noodles. Despite its recognised importance there is no universally excepted definition for wheat hardness. Anjum & Walker (1991) described it as “the resistance to fracture upon grinding, slicing, abrasion or indentation of a single kernel or bulk samples”. The most widely excepted theory on the mechanism of wheat hardness states that the differences in hardness between different wheats result from differences in the strength of the cohesion between starch and protein at the interface in the endosperm (Barlow *et al.*, 1973; Simmonds *et al.*, 1973; Kent & Evers, 1994). True wheat hardness is under strong genetic control although factors such as the environment and protein content can also influence it to a lesser extent (Symes, 1965; Pomeranz & Williams, 1990; Carver, 1994; Kent & Evers, 1994).

There are over a hundred different methods documented for the measurement of wheat hardness (Williams & Sobering, 1986a; Williams & Sobering, 1986b; Norris *et al.*, 1989; Ohm *et al.*, 1998). It is difficult to measure the absolute hardness of wheat because of the geometry of the kernels. Therefore most tests do not measure the breaking strength directly, but rather evaluate hardness-related phenomena by measuring some property of the wheat

during or after grinding (Norris *et al.*, 1989). Such properties include work to grind, time to grind, mechanical resistance of single kernels to crushing and abrasion and particle size distribution measurements (Hoseney, 1987; Norris *et al.*, 1989; Pomeranz & Williams, 1990).

Cutler & Brinson (1939) developed the particle size index (PSI) test to measure relative wheat hardness by determining the particle size distribution of wheat after grinding. The method has since been modified and standardised by Williams & Sobering (1986a). The method involves grinding a bulk sample of wheat into flour after which it is sieved and the throughs weighed. The results are related to hardness in that hard wheats have a higher mean particle size than soft wheats.

More recently radiation scattering properties have been used to define wheat hardness by means of near infrared (NIR) spectroscopy (Norris *et al.*, 1989; Williams 1991; Delwiche & Norris, 1993; Carver, 1994). Near infrared spectroscopy allows differentiation between wheats of different hardnesses due to its sensitivity to variation in particle size and particle size distribution and is recognised as a reliable, rapid and easily standardisable method (Osborne & Fearn, 1983; Williams & Sobering, 1986a; Delwiche *et al.*, 1995). Delwiche & Norris (1993) classified hard red wheat by means of NIR diffuse reflectance spectroscopy. A 5 factor principle component regression (PCR) model gave accurate results with an average misclassification of 5%. These same samples were also used to perform NIR analysis on bulk whole grain wheat samples (Delwiche *et al.*, 1995). An artificial neural network (ANN) model was used and classification results with accuracies in the range of 95 - 98% were obtained.

Although Fourier transform near infrared (FT-NIR) spectroscopy has been employed in determining protein and moisture content in whole wheat flour (Sorvaniemi *et al.*, 1993; Anonymous, 1997a), no FT-NIR work has been done on kernel hardness.

In South Africa wheat is divided into three classes: hard wheat (for bread-making), soft wheat (for biscuit-making) and durum wheat (for pasta-making) (Van Deventer, 1999). The vast majority of South African wheats, however,

forms part of the hard wheat class. In other wheat producing countries the distinction between hard and soft wheats used to be maintained by breeding programs which preserved the morphology of wheat generally recognised as hard or soft wheats. In countries such as Canada and the USA cross breeding has, however, led to the mixing of hardness classes necessitating a reliable method of measuring hardness (Norris *et al.*, 1989; Delwiche & Norris, 1993). This may also occur in South Africa where wheat is not yet specified or categorised according to wheat hardness. Since the price of wheat in other wheat producing countries is customary based on class and their classification system include wheat hardness as a parameter, determining wheat hardness will become important in the new free market system in South Africa (Norris *et al.*, 1989; Van Deventer, 1999).

The aim of this study was to determine the wheat hardness range of Western and Southern Cape bread wheat cultivars and deriving hardness calibrations of ground wheat samples using the PSI method and Fourier transform near infrared (FT-NIR) spectroscopy. The effects of different genotype and growth location on kernel hardness as well as the relationship between hardness and protein and moisture content, respectively, were also investigated.

## **Materials and methods**

### *Sample collection*

A total of 198 whole grain wheat samples were collected from different localities in the Western and Southern Cape in South Africa. The sample set comprised of 3 repetitions each of 11 cultivars collected at 6 different localities (Table 1).

### *Particle size index (PSI) hardness test*

The reference method employed for the determination of wheat hardness was the particle size index (PSI) test as described by Williams & Sobering (1986b). A

**Table 1.** A listing of the relevant wheat cultivars and localities of the 198 Southern and Western Cape samples that were collected.

Southern and Western Cape samples		
Cultivars	Localities	
	Western Cape (Swartland)	Southern Cape (Ruens)
Palmiet	Philadelphia	Matjiesfontein
Nantes	Langgewens	Tygerhoek
SST 825	Porterville	Voorstekop
SST 55		
SST 57		
SST 65		
SST 66		
SST 75		
Kariega		
Adam Tas		
SST38		

representative sample (ca. 50 g) of a whole grain wheat sample was ground using a UDY Cyclone mill fitted with a 1 mm screen. A sample (10 g weighed to the nearest 0.01 g) of the ground wheat was transferred to a 75  $\mu\text{m}$  sieve with a receiving pan. Approximately 50 g of whole grain kernels was added to prevent clogging of the sieves and the sieve covered with a lid. The sample was sieved for exactly 10 minutes on an automatic sieve shaker (Endocott). All the throughs, including those adhering to the bottom of the sieve, was transferred into the receiving pan and the throughs weighed to the nearest 0.01 g. The final result was expressed as percentage throughs (equation 1). Determinations were performed in duplicate and the standard error of laboratory calculated (equation 2).

$$\% \text{ throughs} = \frac{w_1}{w_2} \times 100 \quad \dots 1$$

where  $w_1$  = mass of throughs (g)

$w_2$  = mass of flour before sifting (g)

$$SEL = \sqrt{\frac{\sum (y_1 - y_2)^2}{2n}} \quad \dots 2$$

where  $y_1$  and  $y_2$  = results of duplicate determinations

$n$  = number of samples

The hardness of a number of Canadian wheat samples with known PSI values, as determined by the Canadian Grain Commission (Winnipeg, Canada), was also determined. These samples were used as reference to optimise the accuracy of the method executed in this study.

#### *Fourier transform near infrared measurements*

In Chapter 3 it has been established that the best FT-NIR calibration and prediction results were obtained when the samples' spectra were collected in

individual borosilicate glass vials rather than in individual soda-glass vials or the conventional sapphire-glass sample cup. Each of the 198 Western and Southern Cape whole wheat flour samples was therefore presented to the Perkin Elmer Spectrum IdentiCheck FT-NIR spectrophotometer in individual borosilicate glass vials (Cromacol) and its reflectance spectra collected using the Spectrum IdentiCheck version 2.00 software program. Spectra were collected from  $10\,000\text{ cm}^{-1}$  to  $4000\text{ cm}^{-1}$  at  $4\text{ cm}^{-1}$  intervals and at a resolution of  $16\text{ cm}^{-1}$ . Resolution is inversely proportional to the mirror displacement in the spectrophotometer (Anonymous, 1997b). The higher the resolution the finer the structure will be resolved in the spectrum. By using the lowest adequate resolution the data collection time is reduced and the signal-to-noise ratio improved.

Each final spectrum was the average of 16 scans and had a total number of 1501 data points. The interleaved mode was used, where the instrument performs a series of interleaved sample and background (ceramic tile) scans, compensating for any instrument variation.

#### *Calibration development*

Grain hardness calibrations were derived using the Spectrum Quant+ version 4.10 as well as the Unscrambler Version 6.11 software programmes (kindly provided by Foss Development (UK) Ltd.). Both programmes were used to confirm that the optimum amount of factors was used in deriving the calibration and to obtain both standard error of prediction (SEP) and root mean standard error of prediction (RMSEP) values. Partial least square (PLS) regression was performed on baseline corrected (by means of 1<sup>st</sup> derivative, width = 25) spectra. The calibration sample set comprised of 132 samples, while a validation set of 66 samples were used for independent validation of the model. Normalisation techniques, such as multiplicative scatter correction, were not performed as it would diminish the radiation scattering properties that enables the FT-NIR spectrophotometer to distinguish between wheats of different hardnesses.

The SEP (equation 3), RMSEP (equation 4), correlation coefficient ( $r$ ), bias and F-value were determined to express the accuracy of the calibration model.

$$SEP = \sqrt{\frac{\sum_{i=1}^n (\hat{y}_i - y_i - bias)^2}{n-1}} \quad \dots 3$$

where  $\hat{y}_i$  = predicted property of the  $i^{\text{th}}$  standard of the independent validation sample set

$y_i$  = actual property of the  $i^{\text{th}}$  standard

$n$  = number of spectra

$bias$  = the average differences between reference and predicted values

$$RMSEP = \sqrt{\frac{\sum_{i=1}^n (\hat{y}_i - y_i)^2}{n-1}} \quad \dots 4$$

### *Protein and moisture determinations*

The protein content of all 198 flour samples were determined by means of the Dumas method (AOAC, 1990). All determinations were performed in duplicate on samples of 0.70 g using a Leco ST 2000 apparatus. Duplicate moisture determinations were performed on the flour samples according to the modified method of James (1995). A sample (5 g) was placed into a dry metal dish and dried in an oven (Mettler) at 130°C for two hours. It was subsequently cooled down in a desiccator and the percentage moisture calculated according to equation 5.



$$\% \text{ moisture} = \frac{w_2 - w_3}{w_2 - w_1} \times 100 \quad \dots 5$$

where  $w_1$  = weight of sample before drying (g)

$w_2$  = weight of sample + metal dish before drying (g)

$w_3$  = weight of sample + metal dish after drying (g)

### *Statistical analysis*

Wheat hardness is influenced by many factors including genotype, environment and moisture while its determination can be influenced by protein content (Pomeranz & Williams, 1990). The influence of these factors on wheat hardness were investigated by performing analysis of variance (ANOVA), Student's t-test, correlation analysis and regression analysis on the raw PSI hardness, protein and moisture content values, respectively, for all 198 bread wheat samples. The ANOVA and Student's t-test were used to determine whether significant differences in kernel hardness, protein content and/or moisture content, could be detected between samples of different cultivars and localities. Correlation analysis was employed to determine whether a linear relationship existed between hardness and protein content and between hardness and moisture content for all samples. Where linear relationships were present, regression analysis was subsequently applied to describe the linear relationships by means of regression equations.

## **Results and discussion**

### *Particle size index (PSI) hardness test*

There is a linear correlation between the PSI results for the Canadian wheat samples measured in Canada and those measured locally (Figure 1), having a correlation coefficient ( $r$ ) of 0.99 ( $R^2 = 0.98$ ). With the differences in results

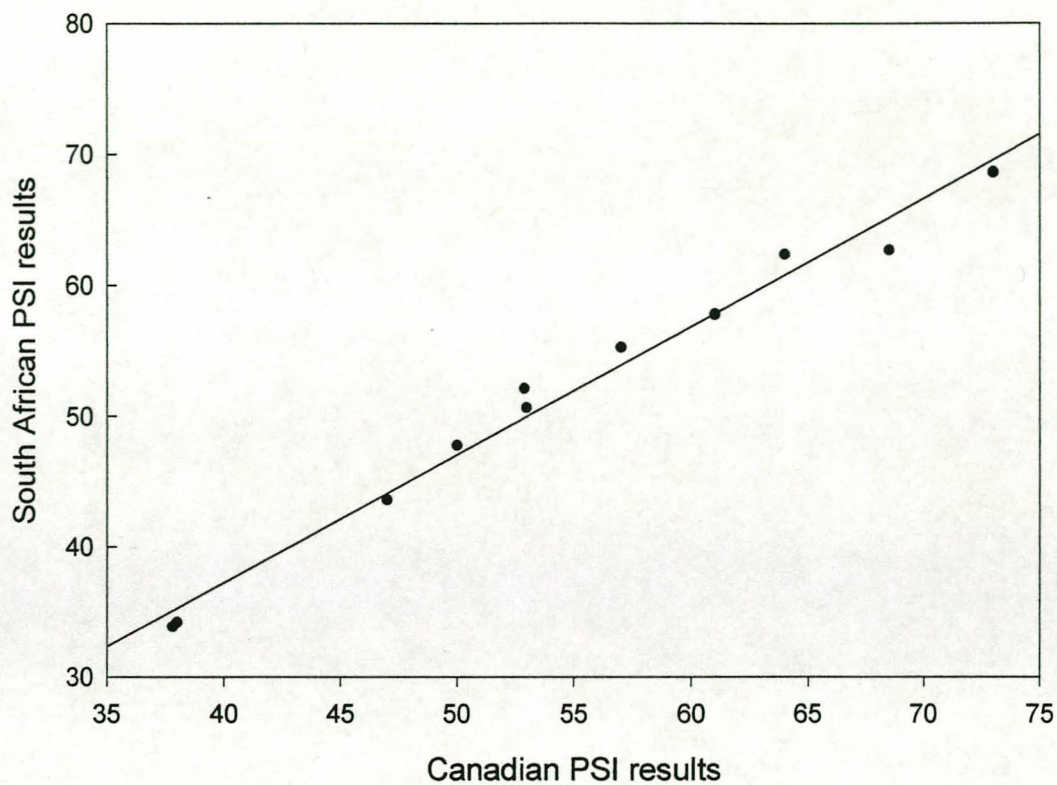


**Figure 1.** A graph of the PSI results for the reference Canadian wheat samples as obtained by the Canadian Grain Commission and obtained locally showing a linear correlation.

remaining constant and hardness values being relevant rather than absolute, the results of the PSI method performed on the local samples could therefore be accepted to be accurate and can be recalculated, if necessary for comparative reasons, using regression equation 6.

$$y = 1.0353x - 4.3661 \quad \dots 6$$

where  $y$  = PSI value of sample determined by the Canadian  
Grain Commission

$x$  = PSI value of sample determined in this study

The PSI results of the 198 Western and Southern Cape wheat samples are given in Table 2. The standard error of laboratory (SEL) for this method was 2.24%. The distribution of the PSI hardness values of the combined calibration and validation sample sets is given in Figure 2. The hardness range of the examined bread wheat cultivars was particularly wide (37.05 - 60.50%), although the majority of determinations were within the range of 45 - 55%.

#### *Calibration development*

The results obtained with the hardness FT-NIR calibration of Southern and Western Cape bread wheats are given in Table 3. The graphs of the scatter plots of actual PSI hardness values against FT-NIR predicted values for both the calibration sample set and the validation sample set are given in Figures 3 & 4, respectively. The skew of the graph in Figure 4 seems to be influenced by certain localities (Tygerhoek, Voorstekop and Porterville).

The SEP and RMSEP values are 2.13% and 4.53%, respectively. This indicates that only an error of a small magnitude is expected when the model is to be used to predict samples. Furthermore the SEP (2.13%) compares well with SEL (2.24%) of the reference method. A reasonable  $r$ -value of 0.89 and a high  $F$ -value (458.9), corresponding to a high signal to noise ratio within the model, were obtained. Calibration results compare well with results obtained in similar

**Table 2.** Reference hardness results as determined by the PSI test.

Location	Cultivar	PSI (%)		
		Repetition 1	Repetition 2	Repetition 3
Philadelphia	Palmiet	50.43	47.63	41.73
	SST 38	50.05	50.05	40.19
	SST 55	42.61	49.95	47.98
	SST 57	42.61	51.87	44.39
	SST 65	49.60	55.55	47.20
	SST 66	50.78	49.67	50.48
	SST 75	50.33	46.22	47.34
	SST 825	57.10	45.63	46.62
	Adam Tas	52.93	47.73	40.10
	Nantes	47.40	49.16	42.69
	Kariega	54.77	48.13	45.46
Langgewens	Palmiet	46.57	45.98	44.66
	SST 38	53.18	52.11	52.38
	SST 55	49.83	44.06	51.05
	SST 57	43.68	45.85	48.23
	SST 65	41.11	43.92	46.98
	SST 66	50.70	51.47	49.44
	SST 75	53.98	48.43	47.32
	SST 825	52.47	48.14	49.70
	Adam Tas	52.44	50.98	50.45
	Nantes	48.20	49.55	50.68
	Kariega	53.32	52.25	50.18
Porterville	Palmiet	55.75	46.50	51.10
	SST 38	54.10	41.43	46.73
	SST 55	55.84	51.15	51.60
	SST 57	50.43	55.68	45.47
	SST 65	53.92	46.44	49.85
	SST 66	59.83	54.52	56.87
	SST 75	55.20	53.56	53.11
	SST 825	51.65	45.60	53.84
	Adam Tas	55.85	50.58	53.27
	Nantes	55.94	50.38	48.95
	Kariega	55.50	50.37	57.94

Table 2 continued / ...

Location	Cultivar	PSI (%)		
		Repetition 1	Repetition 2	Repetition 3
Matjieskloof	Palmiet	49.58	50.05	43.58
	SST 38	52.43	52.68	46.60
	SST 55	53.23	48.75	48.38
	SST 57	49.75	49.23	49.67
	SST 65	45.00	49.70	44.47
	SST 66	44.42	47.29	44.37
	SST 75	43.48	37.05	46.05
	SST 825	50.97	48.98	45.42
	Adam Tas	44.38	46.07	41.43
	Nantes	48.10	43.07	48.63
Tygerhoek	Kariega	52.47	51.53	37.13
	Palmiet	44.55	43.08	48.60
	SST 38	55.80	52.26	40.74
	SST 55	60.51	54.27	49.33
	SST 57	48.00	47.50	46.96
	SST 65	47.72	49.80	48.78
	SST 66	43.43	50.48	47.17
	SST 75	46.01	45.07	45.20
	SST 825	54.39	42.45	48.00
	Adam Tas	51.70	43.10	51.05
Voorstekop	Nantes	43.89	42.94	53.08
	Kariega	48.60	41.47	55.94
	Palmiet	56.21	44.31	41.61
	SST 38	57.87	48.13	45.73
	SST 55	53.15	46.55	47.86
	SST 57	43.46	49.63	47.73
	SST 65	51.30	46.81	44.43
	SST 66	48.15	44.52	48.65
	SST 75	42.76	43.77	42.54
	SST 825	51.23	41.19	46.39
	Adam Tas	46.37	46.08	46.06
	Nantes	46.92	45.95	48.93
	Kariega	50.48	47.63	45.74

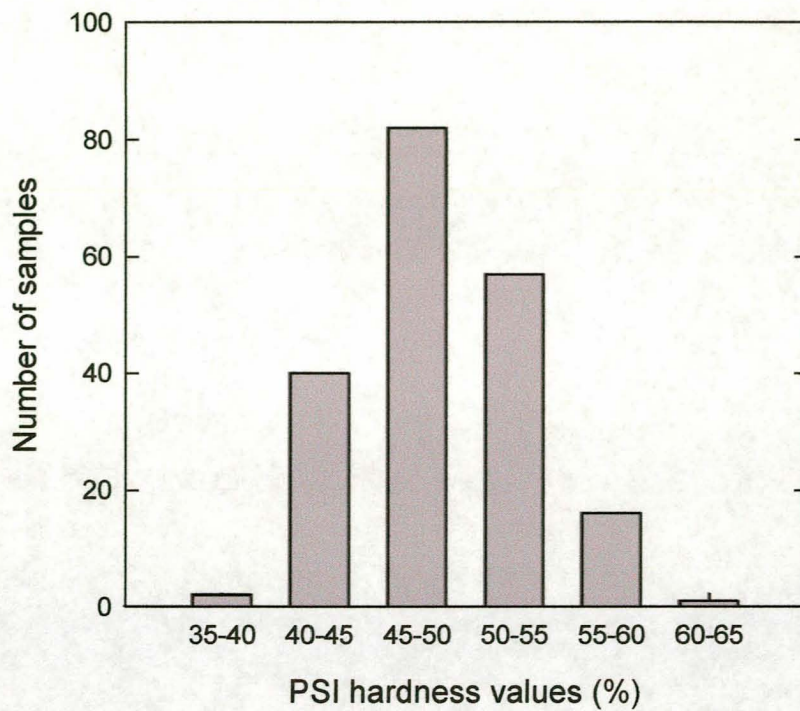


**Figure 2.** A bar chart of the hardness distribution for the samples as determined by the PSI method (with range: 37.05-60.5%).

**Table 3.** Statistical results for the hardness calibration.

<b>SEP</b>	<b>2.13%</b>
<b>RMSEP</b>	<b>4.53%</b>
<b>r</b>	<b>0.89</b>
<b>F-value</b>	<b>458.9</b>
<b>Bias</b>	<b>0.26</b>
<b>Number of PLS factors</b>	<b>8</b>

SEP = standard error of prediction

RMSEP = root mean standard error of prediction

r = correlation coefficient

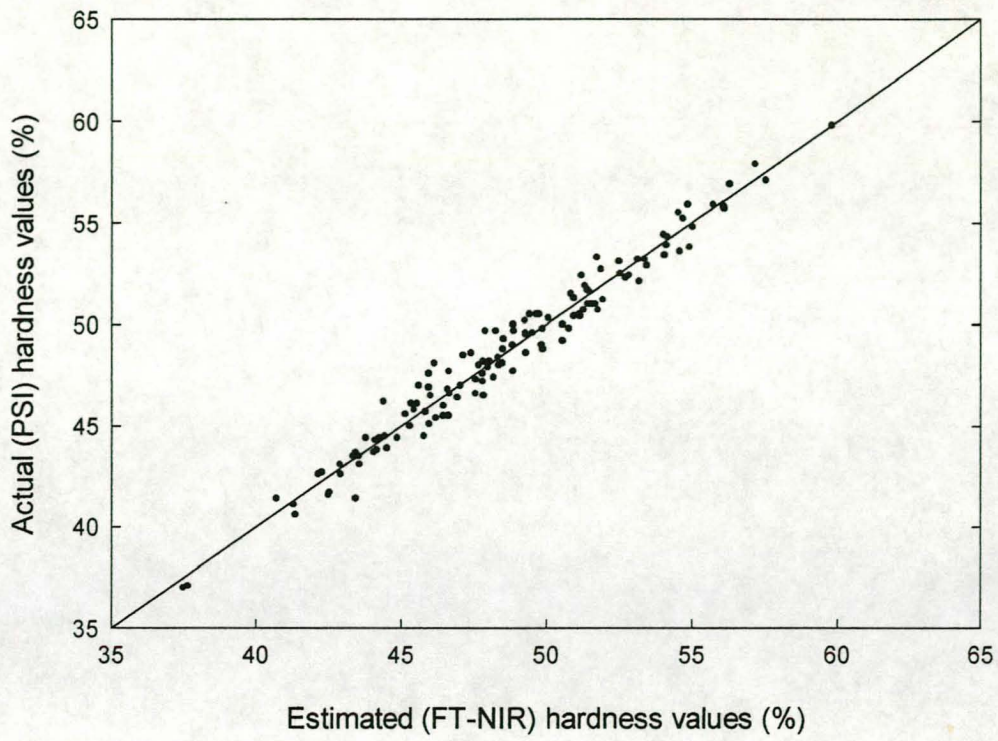


**Figure 3.** Scatter plot of the estimated (FT-NIR) hardness values and the actual (PSI) hardness values for the calibration set of the calibration model.



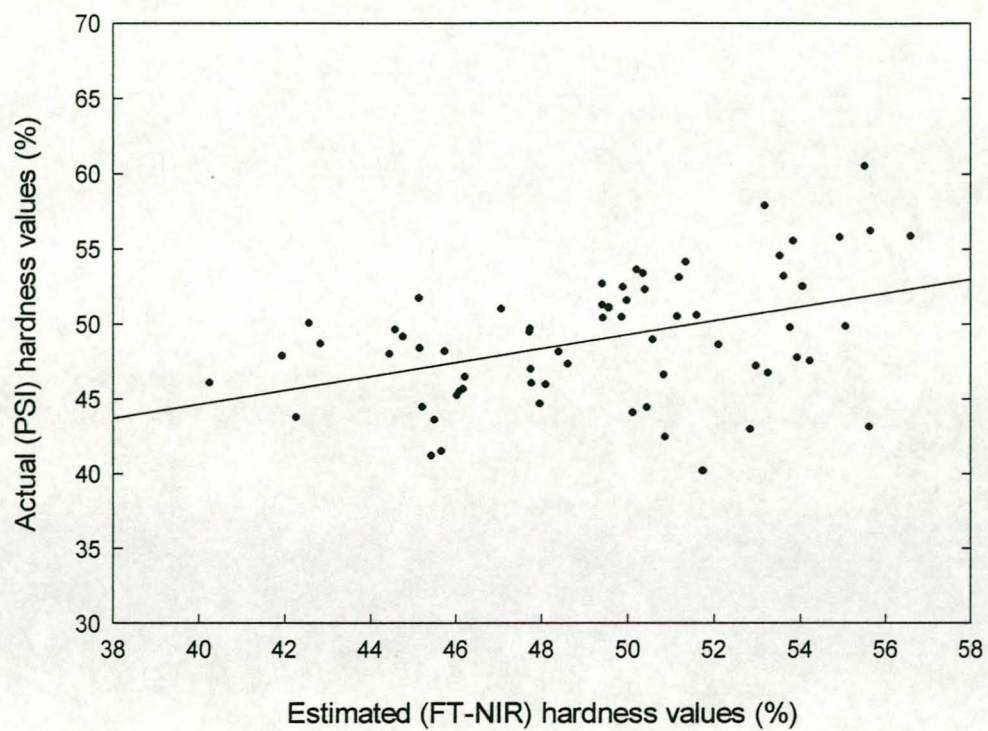


**Figure 4.** Scatter plot of the estimated (FT-NIR) hardness values and the actual (PSI) hardness values for the validation set of the calibration model.

studies in other countries (Williams, 1991; Manley, 1995). Manley (1995), for example, obtained a SEP and  $r$  of, respectively, 1.97% and 0.97 when whole ground wheat were calibrated using NIR reflectance spectroscopy.

### *Protein and moisture determinations*

The average results of duplicate protein and moisture determinations on the whole wheat flour samples are given in Table 4. The protein content ranges from 8.55 -12.70%, while the moisture content ranges from 10.18 - 17.73%.

### *Statistical analysis*

Results of the ANOVA performed on all the PSI hardness data showed that significant differences in hardness values occurred between samples of different cultivars, but that differences over localities were insignificant ( $P \leq 0.05$ ). Furthermore there were significant differences in protein values between samples of different cultivars and between different localities ( $P \leq 0.05$ ). No significant differences in moisture content were detected either between different cultivars or between different localities ( $P \leq 0.05$ ). All results were confirmed by Student's t-test ( $P \leq 0.05$ ). The specific cultivars and localities where differences in hardness and/or protein were detected can be seen in Tables 5 - 7. In Table 5 it is clear that significant differences in hardness especially occurred between the cultivars Kariega and SST 75, while the most significant differences in protein content occurred between Nantes and SST 57 (Table 6). With regards to localities, significant differences in protein content were found between samples obtained from Langgewens and Porterville (Table 7). There were no significant differences in protein content between samples obtained from the remaining 4 localities.

The results of the correlation analysis when the data of all 198 samples were used showed that a positive linear relationships exists between kernel hardness and protein content and a negative linear relationship between kernel hardness and moisture content. Therefore it can be said, with 95% certainty, that

**Table 4.** The protein and moisture content of all the whole wheat flour samples.

Location	Cultivar	Protein (%)			Moisture (%)		
		Rep 1	Rep 2	Rep 3	Rep 1	Rep 2	Rep 3
Philadelphia	Palmiet	11.48	11.03	12.00	9.80	12.00	12.00
	SST 38	11.16	11.09	12.00	11.75	12.10	11.85
	SST 55	11.98	12.83	11.12	12.00	12.10	12.25
	SST 57	10.82	10.86	12.26	11.60	10.90	11.70
	SST 65	12.30	11.03	11.31	9.80	12.20	11.85
	SST 66	11.87	11.77	11.31	12.00	12.20	12.05
	SST 75	12.15	12.26	11.46	11.90	11.95	11.85
	SST 825	10.89	10.94	10.94	10.20	12.35	12.05
	Adam Tas	12.10	13.31	12.17	9.10	11.95	12.00
	Nantes	11.49	16.53	12.45	8.75	12.20	12.00
Langgewens	Kariega	10.97	11.06	11.57	12.15	12.20	12.05
	Palmiet	16.63	17.01	13.36	10.95	11.50	11.75
	SST 38	17.50	15.70	17.01	10.95	11.70	11.95
	SST 55	15.71	14.51	16.50	11.30	11.50	11.80
	SST 57	14.27	14.22	16.64	9.25	11.75	11.80
	SST 65	15.34	15.93	16.44	9.45	11.60	11.80
	SST 66	15.70	16.52	16.33	11.25	11.70	11.65
	SST 75	15.58	15.28	16.27	11.20	11.65	11.50
	SST 825	14.79	16.30	15.39	11.25	11.65	11.75
	Adam Tas	16.82	15.65	16.84	11.40	11.70	8.95
Porterville	Nantes	16.01	15.96	15.70	11.65	11.60	8.55
	Kariega	16.03	15.39	17.73	11.60	11.55	9.80
	Palmiet	14.76	14.42	15.73	11.80	11.90	8.90
	SST 38	17.62	14.76	14.02	11.65	11.80	9.15
	SST 55	14.93	13.74	16.62	11.90	11.95	11.15
	SST 57	15.08	13.77	14.31	11.60	11.70	11.20
	SST 65	15.09	13.62	13.65	11.75	11.80	11.00
	SST 66	15.02	14.68	16.53	11.50	11.85	11.15
	SST 75	14.50	13.71	13.48	11.30	11.40	11.05
	SST 825	14.93	13.25	13.82	11.60	11.80	10.95
	Adam Tas	14.98	13.22	15.25	11.65	11.75	11.00
	Nantes	16.22	13.82	14.79	11.60	11.85	10.95
	Kariega	15.55	13.82	14.56	11.60	11.80	11.70
	SST 38	11.40	11.49	11.17	12.45	12.25	11.60

Table 4 continued / ...

Location	Cultivar	Protein (%)			Moisture (%)		
		Rep 1	Rep 2	Rep 3	Rep 1	Rep 2	Rep 3
Matjiesfontein	Palmiet	11.60	11.46	11.60	12.45	12.55	11.75
	SST 55	11.80	11.54	11.34	12.65	12.55	11.80
	SST 57	11.67	11.26	10.52	12.45	12.65	11.85
	SST 65	11.63	11.71	12.14	12.50	12.45	11.80
	SST 66	11.93	11.97	11.46	12.60	12.60	11.75
	SST 75	11.54	11.69	11.86	12.25	12.15	12.05
	SST 825	11.65	12.14	11.40	12.35	12.45	11.80
	Adam Tas	12.52	12.54	11.37	12.20	12.10	11.90
	Nantes	12.38	12.31	12.01	12.20	12.20	11.95
Tygerhoek	Kariega	11.97	11.86	11.09	12.25	12.40	11.60
	Palmiet	12.84	13.22	10.18	12.45	12.55	12.00
	SST 38	11.25	14.31	12.31	12.55	12.60	11.90
	SST 55	10.92	11.26	12.20	12.70	12.70	11.85
	SST 57	11.24	12.94	11.29	12.45	12.60	11.80
	SST 65	11.13	13.48	11.97	12.50	12.50	11.70
	SST 66	12.13	13.62	12.71	12.20	12.60	11.70
	SST 75	10.62	12.43	11.34	12.35	12.40	11.60
	SST 825	11.14	13.62	12.43	12.30	12.40	11.70
Voorstekop	Adam Tas	13.65	12.00	12.11	12.35	12.50	11.70
	Nantes	12.58	13.05	12.51	12.15	12.55	11.80
	Kariega	12.58	13.31	12.26	12.25	12.65	11.70
	Palmiet	11.56	12.14	12.03	12.35	12.25	12.00
	SST 38	11.17	11.51	11.51	12.45	12.30	12.10
	SST 55	11.84	11.51	11.63	12.60	12.40	12.00
	SST 57	11.89	12.08	11.63	12.25	12.25	12.05
	SST 65	11.09	11.57	11.86	12.15	12.10	12.05
	SST 66	12.11	11.94	11.91	12.50	11.85	11.85
	SST 75	12.23	11.49	11.17	12.50	11.85	11.85
	SST 825	11.37	11.60	12.34	12.15	12.10	11.95
	Adam Tas	12.75	12.03	12.26	12.30	12.10	11.85
	Nantes	11.71	12.45	12.20	12.15	12.00	12.05
	Kariega	11.31	11.46	11.34	12.20	11.34	12.05

**Table 5.** An outlay of the differences in hardness occurring over different cultivars as determined by Student's t-test.

Cultivar	n	Mean PSI (%)	T-grouping <sup>+</sup>			
Kariega	18	50.50		a		
SST 55	18	50.34	b	a		
SST 38	18	49.58	b	a	c	
SST 66	18	49.01	b	a	c	d
SST 825	18	48.87	b	a	c	d
Adam Tas	18	48.37	b	a	c	d
Nantes	18	48.03	b		c	d
SST 57	18	47.95			c	d
SST 65	18	47.92			c	d
Palmiet	18	47.33			c	d
SST 75	18	47.08				d

<sup>+</sup> Means with the same letter indicates no significant differences

**Table 6.** A layout of the differences in protein content values over different cultivars as determined by Student's t-test.

Cultivar	n	Mean protein (%)	T-grouping <sup>+</sup>			
Nantes	18	13.57			a	
Adam Tas	18	13.42	b		a	
SST 66	18	13.31	b		a	c
SST 38	18	13.20	b	d	a	c
Kariega	18	12.99	b	d	e	c
Palmiet	18	12.91	b	d	e	c
SST 55	18	12.88		d	e	c
SST 65	18	12.84		d	e	c
SSt 75	18	12.73		d	e	
SST 825	18	12.71		d	e	
SST 57	18	12.59			e	

<sup>+</sup> Means with the same letter indicates no significant differences

**Table 7.** A layout of the differences in protein content values over different localities as determined by Student's t-test.

Locality	n	Mean protein (%)	T-grouping*
Langgewens	33	15.91	a
Porterville	33	14.67	b
Tygerhoek	33	12.26	c
Voorstekop	33	11.78	c
Philadelphia	33	11.77	c
Matjiesfontien	33	11.70	c

\* Means with the same letter indicates no significant differences

protein content increases and moisture content decreases with increasing kernel hardness in wheat. Upon additional correlation analysis of the samples of each cultivar and within each locality, it was found that these relationships were only present within certain cultivars and localities in the Southern and Western Cape ( $P \leq 0.05$ ). These cultivars and localities, together with the results of the regression analysis, which describes the relationship by means of a regression equation, can be seen in Tables 8 & 9.

## **Conclusions**

The PSI and FT-NIR spectroscopy methods can both be successfully used to measure South African, and specifically Southern and Western Cape bread wheat cultivars for kernel hardness. Fourier transform near infrared spectroscopy calibration results compare well with similar studies in other wheat producing countries (Williams, 1991; Manley, 1995). The hardness range of the examined local wheat samples were particularly wide 37.05 - 60.50%, although the majority of determinations were within the range of 45 - 55%. Statistical analysis determined that wheat hardness values are significantly influenced by genotype, but not by growth location. Hardness has linear relationships with both protein- and moisture content in that there is an increase in protein content and a decrease in moisture content with increasing kernel hardness.

**Table 8.** The cultivars within which linear relationships between hardness and protein and/or moisture content exist and a description of such relationships.

Cultivar	Hardness-protein relationship	Hardness-moisture relationship	Regression <sup>♦</sup> equation
Adam Tas	Positive linear		$y = 26.34 + 1.64x$
Adam Tas		Negative linear	$y = 85.3 - 31.6a$
Nantes	Positive linear		$y = 34.67 + 0.98x$
SST 66	Positive linear		$y = 33.37 + 1.18x$
SST 825		Negative linear	$y = 109.18 - 5.09a$

♦ where  $y$  = PSI hardness (%)  
 $x$  = Protein content (%)  
 $a$  = Moisture content (%)

**Table 9.** The localities within which linear relationships between hardness and protein and/or moisture content exist and a description of such relationships.

Locality	Hardness-protein relationship	Hardness-moisture relationship	Regression equation
Langgewens	Positive linear		$y = 27.47 + 1.36x$
Porterville	Positive linear		$y = 32.60 + 1.31x$
Porterville		Negative linear	$y = 74.60 - 2.01a$

♦ where  $y$  = PSI hardness (%)  
 $x$  = Protein content (%)  
 $a$  = Moisture content (%)



## References

- Anjum, O.S. & Walker, J.H. (1991). Review on the significance of starch and protein to wheat kernel hardness. *Journal of the Science of Food and Agriculture*, **56**, 1-13.
- Anonymous. (1997a). *Perkin Elmer FT-NIR spectroscopy application note: The determination of protein and moisture in samples of wheat*. The Perkin Elmer Corporation. Beaconsfield, UK: Technical Publications.
- Anonymous. (1997b). *Spectrum Quant+ User's Reference*. The Perkin Elmer Corporation. Beaconsfield, UK: Technical Publications.
- AOAC (1990). Protein (crude) in animal feed: Dumas method. Method 68.06. In: *Official Methods of Analysis of the AOAC (15<sup>th</sup> edition)*. Virginia, USA: Association of Official Analytical Chemists Inc.
- Barlow, K.K., Buttrose, M.S., Simmonds, D.H. & Vesk, M. (1973). The nature of the starch-protein interface in wheat endosperm. *Cereal Chemistry*, **50**, 443-454.
- Carver, B.F. (1994). Genetic implications of kernel NIR hardness on milling and flour quality in bread wheat. *Journal of the Science of Food and Agriculture*, **65**, 125-132.
- Cutler, G.H. & Brinson, G.A. (1939). The granulation of wholemeal and a method of expressing it numerically. *Cereal Chemistry*, **12**, 120.
- Delwiche, R., Chen, Y. & Hruschka, W.R. (1995). Differentiation of hard red wheat by near infrared analysis of bulk samples. *Cereal Chemistry*, **72**, 243-247.
- Delwiche, R. & Norris, K.H. (1993). Classification of hard red wheat by near infrared diffuse reflectance spectroscopy. *Cereal Chemistry*, **70**, 29-35.
- Hoseney, R.C. (1987). Wheat hardness. *Cereal Foods World*, **32**, 320-322.
- James, C.S. (1995). Experimental procedures. In: *Analytical Chemistry of Foods*. Pp. 73-74. UK: Blackie Academic & Professionals.
- Kent, N.L. & Evers A.D. (1994). *Kent's Technology of Cereals (4<sup>th</sup> edition)*. Pp.1-5, 78-82. Oxford, UK: Elsevier Science Ltd.

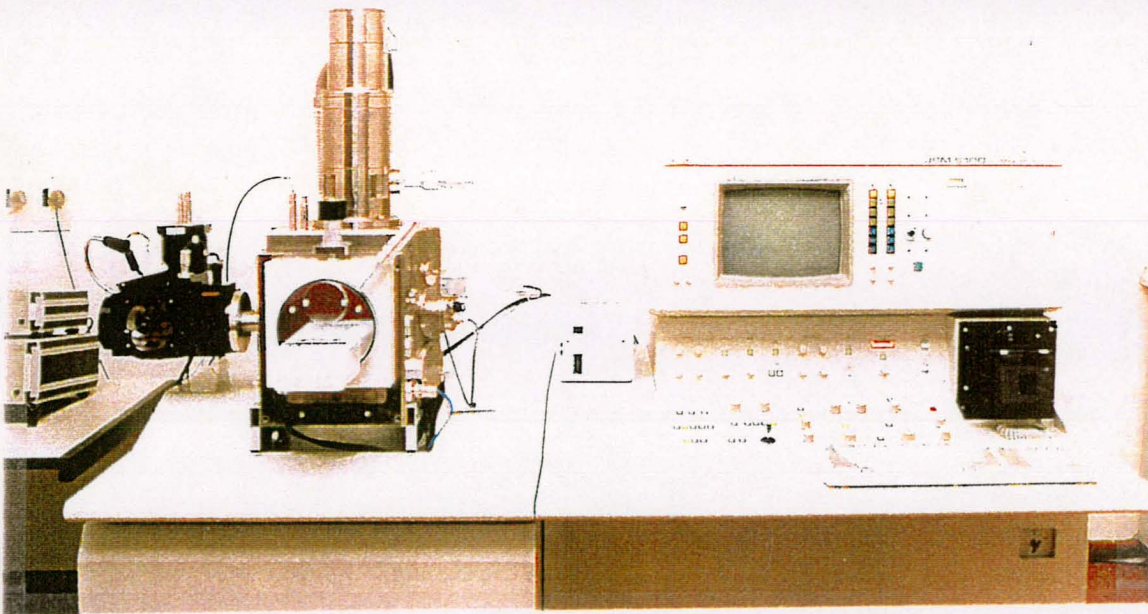
- Manley, M. (1995). *Wheat hardness by near infrared (NIR) spectroscopy: New insights*, PhD. thesis, University of Plymouth, United Kingdom.
- Norris, K.H., Hruschka, W.R., Bean, M.M. & Slaughter, D.C. (1989). A definition of wheat hardness using near infrared reflectance spectroscopy. *Cereal Foods World*, **34**, 696-704.
- Ohm, J.B., Chungm, O.K. & Deyoe, C.W. (1998). Single kernel characteristics of hard winter wheats in relation to milling and baking quality. *Cereal Chemistry*, **75**, 156-161.
- Osborne, B.G. & Fearn, T. (1983). Collaborative evaluation of near infrared reflectance analysis for the determination of protein, moisture and hardness in wheat. *Journal of the Science of Food and Agriculture*, **34**, 1011-1017.
- Pomeranz, Y. & Williams, P.C. (1990). Wheat hardness: its genetic, structural and biochemical background, measurement and significance. In: *Advances in cereal science and technology* (edited by Y. Pomeranz). Pp. 471-548. Minnesota, USA: American Association of Cereal Chemists Inc.
- Simmonds, D.H., Barlow, R.R. & Wrigley, C.W. (1973). The biochemical basis of grain hardness in wheat. *Cereal Chemistry*, **50**, 553-562.
- Sorvaniemi, J., Kinnunen, A., Mälkki, Y. & Tsados, A. (1993). Using partial least squares regression and multiplicative scatter correction for FT-NIR data evaluation of wheat flours. *Journal of Food Science and Technology*, **26**, 251-258.
- Symes, K.J. (1965). The inheritance of grain hardness in wheat as measured by the particle size index. *Australian Journal of Agricultural Resources*, **16**, 113-123 (as cited by Pomeranz & Williams, 1990).
- Van Deventer, C.S. (1999). Koringbedryf moet kyk na nuwe klassifikasie stelsel. *Landbouweekblad*, **1098**, 10-13.
- Williams, P.C. (1991). Prediction of wheat kernel texture in whole grains by near infrared transmittance. *Cereal Chemistry*, **68**, 112-114.

Williams, P.C. & Sobering, D.C. (1986a). Attempts at standardisation of hardness testing of wheat. II. The near infrared reflectance method. *Cereal Foods World*, **31**, 417-420.

Williams, P.C. & Sobering, D.C. (1986b). Attempts at standardisation of hardness testing of wheat. I. The grinding/sieving (Particle Size Index) method. *Cereal Foods World*, **31**, 359-364.

## Chapter 5

A comparative scanning electron microscopy (SEM) study of a number of South African and Canadian wheats of different hardnesses



## Chapter 5

### **A COMPARATIVE SCANNING ELECTRON MICROSCOPY (SEM) STUDY OF SOUTH AFRICAN AND CANADIAN WHEATS OF DIFFERENT HARDNESSES**

#### **Summary**

A number of different South African wheat cultivars were compared for hardness-related structural differences using scanning electron microscopy (SEM). The cultivars examined were Kronos (durum wheat), T4, SST 876, Gariiep, SST 75 (bread wheats) and Wit Wol (soft wheat). Six Canadian wheat samples, one each of the durum and soft wheat classes and four bread wheats (western extra strong, hard red spring, prairie spring red and hard red winter), were also examined for comparative reasons. For each cultivar a cross section of the kernel endosperm and a sample of its whole wheat flour were examined. Kronos and its flour have a similar structure to the Canadian durum wheat and flour, having a tightly packed protein-starch matrix and a high degree of starch damage. Both the South African and Canadian bread wheat samples examined, revealed a large range of hardnesses and therefore a great difference in endosperm structures. The continuity of the protein-starch matrix and the degree of starch damage differ within the South African bread wheat class, with T4 and SST 75 being, respectively, the hardest and the softest of the examined cultivars. The structure of the South African and Canadian soft wheat cultivars are similar, both revealing a discontinuous matrix, free starch granules and little or no starch damage. Results of this study confirm the theory that wheat hardness is determined by the strength of the protein-starch bond in the endosperm. The South African wheat, milling and baking industry may benefit by recognizing the great variety in hardness within the bread wheat class and adopting a classification system similar to the Canadian system, where the bread wheat class is sub-classified according to kernel hardness as determined by the particle size index (PSI) method.

## Keywords

Protein-starch matrix, scanning electron microscopy, starch, wheat hardness

## Introduction

Wheat hardness can be described as "the resistance to fracture upon grinding, slicing, abrasion or indentation of a single kernel or bulk samples" (Anjum & Walker, 1991) or as "not easily penetrated or separated into parts" (Pomeranz & Williams, 1990). It is of great importance in the milling process and affects the end-use properties of wheat. There are many theories on the mechanism of wheat hardness, the most widely accepted one being that differences in hardness between different wheat varieties are the result of differences in the strength of adhesion between the starch granules and storage protein in the endosperm (Barlow *et al.*, 1973; Simmonds *et al.*, 1973). There is a higher degree of adhesion between starch and protein in hard wheats than in soft wheats, causing a higher degree of fracturing to occur through the starch granules rather than at the interface between the starch and protein (Pomeranz & Williams, 1990). Hard wheats would therefore suffer more starch damage from milling, yielding more granular flour suitable for bread-making.

Scanning electron microscopy (SEM) produces magnified images using electrostatic or electromagnetic lenses with fast moving electrons as illumination and is used to study the outside features of bulk materials (Goldstein *et al.*, 1992; Watt, 1997). It has been used successfully in viewing the structural differences between wheats of different hardnesses (Barlow *et al.*, 1973; Hosney & Seib, 1973; Moss *et al.*, 1980; Davis & Eustage, 1984; Glenn & Saunders, 1990). It is preferred over light spectroscopy in the study of the structure of cereal grains as better depth of focus is afforded at equivalent magnifications (Evers, 1969). Furthermore, the problematic swelling of especially protein in the endosperm during light spectroscopy studies is eliminated in SEM studies where an aqueous media is not required (Moss *et al.*, 1980).

Hoseney & Seib (1973) studied the endosperm structure of soft red winter, hard red winter and durum wheats as well as their flours using an ETEC scanning electron microscope. Magnifications of the endosperm showed that the protein was adhered to the starch more tightly and there was a higher degree of starch damage present in the durum and hard red winter wheat than in the case of the soft red winter wheat. Magnifications of the durum and hard red winter wheat flours showed that the protein-starch matrix was still intact and that many starch granules on the surface of particles were damaged. The flour of the soft red winter wheat was a mixture of free starch, free protein and small aggregates of protein and starch, and there were no fractured or damaged starch granules. These findings supported the theory that the hardness of wheat is determined by the strength of the protein-starch bond (Barlow *et al.*, 1973; Simmonds *et al.*, 1973).

In another interesting study SEM was used to provide visual evidence of the great variability in the milling properties of different classes of wheat under commercial milling conditions (Davis & Eustage, 1984). Samples of hard red winter, soft red winter and durum wheat was collected at various stages during the milling process and observed with an ETEC U01 scanning electron microscope. The results suggested that soft wheat endosperm is more readily removed from its bran than is endosperm from hard wheat and that the disintegration of soft wheat endosperm is accomplished more quickly.

As yet no electron microscopy work has been done on the hardness-related structural differences of South African wheats or their flours. It has been established that there is a great variety in hardness within wheats of the South African bread wheat class (Chapter 4). There is, however, no classification system where cultivars can be sub-classified according to kernel hardness as is the case in Canada (Van Deventer, 1999; Williams, 1999). The Canadian bread wheat class also has great variety in kernel texture and is therefore further categorized, according to hardness, as determined by the PSI method, into five sub-classes (western extra strong, hard red spring, hard red winter, prairie red spring and prairie white spring) (Williams, 1999).

The aim of this study was to examine the structure of South African wheat cultivars, particularly bread wheat, and their flours of varying hardnesses. It was further compared to the structure of Canadian wheats and flours with similar hardnesses. If the South African bread wheat cultivars reveal significant differences in endosperm and flour texture, and therefore also in hardness, it may be beneficial for the South African milling and baking industries to consider a new wheat classification system where such differences are accounted for.

## **Material and methods**

### *Scanning electron microscopy*

Six wheat samples of different cultivars and localities in South Africa were selected for scanning electron microscopy examination. The selected cultivars were Kronos (durum wheat), SST 876, SST 75, Gariep, T4 (bread wheats) and Wit Wol (soft wheat). Six Canadian wheat samples (durum, western extra strong, hard red spring, prairie spring red, hard red winter and soft white spring wheat) and their corresponding flours were also selected and examined. In both cases the whole flour was obtained by using a UDY Cyclone mill fitted with a 1 mm screen.

Grains were fractured transversely using a blunt razor blade and applying downward pressure across the mid-dorsal region. Care was taken not to cut the grain to ensure that fractures occurred at the inherent weak points in the endosperm, exposing significant structural details. These wheat cross sections were mounted on aluminium stubs using double-sided adhesive tape and the sides coated with silver paint to minimize the occurrence of charging. The wheat samples were then coated with gold alloy and viewed with a JSM-6100 Scanning Microscope (Jeol). Flour samples were mounted on aluminium stubs and sputtered with gold in preparation for viewing. An accelerating voltage of 7 kV was used.



### *Particle size index (PSI) hardness test*

The hardness of all the South African and Canadian wheat samples was determined by means of the particle size index (PSI) test as described by Williams & Sobering (1986).

A representative sample (ca. 50 g) of a whole grain wheat sample was ground by means of a UDY Cyclone mill with a 1 mm screen. A sample of the ground wheat (10 g weighed to the nearest 0.01 g) was transferred to a 75  $\mu\text{m}$  sieve with a receiving pan. Approximately 50 g of whole grain kernels was added to prevent clogging of the sieves and the sieve covered with a lid. The sample was sieved for exactly 10 minutes on an automatic sieve shaker (Endocott). All the throughs, including those adhering to the bottom of the sieve, was transferred into the receiving pan and the throughs weighed to the nearest 0.01 g. The final result was expressed as the percentage throughs (equation 1). All the tests were performed in duplicate.

$$\% \text{ throughs} = \frac{w_1}{w_2} \times 100 \quad \dots 1$$

where  $w_1$  = mass of throughs

$w_2$  = mass of original flour sample

## **Results and discussion**

The average PSI hardness values for all the examined Canadian and South African wheat cultivars are tabulated in Table 1. The Canadian durum wheat has the lowest PSI result, corresponding to the hardest kernel texture of the examined cultivars, followed by the South African durum cultivar, Kronos. There is a wide range in hardness in both the Canadian and South African bread wheat cultivars. The Canadian bread wheat hardness range includes wheats with particularly high PSI measurements, bordering on the South African soft wheat

**Table 1.** Particle size index (PSI) hardness values for all SEM examined wheat samples.

	<b>Cultivars</b>	<b>PSI hardness values (%)</b>
<b>Canadian</b>	Durum	33.83
	Western extra strong	43.41
	Hard red spring	48.50
	Prairie spring red	55.24
	Hard red winter	58.33
	Soft white spring	62.66
<b>South African</b>	Kronos	34.42
	T4	43.17
	SST 876	46.38
	Gariep	49.10
	SST 75	52.33
	Wit Wol	58.77

hardness range. The examined Canadian soft wheat cultivar is softer than the examined South African soft wheat cultivar.

### *Canadian wheat samples*

#### Durum wheat

Figure 1 shows a cross section of the endosperm of a Canadian durum wheat kernel that has been cut during sample preparation instead of being fractured. All structural detail was lost, illustrating the importance of fracturing the wheat at its inherent weakpoints.

A cross section of the endosperm of a durum wheat kernel, magnified 800X, is shown in Figure 2. A tightly packed structure of protein and starch with essentially no air spaces are noticeable. The protein appears to adhere strongly to the starch exposing little of the starch surface. There is a high number of starch granules that fractured when the kernel broke, indicating the strength of the protein-starch bond. When sufficient force was applied the starch granules rather than the protein-starch bond broke.

#### Bread wheat

In the photomicrograph of the strongest of the Canadian bread wheats, the western extra strong sample (Figure 3), the protein-starch matrix is still continuous, but the endosperm is not as tightly packed compared to the durum sample. More of the starch surface is exposed and the degree of starch damage is slightly less.

The cross section of the hard red spring wheat kernel (Figure 4), magnified 800X, shows protein still adhering tightly to the starch, but more of the starch surface is exposed. The existence in the wheat endosperm of two types of starch granules, differing in shape and size, is well known (Sanstedt, 1946; Evers, 1969; Hosney, 1986). The larger granules are generally lenticular while the smaller ones are spherical. These different types and sizes of granules are

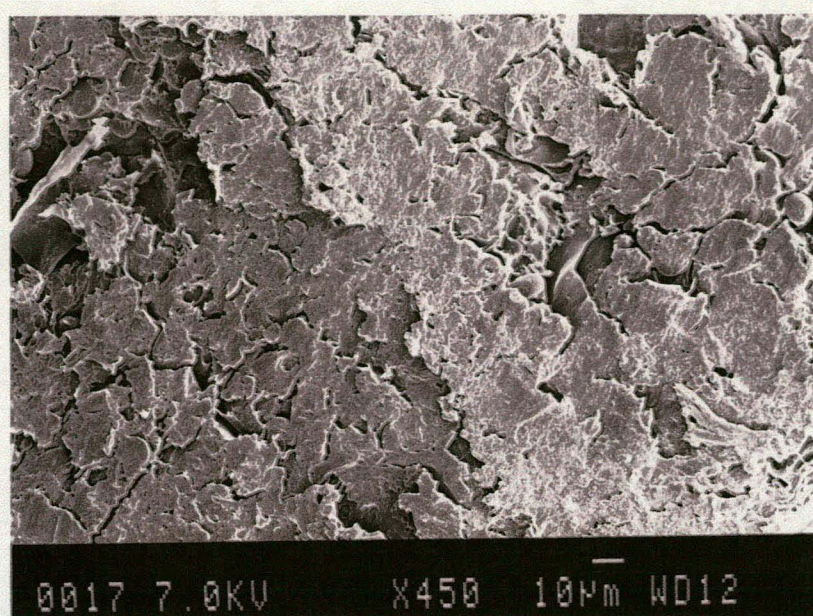


**Figure 1.** An example of the endosperm of a wheat kernel that was cut instead of fractured during cross sectioning.

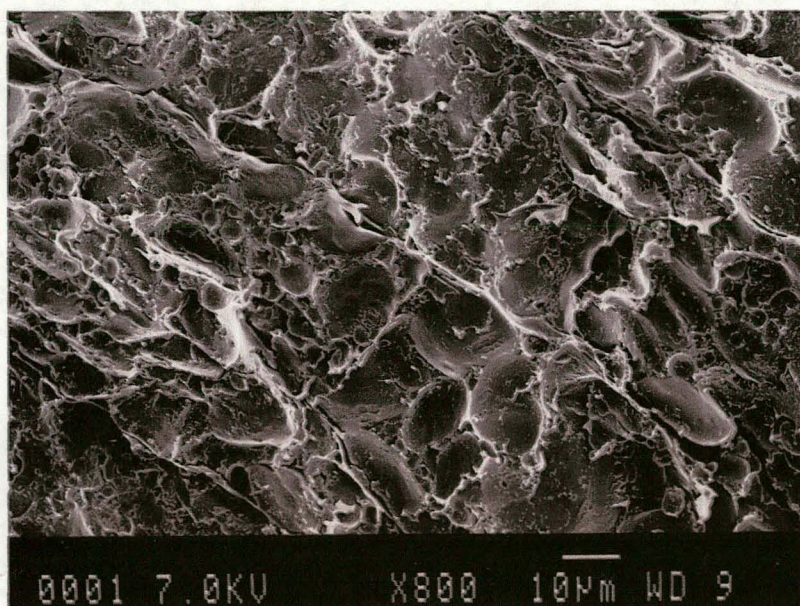


**Figure 2.** A cross section of the endosperm of the Canadian durum wheat sample, magnified 800X.

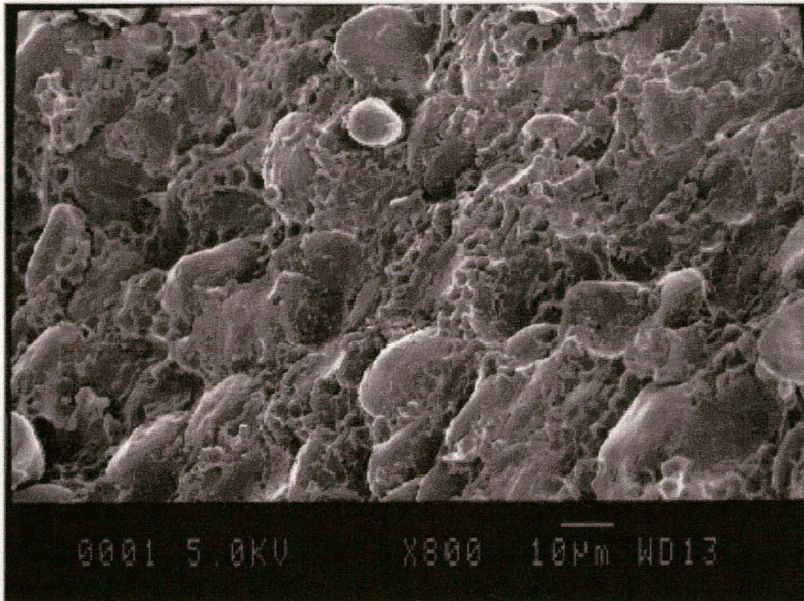


**Figure 3.** A cross section of the endosperm of the Canadian western extra strong wheat sample, magnified 800X.

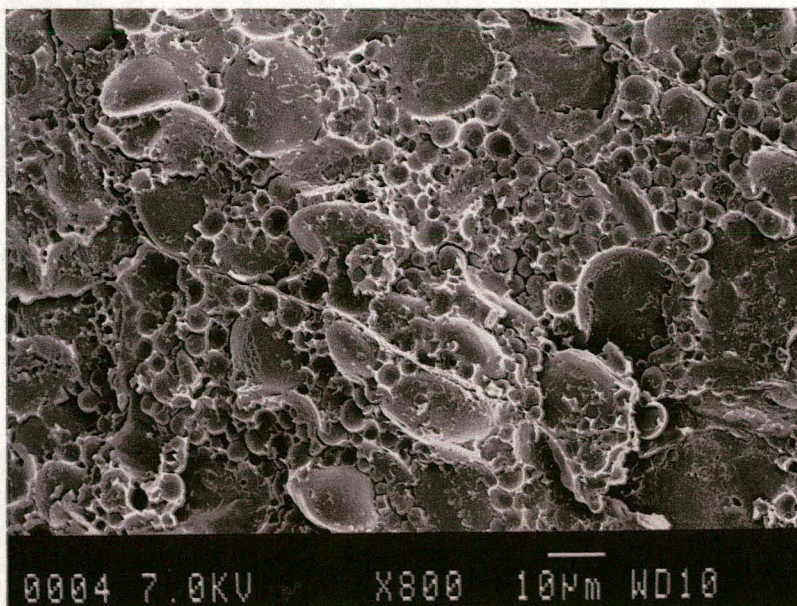


**Figure 4.** A cross section of the endosperm of the Canadian hard red spring wheat sample, magnified 800X.

clearly visible in this photomicrograph. There is a high degree of damaged starch, but there is also an amount of intact starch granules, especially the smaller sized ones. This indicates, as expected, a slightly weaker protein-starch association in the bread wheat compared to the durum wheat.

The prairie red spring wheat (Figure 5) has a greater amount of undamaged starch granules, although some starch damage is still apparent. Undamaged starch granules are becoming even more apparent in the photomicrograph of the endosperm of the hard red winter wheat (Figure 6). The protein-starch matrix is becoming discontinuous with air spaces and protein fragments becoming visible.

#### Soft wheat

Figures 7 & 8 show cross sections of the soft white spring wheat kernel, magnified 800X and 2500X, respectively. The structure appears to be much looser with air spaces becoming apparent. The starch surface is largely exposed and the protein matrix does not appear to be continuous. Again the size and shape of the starch granules varies, but noticeably almost all are intact. There is practically no starch damage, indicating that fracturing occurred through the weak protein-starch bond rather than through the starch granules.

#### *South African wheat samples*

##### Durum wheat

The cross section of the Kronos wheat endosperm (Figure 9) shows great similarities with the Canadian durum wheat sample (Figure 2), having a tightly packed, intact protein-starch matrix and a high degree of starch damage. This similarity is confirmed by their similar PSI hardness values of 34.42% and 33.83%, respectively.

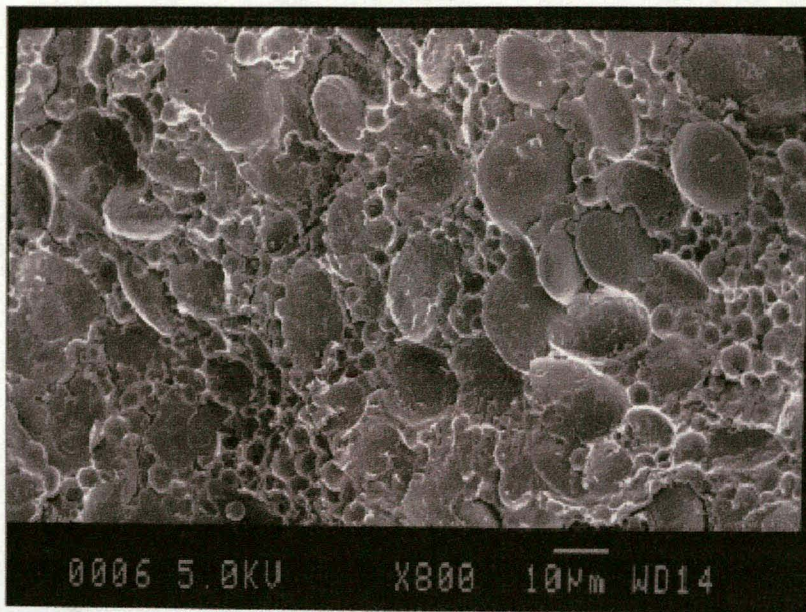


**Figure 5.** A cross section of the endosperm of the Canadian prairie spring red wheat sample, magnified 800X.

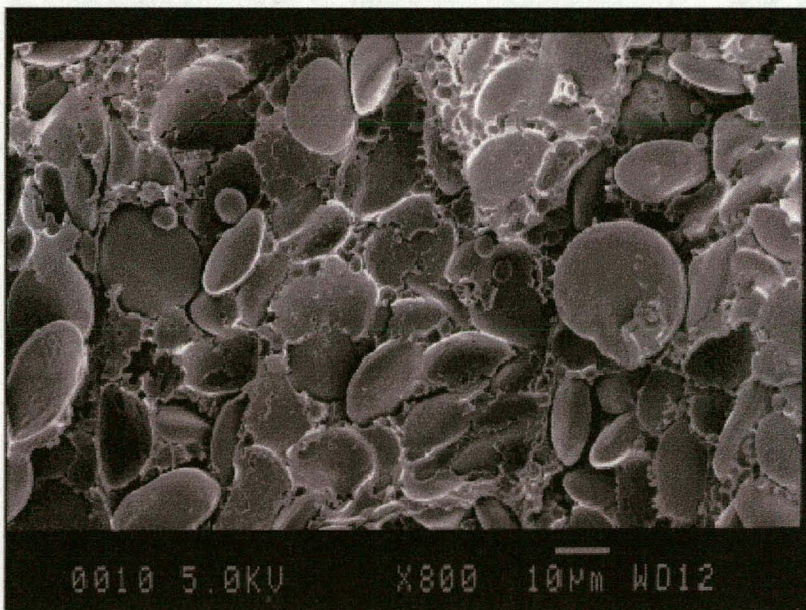


**Figure 6.** A cross section of the endosperm of the Canadian hard red winter wheat sample, magnified 800X.

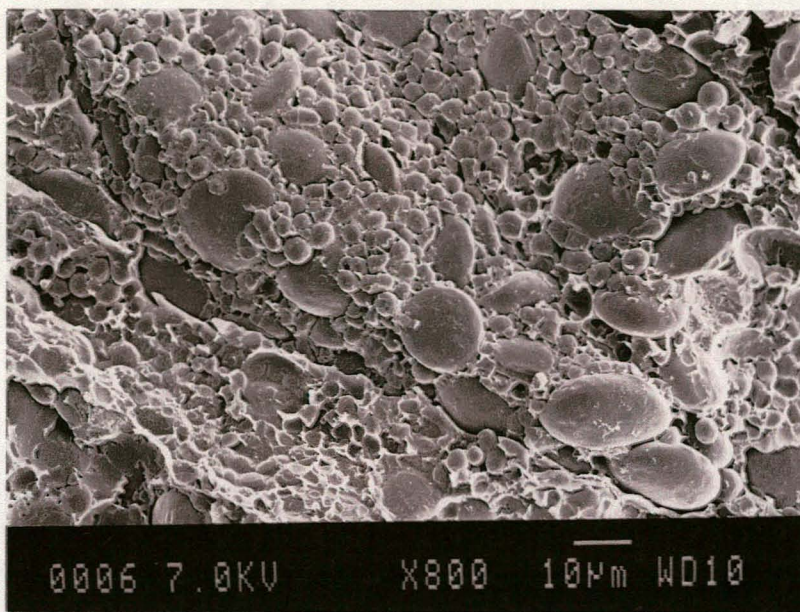


**Figure 7.** A cross section of the endosperm of the Canadian soft white spring wheat sample, magnified 800X.

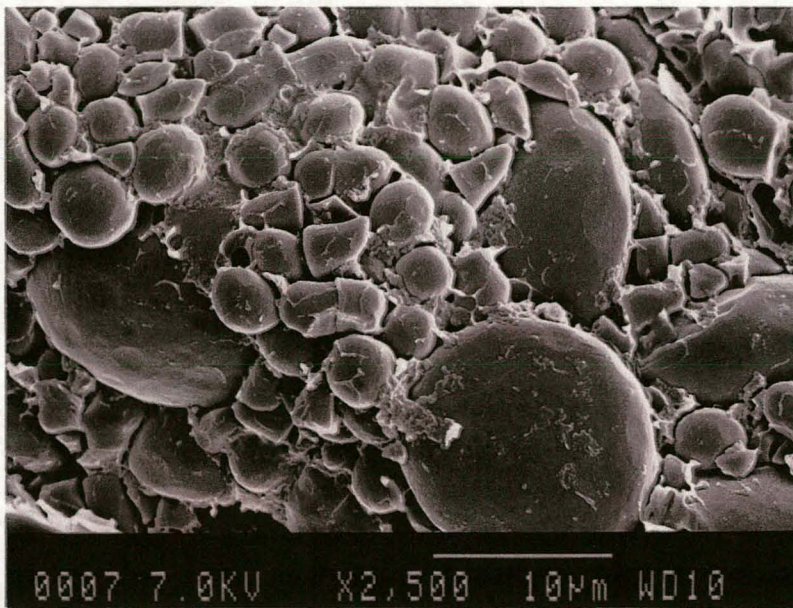


**Figure 8.** A cross section of the endosperm of the Canadian soft white spring wheat sample, magnified 2500X.



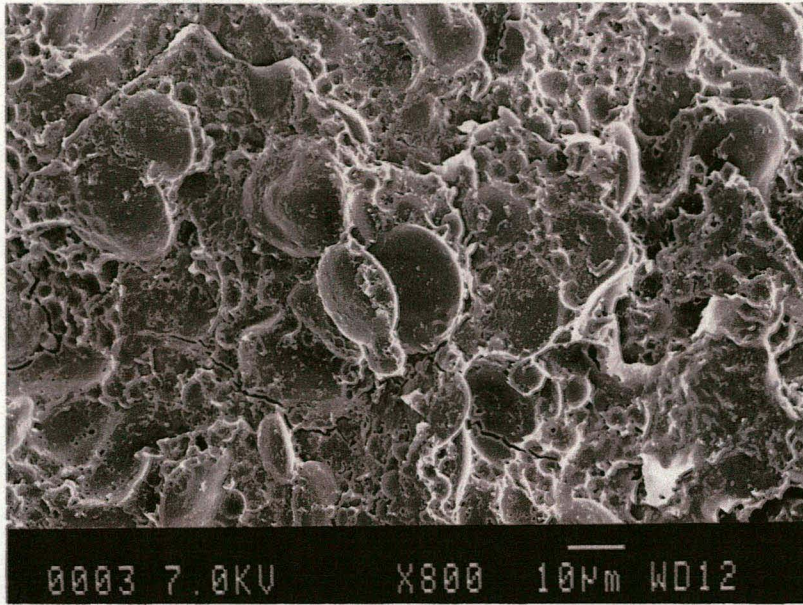


**Figure 9.** A cross section of the endosperm of the South African durum wheat sample, Kronos, magnified 800X.

## Bread wheat

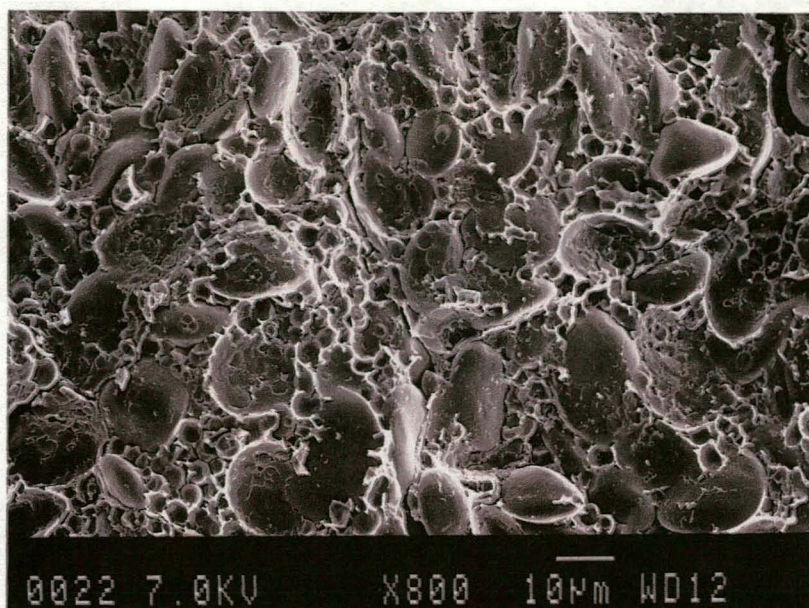
The cultivar T4 is the hardest of the examined bread wheat cultivars, followed by SST 876, Gariep and SST 75 as determined by the PSI test and confirmed by examination of their endosperm structure. In Figure 10, which is a cross section of the endosperm of the cultivar T4, the integrity of the protein matrix structure can still be observed with the protein adhering to the starch surface very well. There are little or no air spaces visible and there is a relatively great amount of starch damage present, especially of smaller sized granules.

The cultivar SST 876 (Figure 11) is slightly softer in comparison to T4. The protein-starch matrix is still continuous but there is a lesser degree of starch damage to particularly the smaller sized granules.

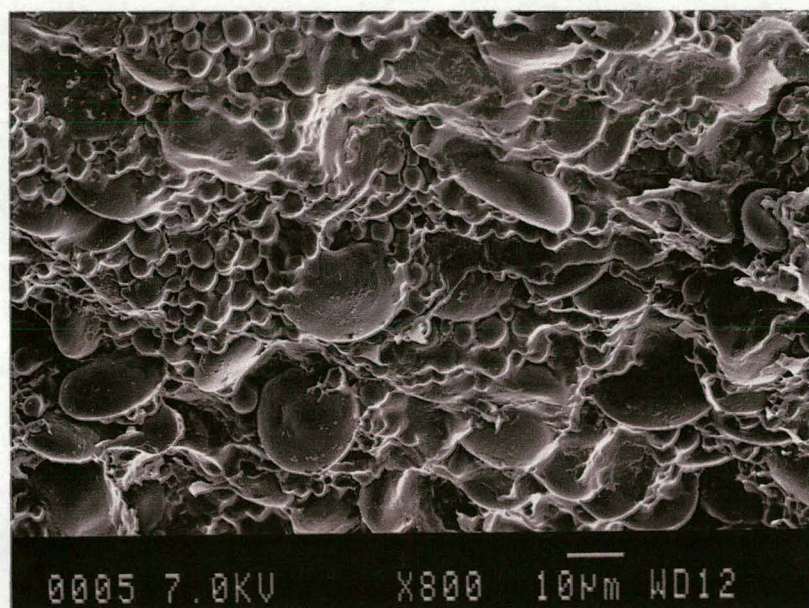
Figure 12 illustrates a cross section of the endosperm of the bread wheat cultivar Gariep, magnified 800X. The protein-starch matrix is breaking up, but protein is still covering much of the surface of the starch. Air spaces are becoming apparent and little starch damage occurred.

Figure 13 illustrates the endosperm of the softest of the examined bread wheat cultivars, SST 75. The protein is not adhering to the starch as much, exposing more of the starch surface. There are some free starch granules and only a small percentage of starch is damaged.

It is interesting to notice the differences in the shape and size of the starch granules between the different examined South African bread wheat samples. The two harder bread wheat samples (Figures 10 & 11) appears to have a larger amount of large spherical or elongated starch granules that are coated, to a large extent, by protein. Only a small amount of smaller sized starch granules are present. The two softer South African bread wheat samples (Figures 12 & 13) differ from this in that small, spherical, almost round starch granules are predominant.



**Figure 10.** A cross section of the endosperm of the South African bread wheat, T4, magnified 800X.



**Figure 11.** A cross section of the endosperm of the South African bread wheat, SST 876, magnified 800X.

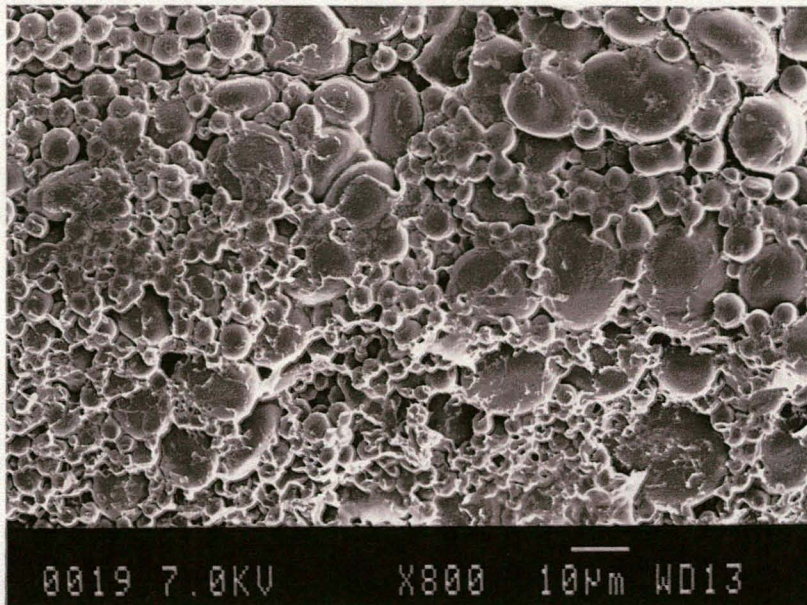


**Figure 12.** A cross section of the endosperm of the South African bread wheat cultivar, Gariep, magnified 800X.

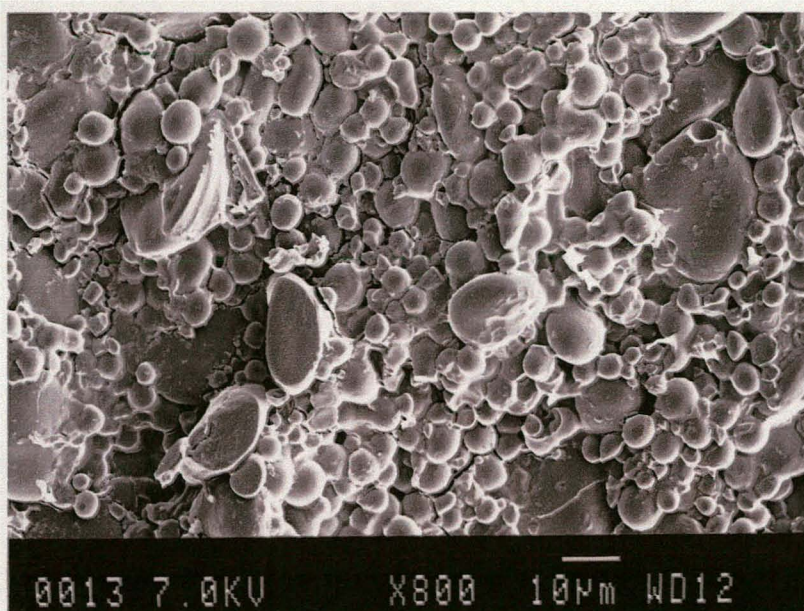


**Figure 13.** A cross section of the South African bread wheat sample, SST 75, magnified 800X.

## Soft wheat

Figures 14 & 15 show the endosperm of the South African soft wheat cultivar, Wit Wol, magnified 800X and 2500X, respectively. Aggregates of protein and starch as well as air spaces have formed. The surfaces of the starch granules are largely uncovered and some free starch granules are visible. The grain surface also reveals a number of cavities which formed when starch granules were dislodged during sectioning. The surfaces of the starch granules are undamaged. The average size of the starch granules is much bigger than that of the South African and Canadian bread wheats as well as the Canadian soft white spring wheat sample.

### *Outer layers and endosperm of wheat kernels*

It is well known that there is an inverse gradient involving protein and starch in wheat, with the protein percentage per unit mass of endosperm tissue increasing towards the periphery (Kent & Evers, 1994). Therefore the whole kernels of the South African wheats were not only investigated at a point deep in the starchy endosperm, but also at a point near the pericarp where protein is more predominant (Figures 16 - 21). For each sample the multi-layered pericarp, the aleuronlayer and the endosperm cells are clearly visible. The same tendency regarding endosperm structure prevailed as with the corresponding starchy endosperm photomicrographs (Figures 10 - 15), the protein-starch matrix becoming more discontinuous and the degree of starch damage decreasing with decreasing kernel hardness.

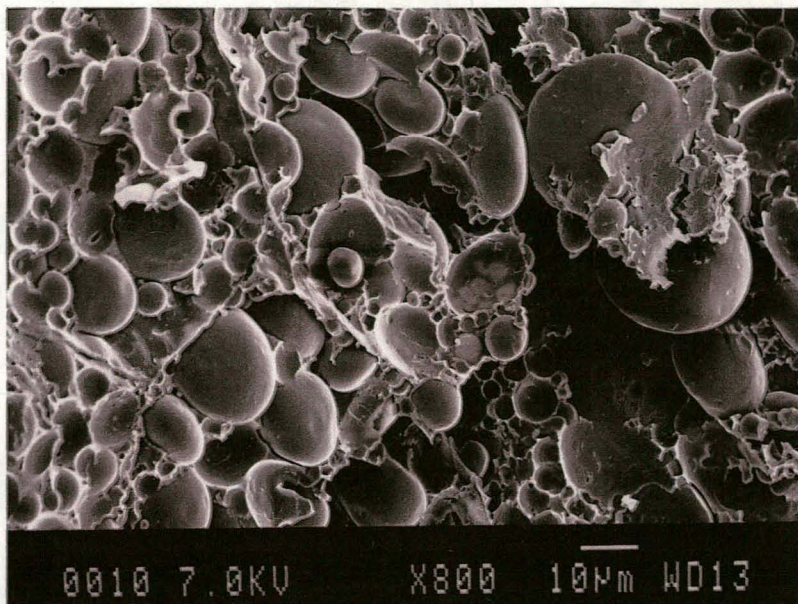


**Figure 14.** A cross section of the South African soft wheat sample, Wit Wol, magnified 800X.

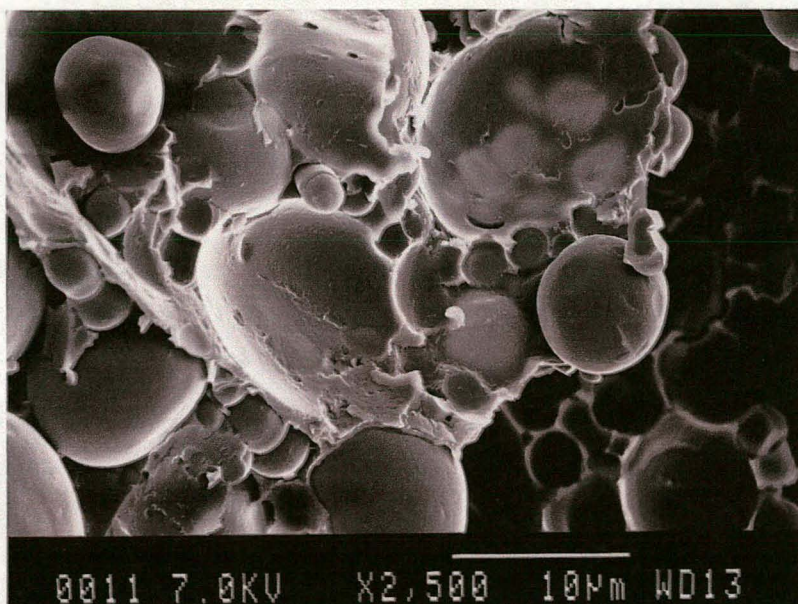


**Figure 15.** A cross section of the South African soft wheat cultivar, Wit Wol, magnified 2500X.

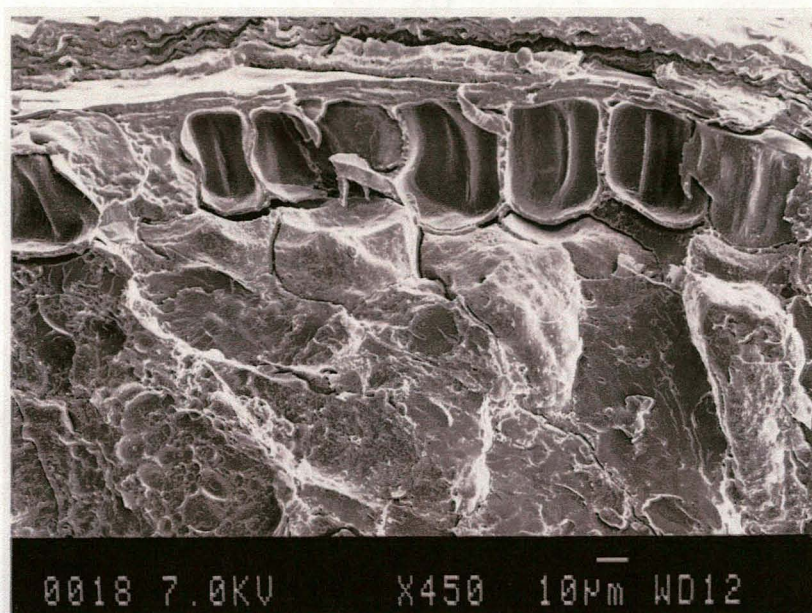


**Figure 16.** A photomicrograph of the different outer layers and the endosperm of the South African durum wheat, Kronos, magnified 450X.

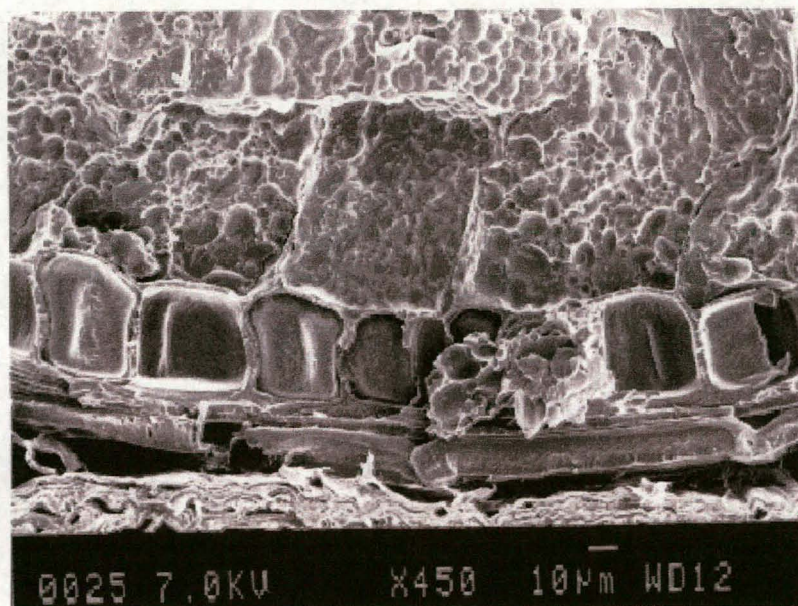


**Figure 17.** A photomicrograph of the different outer layers and the endosperm of the South African bread wheat, T4, magnified 450X.

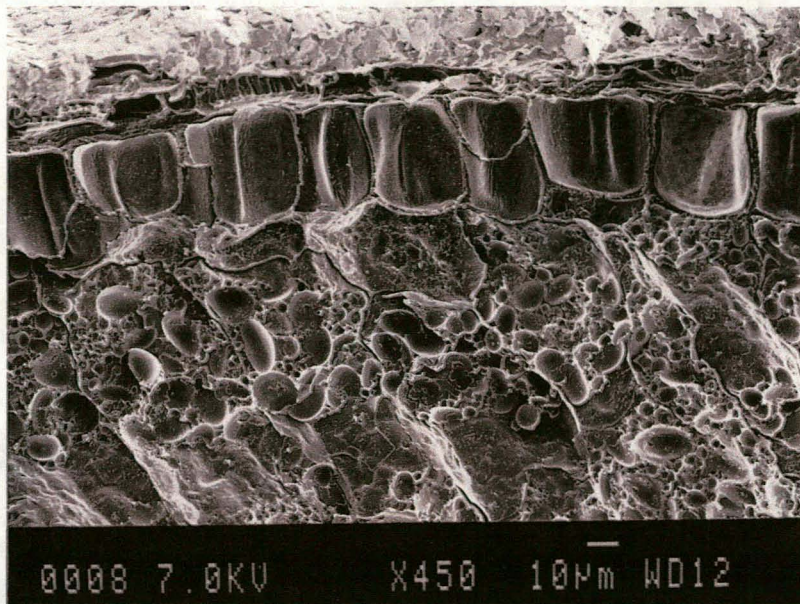


**Figure 18.** A photomicrograph of the outer layers and endosperm of the South African bread wheat, SST 876, magnified 450X.

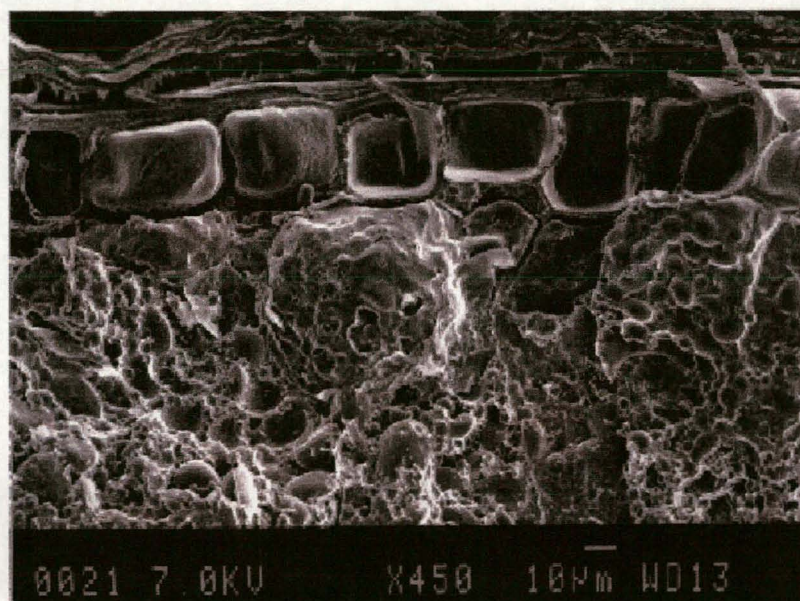


**Figure 19.** A photomicrograph of the outer layers and endosperm of the South African bread wheat, Gariep, magnified 450X.



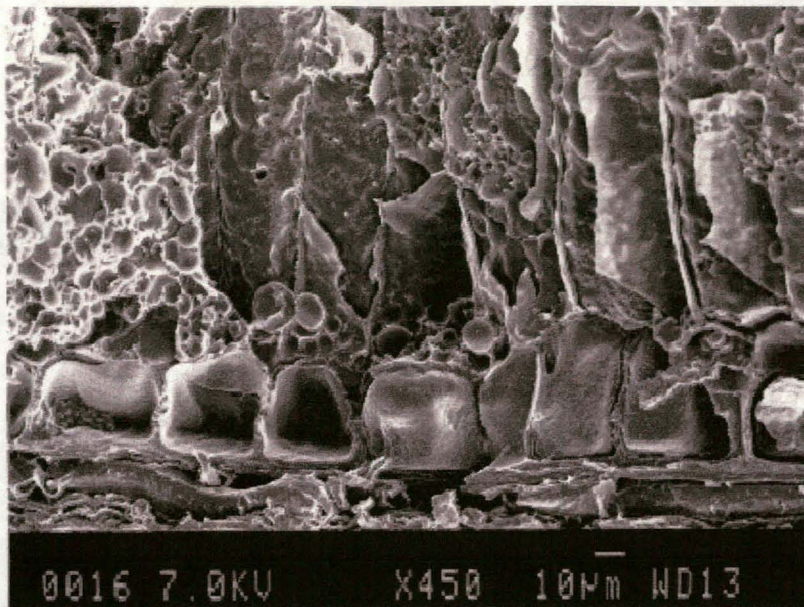


**Figure 20.** A photomicrograph of the outer layers and endosperm of the South African bread wheat, SST 75, magnified 450X.

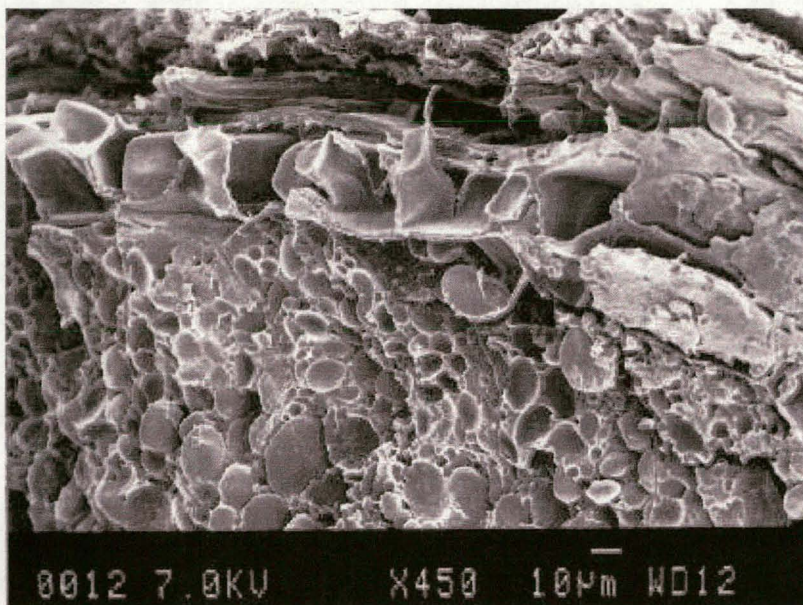


**Figure 21.** A photomicrograph of the outer layers and endosperm of the South African soft wheat, Wit Wol, magnified 450X.

### *Canadian whole wheat flour samples*

The photomicrograph of the whole flour of the durum wheat cultivar (Figure 22), magnified 800X, shows the still largely intact protein-starch matrix. The structure is compact with no air spaces. Almost all starch granules have been fractured during milling.

Figure 23 shows the whole flour of the hard red spring wheat, magnified 800X. The protein-starch matrix is still preserved, but the particle size is greatly reduced and air spaces occur.

Figures 24 & 25 illustrate the structure of the whole flour of the soft winter wheat sample, magnified 800X and 2000X, respectively. The protein-starch matrix has lost most of its structure. Smaller aggregates of protein and starch granules formed, there are some free starch granules and there are almost no fractured or surface-damaged starch granules.

### *South African whole wheat flour samples*

The protein-starch matrix of the whole flour of the durum cultivar, Kronos (Figure 26), is preserved and there are no intact starch granules visible. Some protein fragments are noticeable.

Most of the protein-starch matrix of the bread wheat T4 (Figure 27) is preserved. Some undamaged starch and cavities where smaller starch granules were dislodged during milling, are becoming visible, indicating a weaker protein-starch bond and therefore a relatively softer kernel texture.

The photomicrograph of the whole flour of the bread wheat SST 876 (Figure 28) shows protein still adhering to most of the starch surface, but with less damage to the uncovered starch surface. Some cavities formed by "freed" starch granules are visible on the surface.

Figure 29 illustrates the whole flour of the bread wheat Gariep, magnified 800X. The matrix is still relatively continuous. There is a higher degree of undamaged starch than in Figures 26 - 28, especially the smaller round starch granules that appear to be clustered together.

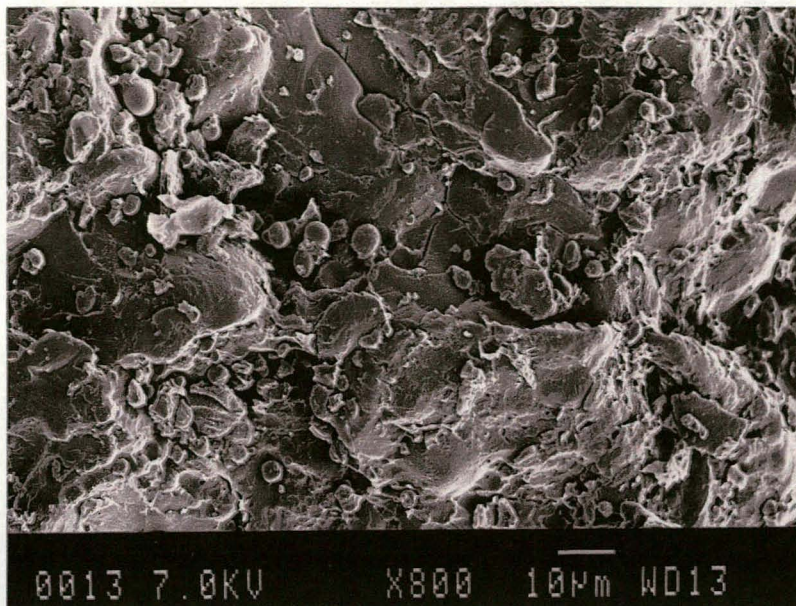


**Figure 22.** A photomicrograph of a sample of the flour of the Canadian durum wheat cultivar, magnified 800X.

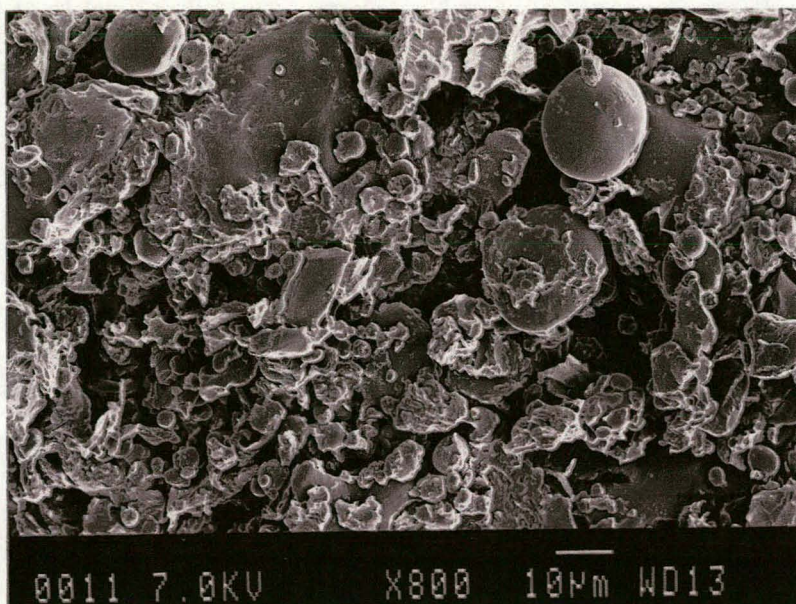


**Figure 23.** A photomicrograph of a sample of the flour of the Canadian hard red spring cultivar, magnified 800X.

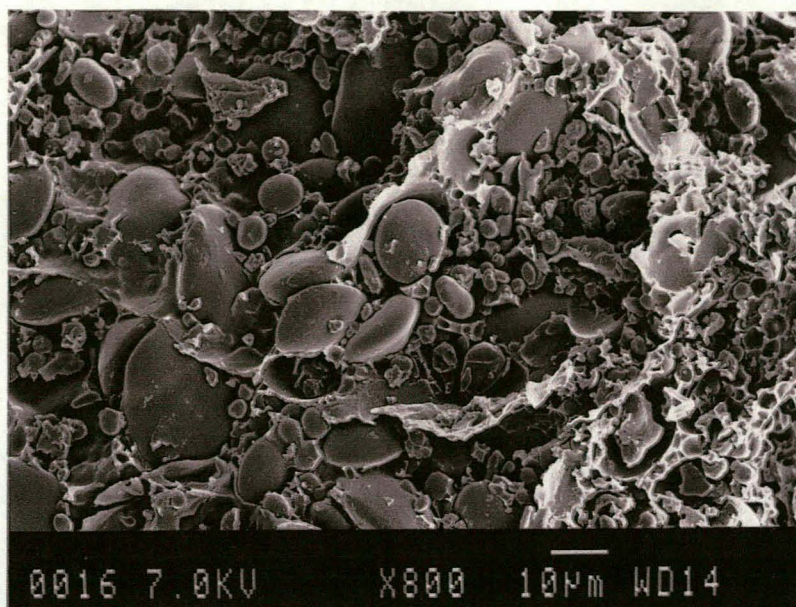


**Figure 24.** A photomicrograph of a sample of the flour of the Canadian soft white spring cultivar, magnified 800X.

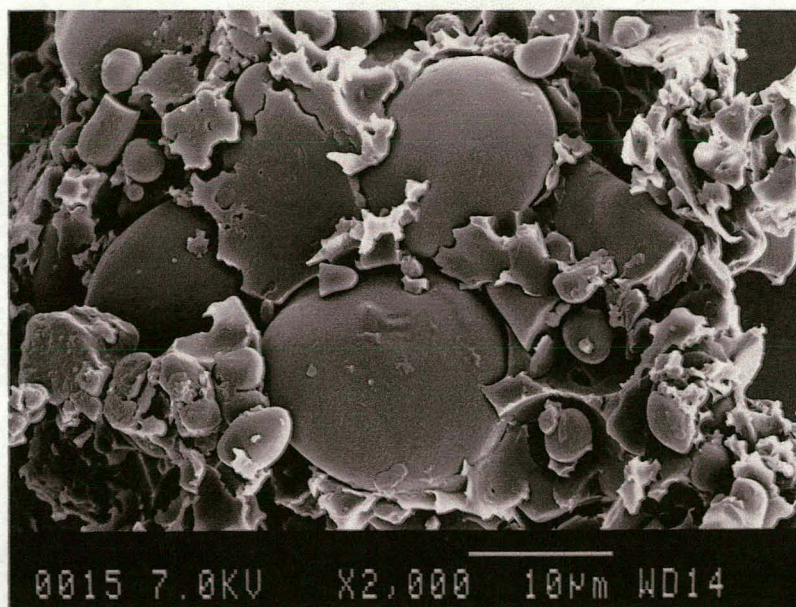


**Figure 25.** A photomicrograph of a sample of the flour of the Canadian soft white spring cultivar, magnified 2000X.

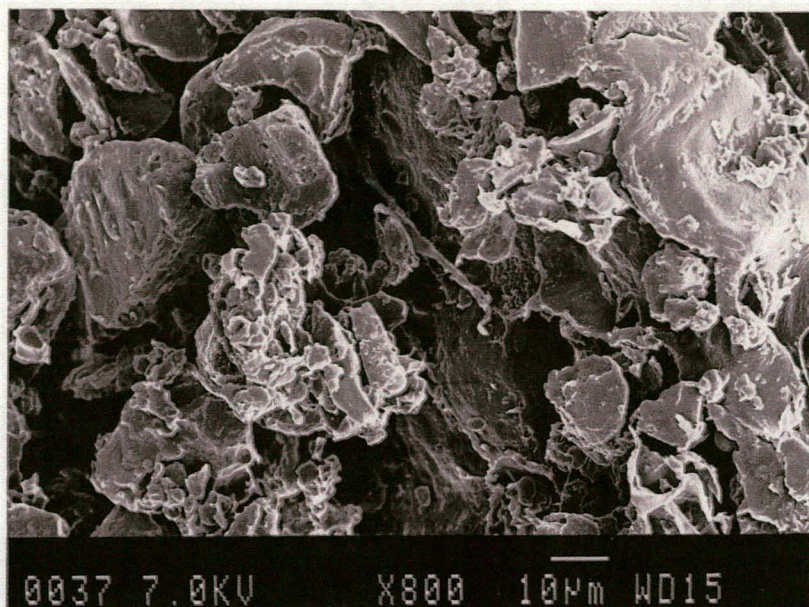


**Figure 26.** A photomicrograph of a sample of the flour of the South African durum wheat cultivar, Kronos, magnified 800X.

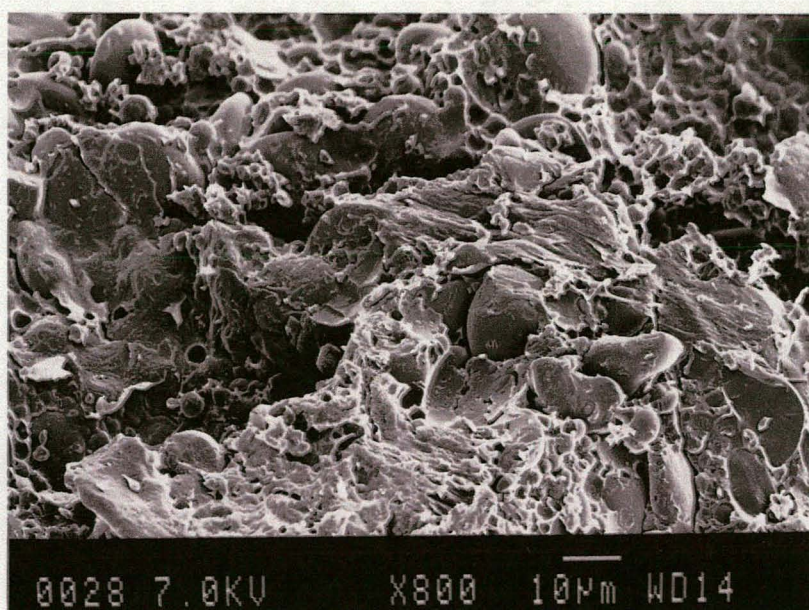


**Figure 27.** A photomicrograph of a sample of the flour of the South African bread wheat cultivar, T4, magnified 800X.

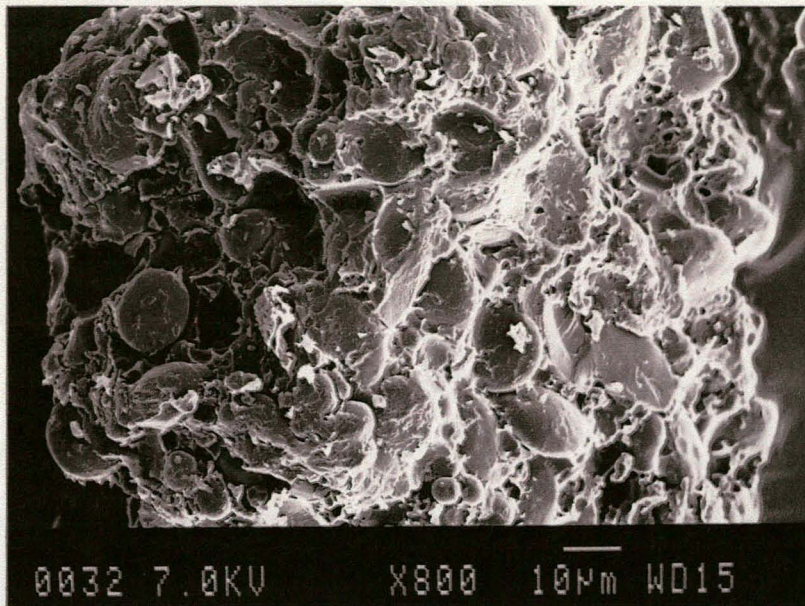


**Figure 28.** A photomicrograph of a sample of the flour of the South African bread wheat cultivar, SST 876, magnified 800X.

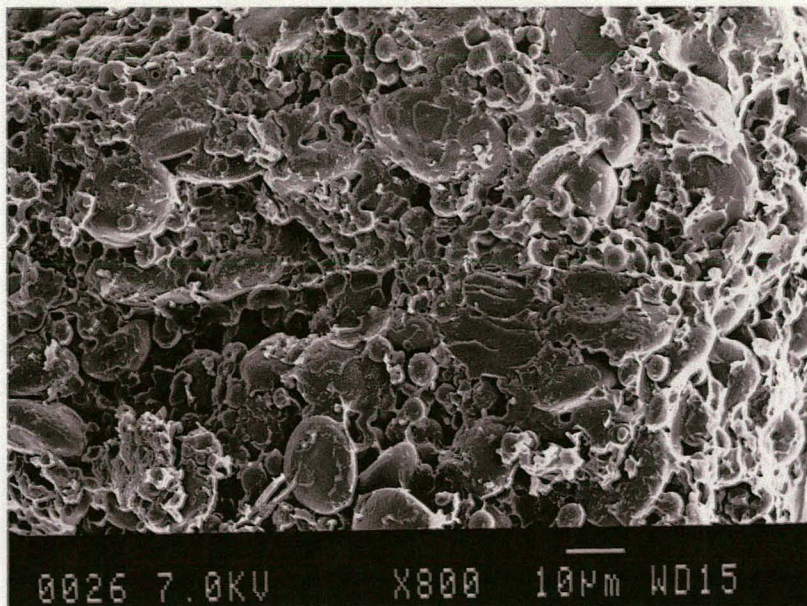


**Figure 29.** A photomicrograph of a sample of the flour of the South African bread wheat cultivar, Gariep, magnified 800X.

The structure of a flour sample of SST 75 (Figure 30) exhibits a discontinuous protein-starch matrix with aggregates of starch and protein, protein fragments, some free starch granules and large air spaces being prominent.

The protein-starch matrix of the whole flour of the soft wheat, Wit Wol, (Figures 31 & 32) has nearly disintegrated. Aggregates of protein and starch granules have formed where the starch is largely exposed, and protein fragments, large air spaces and a large number of free, undamaged starch granules are noticeable. Very little starch damage occurred and cavities left in the matrix by dislodged starch granules are visible.

## **Conclusions**

Scanning electron microscopy studies of wheat endosperm and flour structure confirm the theory that wheat hardness is determined by the strength of the protein-starch bond. The harder the wheat, the stronger the bond and the higher the occurrence of fractures through starch granules rather than at the protein-starch interface. The examined South African durum and soft wheat cultivars seem to resemble the structure of, respectively, the Canadian durum and soft wheat cultivars. There are large differences in hardness, and therefore also in endosperm and flour structure, within the examined samples of both the South African and Canadian bread wheat class. In Canada the wheat classification system acknowledges these differences by sub-classifying the bread wheat class according to kernel hardness. Knowing now that such vast differences in hardness also occur within cultivars of the South African bread wheat class, the South African wheat, milling and baking industry may also benefit from such a sub-classification based on kernel hardness.

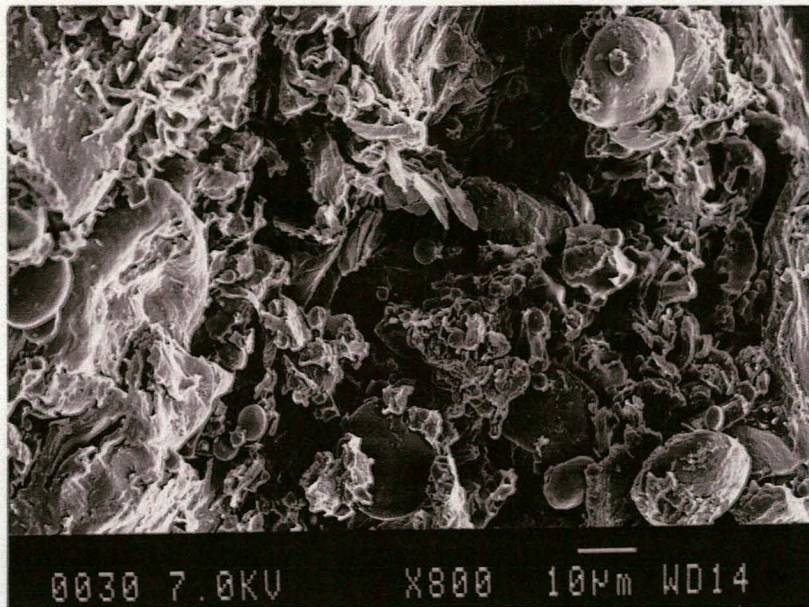


**Figure 30.** A photomicrograph of a flour sample of the South African bread wheat cultivar, SST 75, magnified 800X.

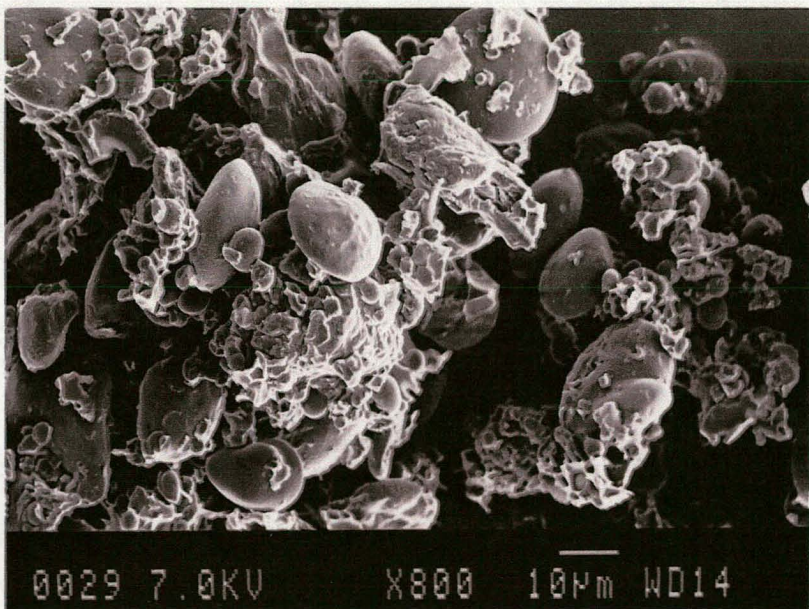


**Figure 31.** A photomicrograph of a sample of the flour of the South African soft wheat cultivar, Wit Wol, magnified 800X.



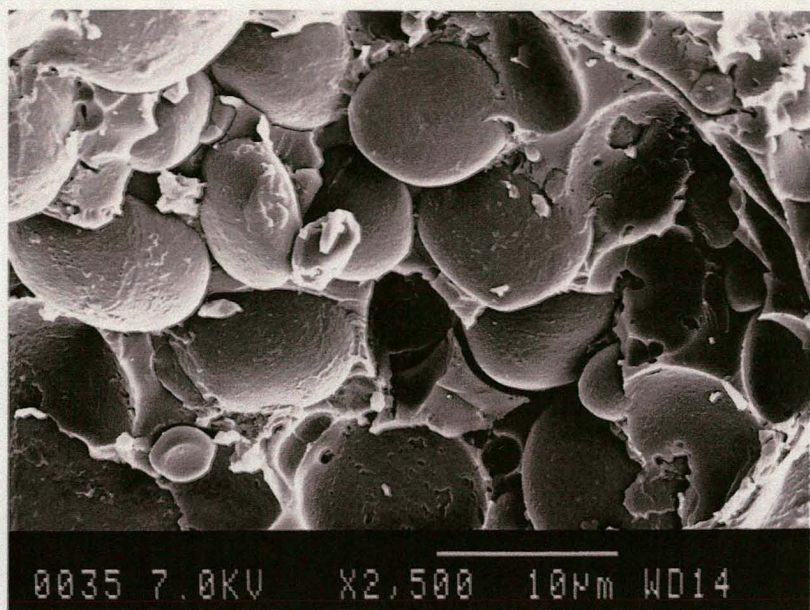


**Figure 32.** A photomicrograph of a sample of the flour of the South African soft wheat cultivar, Wit Wol, magnified 2500X.

## References

- Anjum, O.S. & Walker, J.H. (1991). Review on the significance of starch and protein to wheat kernel hardness. *Journal of the Science of Food and Agriculture*, **56**, 1-13.
- Barlow, K.K., Buttrose, M.S., Simmonds, D.H. & Vesk, M. (1973). The nature of the starch-protein interface in wheat endosperm. *Cereal Chemistry*, **50**, 443-454.
- Davis, A.B. & Eustage, W.D. (1984). Scanning electron microscope views of material from various stages in the milling of hard red wheat winter, soft red wheat winter and durum wheat. *Cereal Chemistry*, **6**, 182-186.
- Evers, A.D. (1969). Scanning electron microscopy of wheat starch. *Die Stärke*, **4**, 96-99.
- Glenn, G.M. & Saunders, R.M. (1990). Physical and structural properties of wheat endosperm associated with grain texture. *Cereal Chemistry*, **67**, 176-182.
- Goldstein, J.I., Newbury, D.E., Echlin, P., Joy, D.C., Romig Jr., A.D., Lyman, C.E., Fiori, C. & Lifshin, E. (1992). Electron optics. In: *Scanning Electron Microscopy and X-ray Microanalysis (2<sup>nd</sup> edition)*. Pp. 21-67. New York, USA: Plenum Press.
- Hoseney, C. (1986). Structure of cereals. In: *Principles of Cereal Science and Technology (student edition)*. Pp.1-32. Minnesota, USA: American Association of Cereal Chemists Inc.
- Hoseney, R.C. & Seib, P.A. (1973). Structural differences in hard and soft wheat. *The Bakers Digest*, **47**, 26-28 & 56.
- Kent, N.L. & Evers, A.D. (1994). Botanical aspects of cereals. In: *Kent's Technology of Cereals (4<sup>th</sup> edition)*. Pp. 29-52. Oxford, UK: Elsevier Science Ltd.
- Moss, R., Stenvert, N.L., Kingswood, K. & Pointing, G. (1980). The relationship between wheat microstructure and flourmilling. *Scanning Electron Microscopy*, **3**, 613-620.

- Pomeranz, Y. & Williams, P.C. (1990). Wheat hardness: its genetic, structural and biochemical background, measurement and significance. In: *Advances in Cereal Science and Technology* (edited by Y. Pomeranz). Pp. 471-548. Minnesota, USA: American Association of Cereal Chemists Inc.
- Sanstedt, R.M. (1946). Photomicrographic studies of wheat starch. I. Development of the starch granules. *Cereal Chemistry*, **23**, 337-359.
- Simmonds, D.H., Barlow, R.R. & Wrigley, C.W. (1973). The biochemical basis of grain hardness in wheat. *Cereal Chemistry*, **50**, 553-562.
- Van Deventer, C. S.(1999). Koringbedryf moet kyk na nuwe klassifikasie stelsel. *Landbouweekblad*, **1098**, 10-13.
- Watt, I.M. (1997). The electron microscope family. In: *The Principles and Practice of Electron Microscopy* (2<sup>nd</sup> edition). Pp. 59-135. Cambridge, UK: Cambridge University Press.
- Williams, P.C. (1999). Personal communication. Grain Research Laboratory. Canadian Grain Commission, Canada.
- Williams, P.C. & Sobering, D.C. (1986). Attempts at standardization of hardness testing of wheat. I. The grinding/sieving (Particle Size Index) method. *Cereal Foods World*, **31**, 359-364.

## Chapter 6

### General discussion and conclusions



## Chapter 6

### GENERAL DISCUSSION AND CONCLUSIONS

In South Africa wheat is not yet categorised or classified according to wheat hardness and little or no information is available on the wheat hardness scenario (Wessels, 1999). In the new free market system of South Africa, however, the price of wheat is playing an important role. Since price is customary based on class, and since kernel hardness is a factor in determining class in other wheat-producing countries (Norris *et al.*, 1989; Williams, 1999), determining wheat hardness will become important for the South African wheat, milling and baking industries. Most of the wheat in South Africa falls under the bread wheat class (Van Deventer, 1999). The aim of this study was therefore to establish a reference method, the particle size index (PSI) test, by which to determine kernel hardness of Southern and Western Cape wheats accurately. This would also give insight into the present variation in hardness of wheats of the bread wheat class in this area. After establishing a reference method, Fourier transform near infrared spectroscopy could subsequently be employed to derive hardness calibrations by which an on-line or in-line result can be obtained within 30 seconds for routine analysis (Osborne *et al.*, 1993).

The PSI method was first described by Cutler & Brinson (1939) and is the most important of the grinding/sieving - type methods for determining hardness (Pomeranz & Williams, 1990). The principle of this method is based on the fact that wheats of different hardnesses produce flours of different particle sizes upon grinding.

The PSI results had a correlation coefficient of 0.99 with results obtained by the Canadian Grain Commission for the same reference Canadian whole wheat flour sample set. A standard error of laboratory of 2.24% was obtained for results of the 198 Southern and Western Cape whole bread wheat flour samples. This indicates that accurate results can be obtained when the method is applied to South African cultivars. The PSI method was therefore successfully

established as a reference method for FT-NIR spectroscopic hardness determinations.

Particle size index results showed that the hardness range of the examined wheat samples were particularly wide (37.05 - 60.50%), although the majority of determinations were within the range of 45 - 55%. Statistical analysis of the hardness, protein content and moisture content of all the samples gave insight into the bread wheat hardness scenario. It was established that kernel hardness values are significantly influenced by genotype, but that influences due different localities are insignificant ( $P \leq 0.05$ ), confirming the fact that hardness is influenced more by genotype than by environment (Pomeranz & Williams, 1990). Furthermore kernel hardness has a linear positive relationship with protein content and a linear negative relationship with moisture content in the Southern and Western Cape. There is, therefore, an increase in protein content and a decrease in moisture content with increasing kernel hardness.

The effect of different sample holders on calibration results using the Perkin Elmer Spectrum IdentiCheck FT-NIR spectrophotometer, was established. Excellent results were obtained for protein and moisture calibrations for 92 South African whole wheat flour samples. Using different sample holders did not affect the calibration and prediction results significantly ( $P \leq 0.05$ ) implying that the conventional sapphire-glass sample cup could be replaced by one of the two types of vials (borosilicate-glass and soda-glass). This would be more convenient as samples could be stored and presented to the spectrophotometer in individual vials, eliminating the time-consuming task of cleaning and refilling the conventional sample cup for each sample. Subsequently borosilicate-glass vials were used in collecting the samples' spectra during FT-NIR hardness determinations.

A FT-NIR hardness calibration was successfully derived for Southern and Western Cape whole bread wheat flour using the PSI values as reference results. A standard error of prediction (SEP) of 2.13% and a correlation coefficient of 0.89 were obtained. Both calibration and prediction results

compared well with similar near infrared spectroscopy studies in other countries (Williams, 1991; Manley, 1995).

A scanning electron microscopy (SEM) study of South African and Canadian wheats of different hardness, particularly bread wheats, and their flours gave further insight into the South African bread wheat hardness scenario. Results confirmed the theory that wheat hardness is determined by the strength of the protein-starch bond (Simmonds *et al.*, 1973). The harder the wheat, the stronger the bond and the higher the occurrence of fractures through starch granules rather than at the protein-starch interface. Both the examined Canadian and South African bread wheats revealed large differences in endosperm and flour structure, indicating large differences in hardness. This confirms PSI results that the local bread wheat class encompasses wheats of a very wide range of hardnesses.

Should the bread wheat cultivars in South Africa differ so significantly in hardness and include such a wide range of hardnesses as is the case in the Southern and Western Cape, it may become necessary to develop a new wheat classification system in South Africa in which kernel hardness is considered. Similar variety in hardness occurs within the Canadian bread wheat class. Recognising these vast differences in hardness, the Canadian bread wheat class has been sub-classified into five sub-classes of different hardness ranges, giving an indication that four or five sub-classes may also be ideal for South Africa. In such a case FT-NIR reflectance spectroscopy and the PSI test could be considered as methods by which to determine wheat hardness accurately.

## References

- Cutler, G.H. & Brinson, G.A. (1939). The granulation of wholemeal and a method of expressing it numerically. *Cereal Chemistry*, **12**, 120.
- Manley, M. (1995). *Wheat hardness by near infrared (NIR) spectroscopy: New insights*, PhD. Thesis, University of Plymouth, United Kingdom.
- Norris, K.H., Hruschka, W.R., Bean, M.M. & Slaughter, D.C. (1989). A definition of wheat hardness using near infrared reflectance spectroscopy. *Cereal Foods World*, **34**, 696-704.
- Osborne, B.G., Fearn, T. & Hindle, P.H. (1993). *Practical NIR Spectroscopy with Practical implications in Food and Beverage Analysis (2<sup>nd</sup> edition)*. Pp. 1-71. Essex, UK.
- Pomeranz, Y. & Williams, P.C. (1990). Wheat hardness: its genetic, structural, and biochemical background, measurement, and significance. In: *Advances in cereal science and technology* (edited by Y. Pomeranz). Pp. 471-548. Minnesota, USA: American Association of Cereal Chemist Inc.
- Simmonds, D.H., Barlow, R.R. & Wrigley, C.W. (1973). The biochemical basis of grain hardness in wheat. *Cereal Chemistry*, **50**, 553-562.
- Van Deventer, C.S. (1999). Koringbedryf moet kyk na nuwe klassifikasie stelsel. *Landbouweekblad*, **1098**, 10-13.
- Wessels, A. (1999). Personal communication. Manager of product quality and development. Pioneer Food Group Ltd., Malmesbury, South Africa.
- Williams, P.C. (1991). Prediction of wheat kernel texture in whole grains by near infrared transmittance. *Cereal Chemistry*, **68**, 112-114.
- Williams, P.C. (1999). Personal communication. Grain Research Laboratory. Canadian Grain Commission, Winnipeg, Canada.